# Flexural Performance of Reinforced Concrete Beams Fabricated with Ground Glass and Fly Ash

A THESIS
SUBMITTED TO THE FACULTY OF THE
UNIVERSITY OF MINNESOTA
BY

Nicholas J. Johnson

IN PARTIAL FULFILLMENT OF THE REQUIREMENTS
FOR THE DEGREE OF MASTER OF SCIENCE

DR. BENJAMIN Z. DYMOND
DR. MARY U. CHRISTIANSEN

May 2020

**Acknowledgements**

I would like to thank both of my advisors, Dr. Dymond and Dr. Christiansen, for guiding me throughout both of my degrees. I am very fortunate to have worked with both of them so closely. I have gained invaluable knowledge from them. They are both very dedicated to their professions and serve as role models to up-and-coming Engineers.

Additionally, I would like to acknowledge both of my parents for not only their moral support throughout the long process of writing a thesis, but also for their help as manual laborers during the fabrication and testing of the concrete specimens. They were always willing to help with anything and everything they could, and I think they may have enjoyed learning a thing or two. Along with my parents, I would like to thank my fiancé who was also there every step of the way. I am excited for the future and to start our lives together. There is no better way to show commitment than listening to me read through my thesis over and over.

**Abstract**

Concrete is an essential construction material; however, the production of cement (a component of concrete) produces large quantities of carbon dioxide. These large quantities of anthropogenic carbon dioxide (along with other reasons) encouraged a shift toward the use of supplementary cementitious materials (SCMs) such as fly ash or granulated blast furnace slag, which are byproducts of other industries. Ground waste glass is another possible SCM that, at the proper particle size and depending on the chemical composition of the glass, can produce concrete with comparable or higher strength than concrete made without SCMs. However, there is a lack of research related to using glass as an SCM in structural concrete with steel reinforcement. In this study, nine concrete mixtures were created using various combinations of two fly ashes and three different types of ground waste glass and were compared to a control batch of concrete without SCMs. Three 6 ft beam specimens were fabricated from each of these ten mixtures (30 beams total) and the flexural behavior was investigated. Results from the 90-day flexural testing demonstrated that three out of the seven mixtures containing ground glass had higher average flexural strengths than the control beams (between 0.5-4% higher). The remaining beams made with glass had approximately 2-5% less flexural strength compared to control beams. However, there was no statistically significant difference in flexural strength between each of the nine SCM mixtures and the control beams without SCMs. Additionally, the beams made with ground glass had a lower displacement at failure in all cases when compared to the control beams.

# Table of Contents

# List of Tables

# List of Figures

# Chapter 1: Introduction

## 1.1 Background

Concrete is the most consumed construction material in the world (Ionescu, Kilpatrick, & Petrolito, 2018). The versatility and inherent properties of concrete allow for various uses in many modern applications including foundations, parking garages, buildings, roadways, and dams. The most predominate properties of concrete are its high compressive strength, low maintenance, long term durability, and the ability to resist degradation from fire and water. Additionally, concrete can be cast into nearly any desired shape. Concrete is created by mixing four fundamental components that are readily available to most of the world: gravel, sand, water, and cement. Concrete obtains its exceptional compressive strength as a result of hydrated cement. When cement and water react, they form a cementitious paste that "glues" the aggregates together.

### 1.1.1 Cement

Cement is a finely ground, gray material that comes in the form of a dry powder. The vast majority of cement produced is portland cement and will be referred to as "cement" within this document. Cement is mostly comprised of calcium silicates, including tricalcium silicate and dicalcium silicate, which are more commonly referred to as alite and belite, respectively. Hydrated calcium silicates form a cementitious paste that is rich in calcium silicate hydrate (C-S-H). The C-S-H is the primary contributor to concrete strength and binds the aggregates together to form concrete (Jennings & Thomas, 2018). Other common reaction products are formed through the hydration of cement such as calcium hydroxide (CH), ettringite, and some other minor phases that have negligible contribution to the strength of the concrete.

Cement is the second most used substance in the world behind water and is manufactured in many locations worldwide (Gartner, John, & Scrivener, 2018). The process for making cement is outlined by Lalande and Tremblay in United States of America Patent No. US6908507B2 (2005) and begins with the mining of raw materials from the earth. These raw materials typically contain calcium from limestone, silica from

clay/sand/shale, alumina from bauxite, and iron from iron ore. Calcium and silica are required to produce the cementitious chemical reaction during hydration; alumina and iron oxide are added as a flux to lower the kiln temperature for cement production. Once the materials are mined, the raw materials are proportioned and interground to the desired particle size. The blend is preheated and placed in a kiln until a temperature of at least 1,450 °C is reached. The heated material is cooled and referred to as clinker. Finally, the clinker is interground with gypsum to form portland cement (United States of America Patent No. US6908507B2, 2005). Consequently, this manufacturing process produces approximately 10% of the total global anthropogenic carbon dioxide emissions each year (Gartner et al., 2018).

The carbon dioxide emissions originate from two distinct processes that occur during cement manufacturing, direct emissions (90%) and indirect emissions (10%). Direct emissions are the result of limestone calcination and fossil fuel burning in the preheater and kiln process, while indirect emissions are primarily from the electricity used in both of the grinding processes (grinding raw materials and intergrinding gypsum) (Han, Wei, & Zhang, 2018). As large countries such as China and India continue to develop, more cement is produced to meet the market demands, ultimately increasing total global carbon dioxide emissions. Advancements in cement production have been made to reduce these emissions, including a switch from a wet kiln process to a dry kiln process in the 1970's. The major difference between these two kiln methods is that the ground material in the wet kiln process enters the kiln in a wet slurry. The slurry makes blending the raw materials together easier but reduces efficiency due to the water having to be evaporated in the kiln. The primary process used after the 1970's is a dry kiln, which uses 50% less energy than the wet kiln process (Gartner et al., 2018). These state-of-the-art kilns are some of the most efficient thermal machines used in the industry (Gartner et al., 2018). Additional efficiency advancements on the dry kilns would be minimal and expensive. Therefore, the use of supplementary cementitious materials (SCMs) to make concrete is being studied in an attempt to reduce the carbon dioxide emissions produced from cement manufacturing.

Rather than reducing the emissions from cement manufacturing, which is already relatively efficient, SCMs are used to partially replace a portion of the cement within concrete.

### 1.1.2 Supplementary Cementitious Materials

SCMs are often industrial waste byproducts that would otherwise have minimal intrinsic value. For example, fly ash is a common SCM that is the byproduct of burning coal in the thermal power industry. By replacing a portion of cement with a waste material, carbon dioxide emissions can be lowered. Other common SCMs include calcined clay, silica fume, and granulated blast furnace slag (GBFS). SCMs are rich in amorphous silica and also contain alumina and calcium oxide. Typical SCM replacement levels are around 5-20% of the cement by mass, but the replacement levels vary between different SCMs (Juenger & Siddique, 2015). SCMs not only help to reduce some of the carbon dioxide emissions but can also add many desirable properties to concrete mixtures.

SCMs are added to concrete for many performance reasons, including increased durability, decreased permeability, mitigation of alkali-silica reaction (ASR), increased long-term strength gain, and increased sulfate resistance. Furthermore, most SCMs tend to be less expensive than cement. However, SCMs do not all perform the same way or exhibit the same properties in concrete compared to each other. For example, fly ash and silica fume are both SCMs, but they can have differing effects on both fresh concrete properties (e.g., set time, workability, and heat of hydration**)** as well as hardened concrete properties (e.g., permeability and compressive strength).

SCMs can be separated into two categories based on their chemical composition: hydraulic SCMs (e.g., Class C fly ash) and pozzolanic SCMs, also referred to as pozzolans (e.g., silica fume and Class F fly ash). The distinguishing difference between the two categories is a hydraulic SCM will react with water to form cementitious compounds, while a pozzolan will not. Additionally, there are some SCMs that fall in between these two categories that have some cementitious properties; these are referred to as latently hydraulic SCMs (e.g., GBFS). Pozzolanic SCMs undergo a reaction known as the pozzolanic reaction when they are included in a portland cement concrete mixture.

Pozzolans can add many benefits to the strength and durability of the concrete when added as a partial replacement of cement (Lefort, Moras, Rodriguez, & Shao, 2000).

The pozzolanic reaction is a delayed reaction that occurs after the initial hydration of cement. During cement hydration, calcium hydroxide (CH) is formed. High concentrations of excess CH can lead to durability problems and have minimal contribution to strength. When a pozzolan is introduced to a mixture of portland cement and water, the silica from the pozzolan reacts with the leftover CH to produce additional C-S-H. This additional C-S-H can be beneficial for the long-term durability and mechanical properties of the concrete, including the compressive and flexural strength. A simplified cement hydration reaction is shown in Equation 1.1 and the pozzolanic reaction is shown in Equation 1.2.

$$\text{Cement Hydration: Cement + Water} \rightarrow \text{C-S-H + CH} \qquad \text{Eq. 1.1}$$

$$\text{Pozzolanic Reaction: Silica + CH + Water} \rightarrow \text{C-S-H} \qquad \text{Eq. 1.2}$$

An effective pozzolan has the following properties: high silica content, an amorphous structure (glassy), and a small particle size distribution (Pavia & Walker, 2011). A pozzolan must contain significant amounts of silica for the secondary conversion of CH to C-S-H to occur. Additionally, an amorphous structure and small particle size are essential for the pozzolan to undergo rapid hydrolysis. In other words, amorphous materials dissolve more readily in an alkaline solution than crystalline materials. Likewise, smaller particles dissolve quicker than larger ones.

The majority of SCMs used in concrete are fly ash and GBFS. However, future availability of these traditional SCMs has become a concern due to the increased demand for concrete that incorporates SCMs (Juenger & Siddique, 2015). With rising concrete demands and shifts toward more sustainable practices, other alternative SCMs such as ground waste glass are being studied.

### 1.1.3 Ground Waste Glass

Glass is an essential part of modern life and is used in countless products including containers, bottles, windows, and lightbulbs. A unique property of glass is that it can be recycled an infinite amount of times without loss in quality. Unfortunately, the United States produced 11.5 million tons of glass in 2015 and only 3 million tons were recycled, which resulted in a 26.4% recycling rate (Enviornmental Protection Agency, 2019). Another 1.5 million tons of glass were combusted with energy recovery, and much of the remaining 60.9% of glass ended up in landfills (Enviornmental Protection Agency, 2019). One common reason for the inadequate glass recycling rates in the United States is the single stream collection method. All recyclable materials are intermixed in single stream collection including glass, paper, plastics, and some miscellaneous non-recyclables. This method often results in broken and contaminated glass and creates issues in the production of new glass products from recycled glass, which is the largest market for waste glass. New glass production requires the glass to be sorted by color and free of debris, and any glass that is too expensive and time consuming to refine often ends up in landfills (Christiansen & Dymond, 2019).

Conveniently, a potential outlet for unsuitable recycled glass is in the concrete industry as a pozzolan. Waste glass can be ground into a fine powder that displays pozzolanic behavior and can be a partial substituted for cement in concrete. This alternative outlet for waste glass would benefit overcrowded landfills, while potentially producing an inexpensive pozzolan for the concrete industry. Ground glass used as a pozzolan in concrete can delay early compressive strength, but it may increase long-term strength when compared to concrete without SCMs (Kumar & Raju, 2014). Studies have shown increased compressive and flexural strength and increased durability through the pozzolanic generation of secondary C-S-H when using ground glass (Aggarwal & Shekhawat, 2014; Shayan & Xu, 2004; Lefort et al., 2000). However, the effectiveness of the pozzolanic reaction is significantly affected by glass composition and particle size.

Glass composition varies widely between source locations and different types of glass. Around 90% of the glass produced in the United States is soda-lime glass (Corning

Museum of Glass, 2002). Soda-lime glass is used to make container (bottles and jars) and plate (windows and flat sheets) glass. Other types of glass include vitreous silica glasses, borosilicate glasses, glass fibers (including E-glass), aluminosilicate glasses, and glass-ceramics. The composition of these glasses is affected by the application in which they are used. The wide variation in composition creates issues when using ground glass as an SCM because glass composition affects concrete properties in different ways, making it difficult to predict concrete behavior. However, the composition of fly ash can vary substantially from different sources, but it is still an effective and critical SCM in the concrete industry because of extensive performance testing and thorough research studies. Similar to fly ash, waste glass has the potential to be a valuable partial cement replacement regardless of its varying composition.

Implementing the use of waste glass in concrete can reduce carbon dioxide emissions and conserve valuable space in landfills. Additionally, ground glass may have the ability to enhance long-term performance of concrete. If traditional SCMs (e.g., fly ash and GBFS) become less available in the future, other alternatives such as glass may become essential for maintaining progress toward more sustainable concretes.

## 1.2 Motivation for Research and Objectives

Waste glass can be found globally and has the potential to be a significant supplementary cementitious material in concrete. The United States alone disposed of 7 million tons of glass in landfills in 2015 (Enviornmental Protection Agency, 2019). Cement replacements such as ground waste glass have become a growing point of interest due to carbon dioxide emissions and a focus on sustainable practices. Ground glass displays effective pozzolanic properties and is less expensive and more environmentally friendly than cement (Kazi, Rahman, & Sadiqul Islam, 2016). Prior studies on concrete with ground glass suggest that long-term compressive strengths and unreinforced flexural strengths are comparable to concrete without SCMs (Nassar & Soroushian, 2011). However, limited research has been conducted on the structural behavior (e.g., steel reinforced flexural strength) of concrete beams fabricated with ground glass.

The objective of the project was to determine if ground waste glass in a binary or ternary blend could be incorporated into structural concrete mixtures with similar or improved flexural strengths compared to beams without SCMs. One of the goals for this research was to determine whether incorporating different types of ground glass in concrete beams would affect the flexural strength compared to beams that did not have SCMs and compared to beams with fly ash. Another goal was to establish if ternary blends of glass and fly ash would affect the flexural strength compared to control beams and compared to mixtures with only glass or fly ash. The final goal was to determine if the flexural strength of the beams would be affected by different fly ashes in a ternary blend with one type of glass. The compressive strength and modulus of elasticity of the mixtures was also examined.

## 1.3 Thesis Organization

Chapter two presents a literature review that examines research on the effects that ternary blends, glass particle size, glass composition, and replacement level have on the compressive strength, modulus of rupture, and modulus of elasticity of concrete containing ground waste glass. Chapter three provides details on the fabrication of the concrete specimens, information on materials, specimen test setup, instrumentation used during testing, and testing procedures. Chapter four provides the compressive strength, flexural strength, and modulus of elasticity testing results, along with a discussion of the results. Chapter five draws conclusions from the findings and provides recommendations for future work using ground waste glass.

# Chapter 2: Literature Review

## 2.1 Introduction

Ground glass is an underutilized concrete pozzolan. This, in part, has to do with glass not being specifically recognized as a pozzolan within current standards or codes. Establishing glass-based concrete standards would aid in the acceptance of a ground glass SCM within the construction industry. Inherently, most glass types could already be described as a pozzolan as defined by both the American Society for Testing and Materials (ASTM) and American Concrete Institute (ACI).

Per the requirements of ASTM C618 *Standard Specification for Coal Fly Ash and Raw or Calcined Natural Pozzolan for Use in Concrete* (2019), most glasses are considered a natural pozzolan. Classification as a natural pozzolan requires a combined chemical composition of at least 70% silicon dioxide, aluminum oxide, and iron oxide and a maximum of 4% sulfur trioxide, which many glasses already meet. Additional requirements include a maximum water content (3%) and loss on ignition value (10%); both of which are negligible or very low in glass. Fineness criteria in ASTM C618 are easily met by grinding glass to the desired size. Additionally, concrete containing a natural pozzolan must have at least 75% compressive strength compared to concrete containing only portland cement at 7 and 28 days to meet the strength activity index (SAI) requirements, which is often met using ground glass. Glass also meets the other physical requirements of ASTM C618 (2019) and thus can be considered a natural pozzolan. By ACI (2019) definition a pozzolan is a "siliceous or siliceous and aluminous material that in itself possesses little or no cementitious value but will, in finely divided form and in the presence of moisture, chemically react with calcium hydroxide at ordinary temperatures to form compounds having cementitious properties." Inherently, glass is a siliceous material that exhibits the properties described by ACI and can be regarded as a pozzolan. Therefore, glass can be used as a partial replacement for cement in concrete. While glass is a pozzolan as defined by ASTM and ACI, concrete containing ground glass and its attributes are not well understood in the academic research community or construction industry.

## 2.2 Glass Composition

Research on many different types of glass by Christiansen and Dymond (2019) has shown that the glass composition has a diverse effect on the compressive strength performance of concrete containing ground glass.

Soda-lime glass is the most available waste glass and the most practical for use as a large-scale cement replacement. The composition of soda-lime glass is 60-70% silica, 12-18% sodium carbonate or "soda", and 5-12% calcium oxide or "lime", along with trace amounts of other components used mostly for glass coloring (Corning Museum of Glass, 2002). Soda-lime glass has been the focus of most research involving glass replacement in concrete (Aggarwal & Shekhawat, 2014; Kumar & Raju, 2014; Shayan & Xu, 2004). However, another less common type of glass used in fiberglass and to reinforce integrated circuit boards known as electrical grade glass or E-glass has been used as a pozzolan in concrete and has shown promising compressive strength results.

According to Chen, Huang, Wu, and Yang (2006), E-glass has approximately 19% less silica, 13% less equivalent alkalis ($Na_2O+K_2O$), 5% more calcium oxide, and 14% more aluminum oxide than soda-lime glass. Chen et al. (2006) reported concrete cylinder (4 in. diameter by 8 in. height) compressive strength results using E-glass that were 17%, 27%, and 43% higher at 28, 91, and 365 days, respectively, compared to control specimens with 100% portland cement. The optimal cement replacement level was identified to be 40-50% E-glass by weight with 40% of the particles being less than 150 μm (Chen et al., 2006). Similar results were demonstrated by Christiansen and Dymond (2019) with 2 in. mortar cubes containing E-glass with 90% of the particles less than 45 μm, where cement replacement with 20% and 30% E-glass had at least 3% and 9% higher compressive strengths, respectively, at 90 days than 17 other glasses including multiple soda-lime glasses. Compressive strengths of cubes with E-glass were 3% and 6% higher than those of control cubes without SCMs at 90 days, with replacement levels of 20% and 30%, respectively. Additionally, compressive strength cubes with 20% and 30% E-glass replacement levels had comparable strengths at 28 days. The results from Christiansen and Dymond (2019) highlighted the difference in concrete compressive strength performance

when various glass compositions were studied, most notably the higher E-glass compressive strength.

Previous research has shown that the composition of glass used in concrete has an impact on the compressive strength of concrete. Further compressive strength testing on concrete containing glass can provide insight into the impact of glass composition. There are many types of glass that may exhibit pozzolanic behavior, but this study focused on soda-lime and E-glass, due to the availability of soda-lime glass and the enhanced compressive strengths demonstrated by E-glass.

## 2.3 Glass Particle Size

Glass particle size is one of the most influential components on how effective the pozzolanic reaction is. A single large particle takes longer to react than the same size particle ground into smaller pieces due to less exposed surface area. This means compressive strength is obtained more slowly with large particles. Additionally, if the particle sizes are too large, a rim of reacted material may form around the particle preventing the interior of the particle from reacting. This reduces the effectiveness of the pozzolan and in some cases, large enough glass particles may cause alkali-silica reaction (ASR) in the concrete (Shayan & Xu, 2004). ASR occurs when large silica rich glass particles react with alkalis in the pore solution, creating an expansive gel that may have long-term detrimental effects on the flexural and compressive strength of the concrete. This occurs more often when glass is used as a fine or coarse aggregate replacement; ASR can mitigated when glass particles are finely ground (Shayan & Xu, 2004). The following studies focus on particle sizes using soda-lime glass.

Studies conducted by Samtur (1974) and Aphale and Sahare (2016) showed that glass particles less than 75 μm in size displayed pozzolanic activity and helped mitigate ASR. According to Lee, Sutan, Tamanna, and Yakub (2013), glass particle sizes between 45 to 75 μm can be used without undesirable long-term effects on durability of the concrete; they also determined that particle sizes below 45 μm may exhibit pozzolanic behavior. An additional study by Baxter and Meyer (1998) established that glass particles less than 45 μm produced a pozzolanic reaction. Lefort et al., (2000) performed a detailed study on

concrete containing 150, 75, and 38 μm glass particles. Concrete batches containing fly ash, silica fume, and control concrete without SCMs were also cast to compare compressive strengths with the different glass particle sizes. Cement replacement levels were 30% for all SCM batches. Twenty cylinders were cast for each test batch and five cylinders from each batch were tested after 3, 7, 28, and 90 days. Concrete control cylinders (2 in. diameter by 4 in. height) had higher compressive strengths than cylinders containing 150, 75, and 38 μm glass for all test ages except for 38 μm glass at 90 days, which had 8% higher compressive strengths than the control. However, concrete containing 38 μm glass had higher compressive strengths at all ages compared to concrete with fly ash, and concrete containing 75 μm glass had similar compressive strengths compared to the concrete with fly ash.

Samtur (1974), Lee et al. (2013), Baxter and Meyer (1998), Lefort et al. (2000), and Aphale and Sahare (2016) concluded that smaller particle sizes produced more effective pozzolanic reactions, with glass particles less than 45 μm being the most effective. Furthermore, inclusion of particles less than 45 μm in size as an SCM may increase the compressive strength of concrete compared to concrete made without ground glass.

### 2.4 Effects of Glass on Compressive Strength and Flexural Modulus of Rupture

Ground glass performance in concrete has been examined in the past, and in most cases, glass increased long-term compressive strengths and the flexural modulus of rupture of concrete when tested at 90 days (Kumar & Raju, 2014). Shayan and Xu (2004) performed compressive strength tests on 4 in. diameter by 8 in. tall concrete cylinders that contained soda-lime glass with replacement levels of 10%, 20%, and 30% of the cement by mass and with particle sizes less than 10 μm. Because some of the cement was replaced with glass and due to the slower pozzolanic reaction of glass, initial compressive strengths at 28 days were lower than that of control specimens without glass by approximately 2%, 4%, and 17% for 10%, 20%, and 30% cement replacement, respectively. However, long-term compressive strengths (56 and 90 days) of specimens with 10% and 20% glass replacement achieved 2% higher and similar compressive strength, respectively, compared to the control cylinders at 56 days and 5% higher and about the same compressive strength,

respectively, as the control cylinders at 90 days. Specimens with 30% replacement had 4% and 7% lower compressive strengths compared to the control at 56 and 90 days, respectively. The long-term strength gain may signify a pozzolanic reaction occurred within the concrete. Shayan and Xu (2004) determined that as glass replacement levels increased beyond 20% the concrete compressive strengths decreased.

Aggarwal and Shekhawat (2014) reported higher compressive strengths from concrete cylinders (6 in. diameter by 12 in. height) with 10% and 20% glass replacement than control cylinders without cement replacement; the author used soda-lime glass ground to particle sizes less than 90 μm. Contrary to the long-term strength gain demonstrated by Shayan and Xu (2004), the higher glass compressive strength results from Aggarwal and Shekhawat (2014) were obtained at 7 and 28 days. Additionally, Aggarwal and Shekhawat (2014) conducted modulus of rupture tests on 4 in. x 4 in. x 20 in. unreinforced beams. The concrete beams with 10% and 20% glass replacement exhibited an increase in modulus of rupture of 8% and 12% at 7 days and 12% and 15% at 28 days, respectively, compared to control specimens without cement replacement. More than 20% glass replacement levels lowered the modulus of rupture and compressive strength of the concrete. The decreased performance above 20% replacement may be caused by too much silica and not enough available calcium hydroxide. In other words, the excess silica does not have calcium hydroxide to react with and provides little strength by itself. Aggarwal and Shekhawat (2014) stated that a maximum of 20% replacement of cement is the optimum replacement level for economy and better performance.

Kumar and Raju (2014) studied 6 in. concrete cubes with glass replacement levels of 5% to 40% in increments of 5% using soda-lime glass with particle sizes less than 45 μm. Their study also concluded that, at a 20% glass replacement level, the maximum compressive strength was achieved, and the compressive strength was higher than their 6 in. control cubes without cement replacement. This was the case for 7, 28, and 90-day test results. Unreinforced 6 in. x 6 in. x 27.5 in. concrete beams were also tested in flexure. The flexural modulus of rupture values for 20% glass replacement specimens were 27%, 20%, and 17% higher than control beams for 7, 28, and 90-day tests, respectively.

The consensus between these sources was that a maximum glass replacement level of 20% is the most effective for optimal performance and economy of the concrete (Aggarwal & Shekhawat, 2014; Kumar & Raju, 2014; Shayan & Xu, 2004). However, replacement levels less than 20% can still be more effective than conventional concretes without glass. The time it takes to develop both flexural and compressive strength with glass replacement specimens varies in the literature, with some research showing strengths higher than control mixes at 7 and 28 days and some research not demonstrating higher strengths until 56 and 90 days. These differences may be attributed to the pozzolanic reactivity of slightly different glasses and different particle sizes. Additionally, concrete specimens with 20% replacement levels satisfied the minimum SAI of ASTM C618 (2019), with many of the specimens having a SAI over 100% at 7 and 28 days (Aggarwal & Shekhawat, 2014; Kumar & Raju, 2014).

## 2.5 Concrete Ternary Blends

Ternary blends are concrete mixtures that incorporate cement and two other cementitious materials such as GBFS, fly ash, metakaolin, silica fume, or glass. Ternary blends are used for a variety of reasons including increasing concrete compressive strength, increasing ASR resistance, increasing sulfate resistance, decreasing thermal differential within concrete, and decreasing permeability (SCA, 2019). Ternary bends can also be used to offset the early strength loss caused by the addition of normally reactive SCMs (e.g., fly ash) by blending them with highly reactive SCMs such as silica fume (Erdem & Kirca, 2008). Erdem and Kirca (2008) determined that cement and silica fume blended with a Class F fly ash, Class C fly ash, or slag had higher compressive strengths than concrete mixtures with cement and one other SCM (binary mixtures) at 7 and 28 days. Chindaprasirt and Rukzon (2014) obtained similar results with high strength concrete where ternary blends with bagasse ash and fly ash or rice husk ash (RHA) improved concrete compressive strength, corrosion resistance, and resisted chloride penetration. Ternary blends can be implemented to improve many aspects of concrete performance including increased concrete compressive strength.

## 2.6 Effects of Glass on the Modulus of Elasticity

The elastic modulus is a material property indicative of that materials ability to resist elastic deformation when a stress is applied. The elastic modulus is used to calculate the displacment as a component of the stiffness ($EI$), where $I$ is the second moment of inertia. The elastic modulus can also be used to calculate creep and shrinkage of concrete. However, the effects of ground glass on the elastic modulus of concrete are not well known. Ghavidel and Madandoust (2013) studied the modulus of elasticity with combinations of RHA and ground glass as a partial cement replacement. They found the optimal cement replacement level for compressive strength and SAI at 28 days to be 5% rice husk ash and 10% glass by weight. Tests were conducted to obtain the modulus of elasticity at 7, 28, 42, and 90 days and results were compared to those from control specimens without SCMs. Initially, the modulus of elasticity for the 5% RHA and 10% glass concrete was approximately 3 GPa (435 ksi), which was 22% less than that of the control specimens at 7 days. At 90 days, the modulus of elasticity increased to within less than 1 GPa (145 ksi) or 3% of the modulus of the control specimens. This pattern was to be expected considering the delayed pozzolanic reaction, with long-term properties generally being similar to concrete specimens fabricated with 100% portland cement.

## 2.7 Summary

The composition of different types of glass can vary substantially, and this ultimately affects concrete performance. Soda-lime glass is the most accessible glass type and is the most likely to be used as a pozzolan in large-scale concrete construction. However, results from using E-glass as a pozzolan in previous research have indicated that it can increase the compressive strength and modulus of rupture at 90 days, potentially outperforming conventional concrete without SCMs. Both soda-lime glass and E-glass have been shown to be effective pozzolans by potentially increasing concrete compressive strengths and modulus of rupture compared to concrete without SCMs at 90 days. Furthermore, it is hypothesized that ternary blends incorporating fly ash and ground glass may increase concrete compressive strength compared to binary blends. Research has demonstrated that smaller glass particles exhibit more pozzolanic reactivity. Pozzolanic reactivity has been

observed with glass particles less than 75 μm in size with little adverse effects on long-term compressive strength and modulus of rupture of concrete. However, results in the literature indicated that particle sizes less than 45 μm were more favorable for increased pozzolanic behavior. The modulus of elasticity, which affects displacement and stiffness of a concrete member, is not well researched for concrete with glass. Concrete with glass may have a lower initial modulus of elasticity than concrete without SCMs, but it is theorized that both have comparable long-term modulus of elasticity values; additional research was required to confirm this.

# Chapter 3: Methods and Materials

A total of ten different concrete mixtures were developed. Nine of the mixtures had various combinations of two different fly ashes and three different ground waste glasses, with a maximum cement replacement level of 20% for each mixture. The remaining mixture was a control with no cement replacement. For each mixture, three concrete beams and 15 concrete cylinders were fabricated, for a total of 30 beams and 150 cylinders. The dimensions of the concrete beams were approximately 6 ft 3 in. long by 6 in. wide and 10 in. deep, and the cylinders were 3 in. in diameter by 6 in. in height. The target water-to-cementitious materials (w/cm) ratio for all of the mixtures was approximately 0.42. No air-entrainment was added in any of the mixtures, and the nominal target concrete compressive strength was 4,000 psi at 28 days. Three concrete cylinders were tested to quantify the compressive strengths of each mixture at 1, 7, 28, 90, and 180 days after casting in accordance with ASTM C39 (2018). All 30 beams were flexurally tested using a third-point loading setup 90 days after casting in accordance with ASTM C78 (2018).

## 3.1 Variables Investigated

A testing matrix was developed to investigate three distinct areas of interest. The first area of interest was the difference in flexural strength of beams containing three different types of glass: W-glass (soda-lime container), Q-glass (E-glass), and UV-glass (soda-lime plate). The naming conventions for the glasses are arbitrary. Three mixtures were created to investigate the flexural strength of the concrete made with glasses: a mixture with 20% W-glass replacement, 20% UV-glass replacement and 20% Q-glass replacement by mass. Additionally, mixtures with 20% Fly Ash 1 (Class F fly ash) and 20% Fly Ash 2 (Class F fly ash) were created to investigate the flexural strength of beams made with fly ash compared to those made with glass. Two local fly ashes were used to represent variability within Class F fly ash. The second focus examined the flexural strength of beams containing 10% W-glass in combination with 10% Fly Ash 1 and 10% W-glass in combination with 10% Fly Ash 2. The intent was to study the most common type of glass (soda-lime glass) blended with two different fly ashes. The third area of interest examined mixtures containing 10% Fly Ash 2 and 10% of each of the three types

of glasses (i.e., 10% Fly Ash 2 with 10% W-glass, 10% Fly Ash 2 with 10% Q-glass, and 10% Fly Ash 2 with 10% UV-glass). These three sets of beams were used to investigate the flexural performance of beams with different glass types in conjunction with a single fly ash. The control mixture without cement replacement served as a baseline for comparison between the other nine mixtures with cement replacement. A concrete testing matrix containing all ten mixtures and SCM replacement levels can be seen in Table 3.1. The 20% SCM replacement levels are based on the cement weight of the control mixture shown in Table 3.2.

## 3.2 Concrete Beam Design and Fabrication

The beams were fabricated with shear and flexural reinforcement to simulate a realistic reinforced concrete beam scenario. Preliminary flexural testing conducted at the University of Minnesota Duluth (UMD) used the same beam dimensions and reinforcing layout, making comparisons between previous studies consistent (Christiansen & Dymond, 2019). The beams were reinforced with uncoated No. 3 transverse shear stirrups placed at 4 in. on center along the length of the beam, for a total of 18 stirrups. The stirrup spacing prohibited a shear failure while encouraging a tension-controlled flexural failure. All of the stirrups were bent into a closed loop and placed in the beam to allow for a 0.75 in. clear cover. The stirrups were provided by Harris Rebar. The clear cover was in accordance with ACI 318 (2014) requirements for precast nonprestressed members manufactured under plant conditions. Dimensions of the stirrups can be seen in Figure 3.1 and their location within the beam can be seen in Figure 3.2. Three uncoated No. 3 bars were placed in a single longitudinal layer 8.7 in. ($d$) from the top of the beam to provide flexural reinforcement for resisting positive bending. Dayton Superior 0.75 in. tall slab bolsters were used to provide the required cover on the bottom of the beam. The bolsters came in 5 ft lengths, with legs at every 5 in. The bolsters were cut to 5 in. long sections, with a section of the bolster tied to the bottom of the stirrups at each end of the rebar cage and one section supporting the middle, as seen in Figure 3.2. The longitudinal reinforcement was cut to a 5 ft 11 in. length and was also provided by Harris Rebar. After considering the one-half bend diameter space required between the inside of the stirrup and the center of the outside

rebar, the longitudinal bars did not satisfy ACI 318 (2014) minimum reinforcement spacing of at least 1 in. Instead, the as-built transverse spacing between the longitudinal bars was approximately 0.75 in. Two round 0.25 in. diameter smooth bars were tied to the top corners of the stirrups for constructability of the rebar cage. A beam cross section in Figure 3.1 shows the location and spacing of the bars. Two lifting hooks placed in each beam were used for demolding and maneuvering the beams during testing. The lifting hooks were located approximately 1 ft 6 in. from each end of the beams and were tied to the inside of the stirrups as shown in Figure 3.2.

## 3.3 Materials

### 3.3.1 Cement

The cement used for each mixture was type I/II portland cement, with a specific gravity of 3.15. The cement was manufactured by Grupo Cementos de Chihuahua (GCC) of America in Rapid City, South Dakota. The material certification report is shown in Appendix A, Table A.1. The same source and batch of cement was used for all the beams and 3 in. by 6 in. cylinders to minimize the experimental error between mixtures. The cement met all ASTM C150 (2019) and C1157 (2017) requirements.

### 3.3.2 Supplementary Cementitious Materials

Two different fly ashes (Fly Ash 1 and Fly Ash 2) and three different glasses (W, Q, and UV) were used in different combinations in nine of the mixtures. Both Fly Ash 1 and Fly Ash 2 were Class F fly ash per ASTM C618 (2019). The chemical compositions of the fly ashes are shown in Table 3.3. The W-glass (container glass) and the UV-glass (plate glass) were classified as soda-lime glass. The UV-glass was originally two separate plate glasses (U-glass and V-glass); however, they were blended together due to their similar chemical composition to form UV-glass. The third type of glass was Q-glass, which was an electrical grade glass (E-glass). The composition of W, Q, and UV-glass are also shown in Table 3.3. The chemical compositions of the fly ashes and glasses were determined using x-ray fluorescence (XRF). All of the glasses were ground using a rod-mill until 90% of the particles were 45 μm or less. The glass particle size distribution was determined using a CILAS particle size analyzer. The particle size test results are provided

in Table 3.4. All of the SCMs were assumed to have a specific gravity of approximately 2.6 based on previous studies by Christiansen and Dymond (2019) that used the same SCMs.

### 3.3.3 Coarse Aggregate

Coarse aggregate was donated by Ulland Brothers, Inc. from a local source near Duluth, Minnesota. The coarse aggregate was clean (minimal debris and dust) with a nominal size of 0.75 in. The specific gravity and absorption of the coarse aggregate were determined following ASTM C127 (2015) procedures. The oven-dry (OD) specific gravity, saturated-surface-dry (SSD) specific gravity, and apparent specific gravity were 2.64, 2.67, and 2.73, respectively. The absorption was calculated to be 1.2%. ASTM C29 (2017) was used to determine the bulk density of the coarse aggregate, which was 100 pcf. The coarse aggregate gradation was determined in accordance with ASTM C136 (2014) and is shown in Figure 3.3.

### 3.3.4 Fine Aggregate

The fine aggregate (sand) was also provided by Ulland Brothers, Inc. from the same source as the coarse aggregate with a nominal size of 0.187 in. (No. 4 sieve). The OD specific gravity (2.71), SSD specific gravity (2.75), apparent specific gravity (2.82), and absorption (1.4%) were determined in accordance with ASTM C128 (2015). Additionally, the fineness modulus of the fine aggregate was determined to be 2.71 per ASTM C136 (2014).

### 3.3.5 Steel Reinforcement

All of the transverse and longitudinal No. 3 reinforcing bars were grade 60 (i.e., minimum yield strength of 60,000 psi) and conformed to ASTM A706 (2016). Yield strength testing was performed on pieces of the longitudinal reinforcement using three, 8 in. long specimens in accordance with ASTM E8 (2016), which resulted in an average yield strength of 90,000 psi. Stress-strain curves for the three specimens are seen in Figure 3.4. The maximum stress is shown on each curve; these data were used to calculate the average.

## 3.4 Mixing Procedures

A mixture design spreadsheet was created using the absolute volume method to determine the required quantities of coarse aggregate (CA), fine aggregate (FA), cement, SCMs, and water for each of the ten mixtures. Initial trial batches produced concrete with a 12 in. slump, which was not the target slump of 3±0.75 in. The total water content for all mixtures was reduced by 45 lb per cubic yard of concrete, based on the CA being classified as "round" by the Portland Cement Association (PCA) (2016). Subsequent trial batches with adjusted water contents achieved the desired slump.

A total volume of 9.6 $ft^3$of concrete was required to fabricate three beams and 15 cylinders for each mixture. This volume of concrete could not be mixed in a single mixer available at UMD because the actual concrete mixing capacity of a mixer is around half of the manufacturers' specified volume due to exceeding the weight capacity of the mixer. Therefore, the mixture ingredients were split proportionally into two mixers, a 12 $ft^3$ mixer and a 9 $ft^3$ mixer. The 12 $ft^3$ mixer had the capacity to hold the ingredients needed to fabricate two beams (6 $ft^3$), while the material for the other beam and 15 cylinders (3.6 $ft^3$) were mixed within the 9 $ft^3$ mixer.

Several tasks were completed before mixing began. The formwork was inspected for damage before each mixture and inner length, height, and width dimensions were verified. Kleen Kote form oil was applied to the bottom and both sides of the formwork to prevent concrete from adhering to the plywood. Additionally, form oil was applied to the 15, 3 in. diameter by 6 in. tall cylinder molds. Preassembled rebar cages were centered within the formwork and adequate concrete cover was provided around the rebar cage. Moisture contents were calculated from representative FA and CA samples, which were oven-dried at 230 °F for 12-16 hours in accordance with ASTM C566 (2013). The mixture design spreadsheet calculated the required quantities of CA, FA, cement, water, and SCMs. Material quantities for each mixture are seen in Appendix A, Table A.2.

Machine mixing of the concrete in both mixers was completed in accordance with ASTM C192 (2013). The CA was weighed and distributed into both the 12 $ft^3$ and 9 $ft^3$ mixers. The other materials were pre-weighed and stored in 5-gallon buckets. Concrete

was mixed in the 12 $ft^3$ mixer first, and during this time materials for the 9 $ft^3$ mixer were covered with plastic sheeting to prevent water evaporation. With the mixer turned off, a portion of the water (approximately a third) was added to the mixer. The mixer was started, coating the CA and inside of the mixer with water. The mixer ran for 30-60 seconds before the FA was added. After the FA was loaded in the mixer, the cement, SCMs, and most of the water (approximately 5 lb of water was set aside for later use) were incorporated into the mixer and mixed for 3 minutes. The mixer was turned off after 3 minutes and the concrete was allowed to rest for 3 minutes. After the resting period, the concrete was mixed for a final 2 minutes. During these 2 minutes, the remaining water was added, as necessary, until the approximate concrete slump was achieved as determined through visual observation. The slight change in water demand between mixtures was caused by the different SCMs and their properties (e.g., surface area, particle shape); consequently, some mixtures required less water. These variances in water demand were not accounted for in the mixture design spreadsheet. However, the adjusted water-to-cementitious material ratios are provided in Table 3.5. After the final 2 minutes of mixing, tests to obtain fresh concrete properties were performed and the results were recorded. Two concrete beams were cast into the formwork from the 12 $ft^3$ mixer. The same mixing procedures were followed for fabrication of the other beam and 15 cylinders using the 9 $ft^3$ mixer immediately after the casting of the two initial beams.

## 3.5 Fresh Concrete Properties

Tests to obtain fresh concrete properties including slump, air content, unit weight, and temperature were performed on all ten concrete mixtures and for both mixers in accordance with ASTM C143 (2015), ASTM C231 (2017), ASTM C138 (2017), and ASTM C1064 (2017), respectively. Fresh concrete properties were recorded for each mixture as shown in Table 3.5.

## 3.6 Casting of the Concrete Specimens

Concrete was shoveled from the mixer and placed into the formwork until a uniform layer of approximately 3 in. of concrete was distributed over the length of the beam mold.

The concrete was vibrated with a Northrock internal vibrator conforming to ASTM C192 (2016), with at least 9000 vibrations per minute (150 Hz), until the surface of the concrete appeared smooth. The internal vibrator was removed slowly to prevent entrapping air within the concrete. The concrete was vibrated in two, 3 in. lifts at 6 in. increments along the length of the beam. Care was taken not to over vibrate the concrete in order to minimize aggregate segregation within the beam. The top surfaces of the beams were finished to provide a smooth, uniform bearing surface for testing. Additionally, concrete cylinders were constructed with three lifts of concrete, and each lift was tamped 25 times for consolidation of the concrete. Per ASTM C39 (2018), 3 in. diameter concrete cylinders are required to have two lifts of concrete rather than three. Other than this slight variation from ASTM procedures, the concrete cylinders were fabricated according to ASTM specifications. The top surfaces of the concrete cylinders were then struck flush with the cylinder molds. Average concrete densities for each mixture are shown in Appendix A, Table A.4. However, there was not enough concrete to make three, 180-day cylinders for the initial control mixture; therefore, a separate small batch of concrete was created to determine the 180-day compressive strength for the 100PC mixture using three cylinders. Material quantities and fresh concrete properties of these three cylinders can be seen in Table 3.6 and Table 3.7, respectively.

## 3.7 Curing of the Concrete

Concrete beams and cylinders were moist cured in accordance to ASTM C192 (2016). For the first 24 hours after casting, the formwork containing the beams was covered with wet burlap and plastic sheeting to prevent water from evaporating. The beams were demolded and labeled after 24 hours. The beams were labeled according to the type(s) of SCMs within the concrete and, additionally, they were labeled corresponding to the mixer in which the concrete came from. Beams labeled "O" were from the orange mixer (12 $ft^3$) and, beams labeled "R" were from the red mixer (9 $ft^3$). Beam labeling conventions are shown in column one of Table 3.1. Once demolded, the concrete beams were draped in wet burlap and plastic sheeting and were stored in the UMD structures laboratory at room

temperature for 90 days until testing. The burlap was wetted as needed throughout the 90 days.

The concrete cylinders were cured separately from the beams in a curing chamber with a relative humidity of 98% at a temperature of 73.4 °F (23 °C). The cylinders were demolded and labeled 24 hours after casting. The concrete cylinders were left in the curing chamber until they were tested at 1, 7, 28, 90, and 180 days. In hindsight, curing the cylinders in the same environment as the concrete beams may have minimized any potential sources of error between the data collected from the beams and cylinders.

## 3.8 Test Setup, Instrumentation, and Procedures

### 3.8.1 Flexural Strength Test Setup

The test beams were simply supported by a steel pin-and-roller, with 1.5 in. of bearing on each end of the beam. The clear span between supports was 6 ft for all tests. The beams were centered along their longitudinal and transverse axes under a single actuator to minimize eccentric loading. A W8x31 spreader beam attached to the hydraulic actuator applied the force at two, third-point locations along the top compression flange of the concrete beam in conformance with ASTM C78 (2018). The two point loads were applied along the top of the beam using additional steel pins and rollers, as shown in Figure 3.5. Leather/rubber strips were used between all pin/roller points and the concrete surfaces to distribute the applied load uniformly against any concrete imperfections. The pins and rollers uniformly applied the load over the entire 6 in. width of the beam. The actuator was fixed in the transverse direction to prevent movement during testing. Additionally, the steel load frame was anchored to the UMD structures laboratory floor. To prevent interference with the spreader beam, all of the lifting hooks were cut off using a grinder prior to testing the beams.

### 3.8.2 Testing Instrumentation and Data Acquisition

A linear variable differential transformer (LVDT) and a load cell within the actuator determined the displacement and applied load, respectively, during the testing of each beam. The applied load was measured by an Interface model 1000 fatigue rated load cell, with a load capacity of 100 kips. The location of the load cell on the actuator is shown in

Figure 3.5. The load cell and LVDT collected data at 10 samples per second (10 Hz). The data were recorded using a Shore Western control system throughout the duration of the testing and stored via a text file. The text files were converted to Microsoft Excel files for data analysis. Additionally, the displacement and crack patterns from the flexural failure of each beam were photographed for visual comparisons after the beams had failed.

### 3.8.3 Flexural Strength Test Procedure

The dimensions of each beam were recorded prior to testing; three measurements were taken and averaged for both the width and height of each beam as shown in Table A.3. The measurements were taken at mid-span and third-points of the beams, since flexural failure was anticipated to occur near the mid spans of the beams. The beams were aligned under the actuator and a photograph was taken of the beam setup before each test. The actuator was lowered until contact was made between the spreader beam and the top pin and roller, which is when approximately 50-100 lb was applied. The load cell and LVDT were tared before beginning the test. The load was applied at a rate of 0.001 in./sec, based on a desired test time of approximately 30 minutes. The average testing time for all of the beams was approximately 23 minutes.

The concrete beams were visually inspected for initial cracking and the load at which flexural cracking occurred was recorded. The applied load was stopped after the concrete on the top compression flange crushed and a peak loading was achieved. The load and displacement were recorded while the actuator was retracted. Both sides of the beam were examined to ensure similar failure patterns had occurred, and cracks were traced with black permanent marker to help distinguish the crack patterns after unloading; another photograph was taken of each beam after failure with all of the cracks marked. The before and after photographs for each beam are in Appendix C. Photographs documenting the post-test cracking pattern of the top, side, and bottom of each beam are provided in Appendix D.

## 3.9 Modulus of Elasticity Testing

Modulus of elasticity testing could not be completed on the 3 in. diameter concrete cylinders used for compressive strength testing because the available modulus of elasticity

testing apparatus was for 4 in. diameter cylinders. Therefore, 4 in. diameter by 8 in. long concrete cylinders were fabricated for modulus of elasticity testing. The 4 in. diameter concrete cylinders were fabricated with different cement than the 3 in. diameter concrete cylinders and the flexural beams due to a shortage of the original cement. Besides using different cement, the fine aggregates, coarse aggregates, and SCMs remained the same in all concrete specimens within this research and were proportioned the same as the original mixtures. The cylinders were mixed, cast, and cured using the procedures outlined in Section 3.4, 3.6, and 3.7, respectively. Additionally, fresh concrete properties were performed as stated in Section 3.5. Fresh concrete properties can be seen in Table 3.8. The modulus of elasticity testing was performed according to ASTM C469 (2014).

Table 3.1. Matrix of concrete beams tested.

| Concrete Mixtures | Soda-lime Container (W) | E-Glass (Q) | Soda-lime Plate (UV) | Fly Ash 1 | Fly Ash 2 | Number of Beams |
|---|---|---|---|---|---|---|
| Control (100% PC) 100PC | - | - | - | - | - | 3 |
| 20W | 20% | - | - | - | - | 3 |
| 20Q | - | 20% | - | - | - | 3 |
| 20UV | - | - | 20% | - | - | 3 |
| 20FA1 | - | - | - | 20% | - | 3 |
| 20FA2 | - | - | - | - | 20% | 3 |
| 10W10FA2 | 10% | - | - | - | 10% | 3 |
| 10Q10FA2 | - | 10% | - | - | 10% | 3 |
| 10UV10FA2 | - | - | 10% | - | 10% | 3 |
| 10W10FA1 | 10% | - | - | 10% | - | 3 |

Table 3.2. Control mixture material quantities for 9.6 $ft^3$ of concrete.

| Material | Quantity (lb) |
|---|---|
| Water | 102.4 |
| Portland Cement | 248.4 |
| Coarse Aggregate | 593.4 |
| Fine Aggregate | 492.9 |

Table 3.3. Chemical composition of the portland cement, fly ashes, and glasses as determined by XRF; values in weight percent oxide.

| Material | Oxides | | | | | | | | | | LOI | Sum of Oxides | $Na_2O_{eq}$ |
|---|---|---|---|---|---|---|---|---|---|---|---|---|---|
| | $SiO_2$ | $Fe_2O_3$ | $Al_2O_3$ | CaO | $Na_2O$ | MgO | $K_2O$ | $TiO_2$ | $P_2O_5$ | SrO | | | |
| **PC** | 20.20 | 3.30 | 4.60 | 64.00 | 0.12 | 1.20 | 0.70 | - | - | - | 1.7 | 28.1 | 0.58 |
| **Fly Ash 1** | 54.81 | 5.91 | 16.77 | 12.56 | 1.47 | 4.29 | 2.73 | 0.65 | 0.20 | 0.25 | 0.70 | 77.49 | 0.55 |
| **Fly Ash 2** | 51.10 | 7.74 | 13.10 | 15.90 | 3.34 | 3.63 | 2.64 | 0.86 | 0.16 | 0.40 | - | 71.94 | 5.08 |
| **W** | 70.50 | 1.47 | 1.84 | 13.20 | 10.60 | 1.13 | 0.88 | 0.08 | 0.00 | 0.03 | - | 73.81 | 11.18 |
| **Q** | 61.30 | 12.64 | 0.36 | 21.90 | 0.81 | 2.88 | 0.05 | 0.09 | 0.07 | 0.02 | 1.33 | 74.30 | 0.84 |
| **UV** | 72.56 | 0.00 | 0.40 | 8.72 | 12.55 | 3.34 | 0.09 | 0.11 | 0.01 | 0.01 | 0.06 | 72.96 | 12.61 |

Table 3.4. Glass particle size information determined by laser particle size analysis; all values in microns.

| Percent of Particles Less than Diameter | Glass Type | | |
|---|---|---|---|
| | **W** | **Q** | **UV** |
| **d10** | 1.83 | 2.04 | 2.26 |
| **d50** | 10.11 | 11.12 | 13.56 |
| **d90** | 32.47 | 26.74 | 28.23 |

Table 3.5. Fresh concrete properties and adjusted water to cementitious material ratios after accounting for the water withheld from mixing.

| Concrete Mixtures* | Mixer "O"(12 ft$^3$) "R" (9 ft$^3$) | Concrete Slump (in.) | Concrete Air Content (%) | Concrete Temp. (°F) | Concrete Unit Weight (pcf) | W/CM |
|---|---|---|---|---|---|---|
| 100PC (Control) | O | 3.50 | 2.6 | 69.5 | 150.1 | 0.42 |
| | R | 3.75 | 2.6 | 67.5 | 152.0 | 0.42 |
| 20FA1 | O | 3.75 | 2.7 | 73 | 150.9 | 0.40 |
| | R | 2.50 | 2.3 | 71.8 | 151.7 | 0.36 |
| 20FA2 | O | 4.25 | 2.8 | 72 | 149.3 | 0.40 |
| | R | 3.50 | 2.1 | 70.8 | 152.1 | 0.37 |
| 20Q | O | 2.5 | 2.0 | 70.9 | 151.7 | 0.41 |
| | R | 2.75 | 2.4 | 66.1 | 151.7 | 0.42 |
| 20W | O | 3.5 | 2.8 | 62.4 | 148.9 | 0.40 |
| | R | 3.5 | 2.8 | 58.2 | 148.9 | 0.40 |
| 20UV | O | 2.75 | 2.1 | 71.6 | 149.3 | 0.42 |
| | R | 2.0 | 2.2 | 70.1 | 151.3 | 0.37 |
| 10Q10FA2 | O | 3.5 | 2.1 | 67.9 | 151.3 | 0.39 |
| | R | 3.25 | 2.4 | 64.8 | 151.7 | 0.40 |
| 10W10FA2 | O | 2.25 | 2.6 | 72.2 | 151.7 | 0.39 |
| | R | 2.5 | 2.6 | 70.8 | 151.3 | 0.39 |
| 10UV10FA2 | O | 3.75 | 2.7 | 71.7 | 150.1 | 0.37 |
| | R | 2.25 | 2.3 | 69.6 | 150.9 | 0.31 |
| 10W10FA1 | O | 3.75 | 2.9 | 60.4 | 149.3 | 0.39 |
| | R | 3.25 | 2.3 | 59.2 | 150.1 | 0.40 |

*Concrete mixtures were named according to the type of SCM and the percentage of replaced cement. For example, the mixture 10W10FA2 had a cement replacement of 10% W-glass and 10% Fly Ash 2. The beams were also labeled according to which mixers they came from.

Table 3.6. Material quantities for the three, 180-day control mixture (100PC) cylinders.

| Materials | (lb.) |
|---|---|
| Water Content | 13.3 |
| Portland Cement Content | 31.2 |
| Coarse Aggregate Content | 74.8 |
| Fine Aggregate Content | 61.2 |

Table 3.7. Fresh concrete properties and water to cement ratios for the three, 180-day control cylinders.

| Concrete Mixtures | Concrete Slump (in.) | Concrete Air Content (%) | Concrete Temp. (°F) | Concrete Unit Weight (pcf) | W/C* |
|---|---|---|---|---|---|
| 100PC (Control) | 2.50 | 2.9 | 67.8 | 150.5 | 0.42 |

*Adjusted water-to-cement ratio after accounting for water withheld from mixing.

Table 3.8. Fresh concrete properties for each of the ten modulus of elasticity mixtures.

| Concrete Mixtures | Concrete Slump (in.) | Concrete Air Content (%) | Concrete Temp. (°F) | Concrete Unit Weight (pcf) |
|---|---|---|---|---|
| 100PC (Control) | 2.50 | 1.9 | 64.5 | 152.5 |
| 20FA1 | 2.25 | 2.0 | 64.5 | 152.1 |
| 20FA2 | 3.25 | 1.9 | 62.6 | 151.7 |
| 20Q | 2.25 | 2.0 | 58.8 | 151.3 |
| 20W | 2.25 | 2.2 | 59.5 | 152.1 |
| 20UV | 3.0 | 2.9 | 50.3 | 151.3 |
| 10Q10FA2 | 3.5 | 2.1 | 51.3 | 150.9 |
| 10W10FA2 | 3.0 | 1.8 | 64.5 | 151.7 |
| 10UV10FA2 | 3.5 | 2.9 | 60.5 | 150.9 |
| 10W10FA1 | 3.5 | 1.7 | 64.5 | 151.7 |

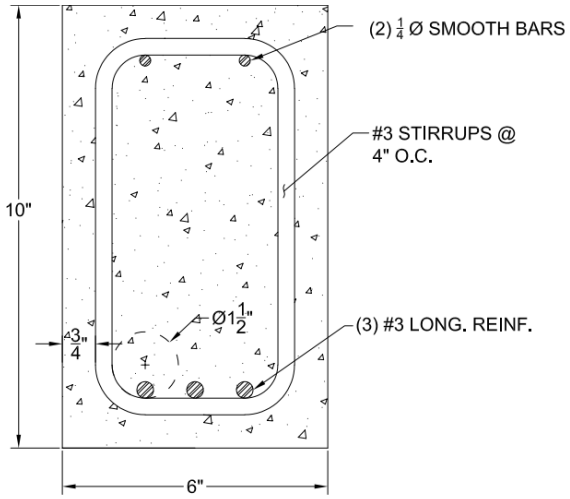


Figure 3.1. Concrete beam cross section showing steel reinforcement and dimensions.

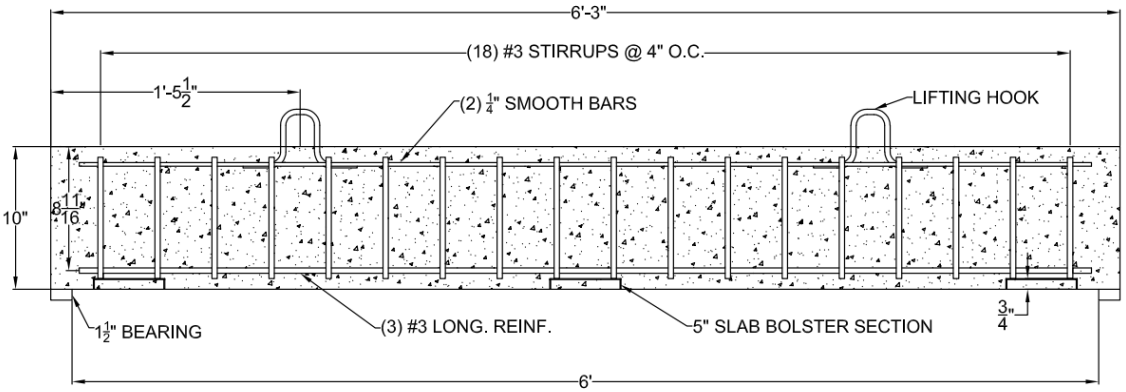


Figure 3.2. Concrete beam elevation showing the steel reinforcement layout.

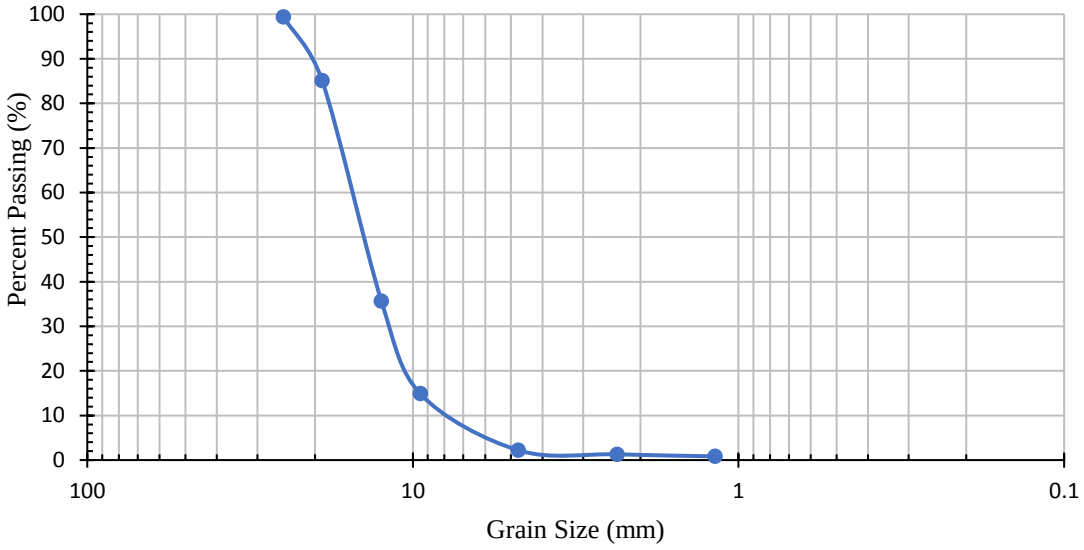


Figure 3.3. Coarse aggregate gradation curve.

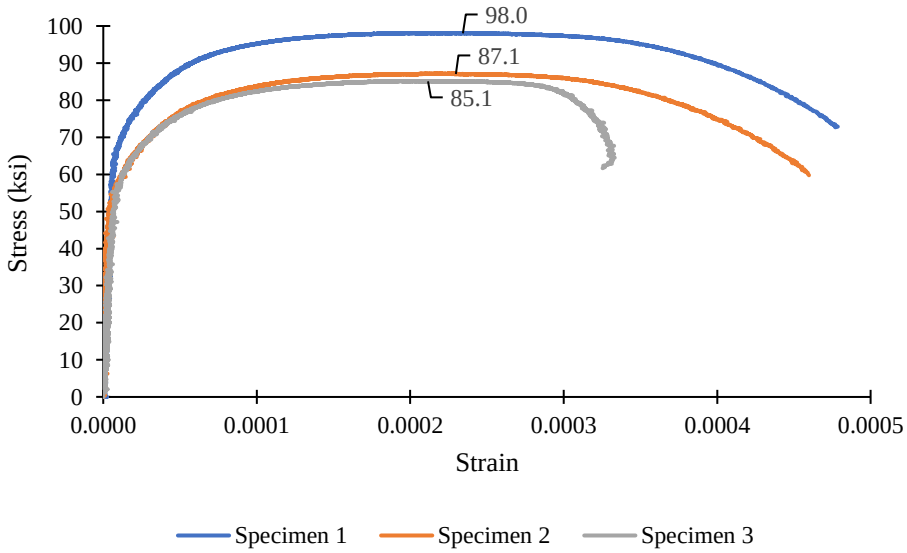


Figure 3.4. Longitudinal steel reinforcement stress-strain curves for three test specimens.

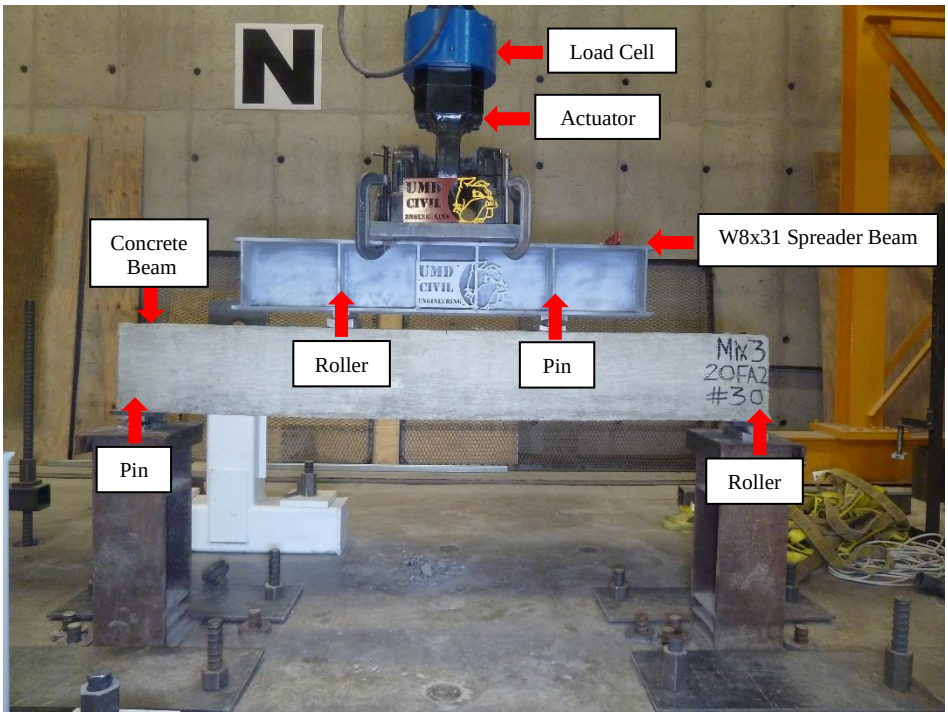

Figure 3.5. Concrete beam test setup.

# Chapter 4: Results and Discussion

Compressive strength data were collected at 1, 7, 28, 90, and 180 days after casting the cylinders. Three cylinders were tested per concrete mixture on each of these days, and the three values were averaged to obtain a single average compressive strength. Cylinder compressive strength results are shown in Figure 4.1. All cylinders were fabricated from concrete out of the 9 $ft^3$ mixer. Three beams were tested in flexure for each of the ten different concrete mixtures; a total of 30 beams were tested. Applied moment was calculated from the applied force data collected during the third-point loading. The modulus of elasticity was obtained at 90 days after casting by averaging the data from the two tests on a single specimen. The modulus of elasticity results are not directly comparable to the beam or cylinder results because the cement used for the modulus of elasticity cylinders was different than the cement used in the flexural beams and compressive strength cylinders. The following section presents and discusses the compressive strength, flexural strength, and modulus of elasticity results.

## 4.1 Compressive Strength

### 4.1.1 Control Cylinders

One day after casting, control cylinders (100PC) had an average compressive strength of 3,720 psi. The average compressive strength for the control cylinders increased to 6,790 psi at 7 days, 7,970 psi at 28 days, and 9,760 psi at 90 days. However, at 180 days, the average compressive strength for the control cylinders decreased from the 90-day compressive strength (9,760 psi) to 8,860 psi. This was likely attributed to there not being enough concrete to make three, 180-day cylinders for the initial control mixture and having to test three, 180-day cylinders from a separate small batch of control concrete. The average compressive strength data obtained from the control cylinders are used as a baseline for comparison to the other nine mixtures.

### 4.1.2 Control Cylinders Compared with 20% Fly Ash Replacement Cylinders

Compared with the control cylinders, the 20FA1 cylinders had at least 90% compressive strength during all test days (1, 7, 28, 90, and 180 days). At 7 and 180 days,

20FA1 cylinders had 1% and 10% higher compressive strengths than control cylinders. Similarly, besides one-day strengths, 20FA2 cylinders had at least 99% compressive strength compared to control cylinders, with 7 and 180-day compressive strength cylinders being 3% and 10% higher than control cylinders, respectively. Even though the SAI is only measured at 7 and 28 days per ASTM C618 (2019), 20FA1 and 20FA2 specimens easily passed the SAI requirement of 75% compressive strength of control cylinders on all test days. There was not a substantial difference in compressive strength between either of the concrete mixtures with fly ashes and the control concrete mixture at any of the test days. Often, Class F fly ashes (20FA1) will reduce early concrete compressive strength and increase long-term strength when compared to specimens containing 100% portland cement due to the silica content and the delayed pozzolanic reaction. However, both Fly Ash 1 and Fly Ash 2 had moderate amounts of calcium oxide (12.56% and 16.30%, respectively) which may have offset the delayed pozzolanic reaction caused by the silica. Average compressive strengths for control cylinders and fly ash cylinders are compared in Figure 4.2.

### 4.1.3 Control Cylinders Compared with 20% Q-, W-, or UV-Glass Replacement Cylinders

Compressive strength data from the control mixture and mixtures with 20% fly ash were used as a baseline for comparison with the 20% glass replacement specimens. The 20Q cylinders had 80-85% of the compressive strength of the control cylinders at 1, 7, 28, and 90 days. The 20Q cylinders had 4% higher compressive strength at 180 days compared to the compressive strength of the control cylinders. These results were unexpected for Q-glass specimens; research demonstrated E-glass specimens had comparable or higher compressive strengths compared to control cylinders as early as 28 days (Chen et al., 2006; Christiansen & Dymond, 2019). Additionally, Q-glass had 61.30% silica content, which should have improved long-term strength through a strong pozzolanic reaction. It was also expected that the high calcium oxide content (21.90%) of Q-glass would offset the initial strength delay caused by the pozzolanic reaction. However, the 20Q cylinders had 80% and 85% of the compressive strength of the control cylinders at 1 and 7 days, respectively.

The particle size distribution (90% less than 26.74 μm) was well under 45 μm as recommended in the literature for strong pozzolanic reactivity. Although, previous research demonstrated increased concrete compressive strength when concrete was made with E-glass at replacement levels of 40-50% (higher than 20%) (Chen et al., 2006). In short, it would appear that the Q-glass had a moderate pozzolanic reaction.

Compressive strength results for 20W specimens were similar to those from 20Q cylinders. 20W cylinders had a very low compressive strength compared to results from control cylinders at 1 day (38% less), which may have been a consequence of the lower calcium oxide content (8.80%) of the W-glass. Additionally, 20W cylinders had lower compressive strengths at 7, 28, 90, and 180 days compared to the compressive strength results from control cylinders (3-13% lower). W-glass had the largest particle sizes of the glasses (90% less than 32.47 μm) but it was well below the 45 μm size recommendation noted in the literature. Additionally, W-glass had a higher silica content compared to the other glasses (65.30%). 20W cylinders likely had a moderate pozzolanic reaction. On the other hand, at 7, 28, and 180 days, 20UV cylinders had higher compressive strengths compared to those of the control cylinders (106-111% higher). Even at 1 and 90 days, the compressive strengths were almost the same as those form the control cylinders, 87% and 91%, respectively. It is likely that 20UV cylinders had a strong pozzolanic reaction based on the silica content of the UV-glass, which had the highest silica content out of all of the SCMs (72.56%). A strong pozzolanic reaction from the silica rich UV-glass may have contributed to the higher compressive strengths. Additionally, UV-glass had the lowest calcium oxide content (8.72%) of the SCMs, which could explain the 87% compressive strength of the control cylinders at one-day. Even with high silica content and low calcium oxide content, 20UV specimens had higher compressive strengths than control cylinders as early as 7 days. UV-glass had 90% of the particles less than 28.23 μm in size.

All of the 20% glass replacement specimens satisfied the ASTM C618 (2019) SAI requirement at 7 and 28 days. Besides 20W cylinder compressive strengths at 1 day, the 20% glass specimens had at least 75% of the compressive strength as control cylinders at all test days. Average compressive strengths for control cylinders and glass cylinders are

compared in Figure 4.3. Additionally, since fly ash and control specimens had similar compressive strengths at each test day, 20% glass replacement specimens performed about the same compared to the fly ash specimen as they did to the control specimens.

### 4.1.4 Control Cylinders Compared with the Ternary Blend Cylinders

The 10Q10FA2 specimens had the same or higher compressive strength compared to control specimens at 1, 28, 90, and 180 days (0-15% higher); the compressive strength was 98% of the control cylinders at 7 days. These results were expected from specimens containing Q-glass based on the literature, unlike the results demonstrated by the 20Q specimens. It is difficult to determine why the Q-glass performed 20-25% better in a ternary blend rather than by itself, but use of ternary blends have been shown to increase concrete strength compared to binary blends (Chindaprasirt & Rukzon, 2014; Slag Cement Association (SCA), 2019). Excluding 1-day compressive strengths, the remaining ternary blends (10W10FA2, 10UV10FA2, and 10W10FA1) had 86-117% of the compressive strength of the control cylinders at all other test days. 1-day strengths for 10W10FA2, 10UV10FA2, and 10W10FA1 had 97%, 76%, and 61% of the compressive strength of the control cylinders, respectively. Overall, the four ternary blend mixtures had relatively similar compressive strength results compared to control cylinders throughout all the testing days, with the vast majority of ternary blend specimen being at least 90% of the compressive strength of the control cylinders at most test days. All of the ternary blend specimens, not including 10W10FA1 at 1-day, had at least 75% compressive strength of the control cylinders on all test days (1, 7, 28, 90, and 180 days). Besides 10UV10FA2 concrete cylinders, which had lower compressive strengths than 20UV cylinders, concrete with ground glass typically performed slightly better in a ternary blend rather than their binary blend counterparts. This was corroborated by results from previous research that suggested concrete mixtures made with a ternary blend increased compressive strength compared to 100% portland cement mixtures (Chindaprasirt & Rukzon, 2014; Erdem & Kirca, 2008). Furthermore, two ternary blends, 10Q10FA2 and 10W10FA1, had compressive strengths over 10,000 psi at 180 days, which is significant considering ACI (2019) defines high-strength concrete as compressive strength over 6,000 psi. Average

compressive strengths form the control cylinders and ternary blend cylinders are compared in Figure 4.4.

### 4.1.5 All Cylinders Containing W-glass

1-day after casting, the 20W and 10W10FA1 cylinders had similar compressive strength results that were about 7% apart, while 10W10FA2 cylinders had higher compressive strengths than both 20W and 10W10FA1 mixtures (35% higher). At 7, 28, and 90 days, all the W-glass specimens (20W, 10W10FA1, and 10W10FA2) had compressive strengths within 7%, 4%, and 4% of each other, respectively. Compressive strengths began to differ at 180 days where 10W10FA1 cylinders had the highest compressive strength, which was 17% higher than results from 20W cylinders and 13% higher than results from 10W10FA2 cylinders. In summary, W-glass in a ternary blend (10W10FA1 and 10W10FA2) typically had higher compressive strengths than the binary mixture (20W), which was consistent with the literature on ternary and binary blends (Chindaprasirt & Rukzon, 2014; Erdem & Kirca, 2008). However, all W-glass specimens had similar compressive strength results for all of the test days. Average compressive strengths from control cylinders and W-glass specimens are compared in Figure 4.5.

### 4.1.6 All Cylinders Containing Fly Ash 2

The 1-day compressive strength results varied amongst the Fly Ash 2 specimens. Both 10Q10FA2 and 10W10FA2 cylinders had similar compressive strengths at 1-day (4% different). Both of these mixtures had approximately 12% and 23% higher compressive strengths compared to results from the 20FA2 and 10UV10FA2 cylinders at 1-day, respectively. At 7 and 28 days, all Fly Ash 2 specimens had compressive strengths within 11% and 7% of each other, respectively. Similar trends were observed between 90- and 180-day compressive strengths, where the 10Q10FA2 cylinders had the highest compressive strength, followed by 20FA2, 10UV10FA2, and lastly 10W10FA2 cylinders. At 90 days, 10Q10FA2 cylinders had a compressive strength 6% higher than 20FA2, 14% higher than 10UV10FA2, and 19% higher than 10W10FA2. Similarly, at 180 days, 10Q10FA2 had a compressive strength 4% higher than 20FA2, 5% higher than 10UV10FA2, and 12% higher than 10W10FA2. For the most part Fly Ash 2 ternary blends

did not perform better than specimens made with the binary blend of Fly Ash 2. Fly Ash 2 likely had a stronger pozzolanic reaction than the glasses, which is why specimens with 20% Fly Ash 2 performed better than 10% Fly Ash 2 and 10% glass specimens. Average compressive strengths for control cylinders and Fly Ash 2 specimens are compared in Figure 4.6.

### 4.1.7 Statistical Analysis

An independent sample *t*-test was performed to determine if the compressive strengths of the nine SCM mixtures were significantly greater than the compressive strength of control cylinders. The left-tailed test was set up with a null hypothesis shown in Equation 4.1 and an alternative hypothesis in Equation 4.2. A left-tailed *t*-test was used because the compressive strength data from some of SCM mixtures appeared to have higher compressive strengths from that of the control mixture.

Null Hypothesis: $H_0: \mu_1 - \mu_2 = 0$ Eq. 4.1

Alternative Hypothesis: $H_a: \mu_1 - \mu_2 < 0$ Eq. 4.2

The null hypothesis stated that there was no difference between the compressive strength of control cylinders and each of the 20% SCM replacement cylinders. Additionally, the null hypothesis would not be rejected if the control cylinders had significantly higher compressive strengths than SCM mixtures. The alternative hypothesis stated that the SCM mixtures had significantly higher compressive strengths compared with control cylinders. The *t*-test used a significance level ($\alpha$) of 1%. P-values comparing the compressive strength of control cylinders to each of the nine SCM mixtures can be seen in Table 4.4. Results from compressive strength *t*-test data at 1 day showed that none of the SCM mixtures had significantly higher compressive strengths compared to control cylinders. However, 20UV and 20FA2 cylinders had significantly higher compressive strengths at 7 days. Similarly, 20UV cylinders had significantly higher compressive strengths than control cylinders at 28 days. At 90 days, 10Q10FA2 cylinders had significantly higher compressive strengths than control cylinders. Only one mixture (20W) did not have significantly higher compressive

strengths than control cylinders at 180 days. As expected, very few of the nine SCM mixture had significantly higher compressive strengths than control cylinders at 1 and 7 days, as the pozzolanic reaction often causes early strength delays. However, it was not expected that only one mixture (10Q10FA2) would have significantly higher compressive strength at 90 days as the pozzolanic reaction usually provides long-term strength. All but one mixture had significantly higher compressive strengths than control cylinders at 180 days. However, the three, 180-day control cylinders were from a separate batch of concrete than the 1, 7, 28, and 90-day control cylinders.

### 4.1.8 Summary

Excluding 180-day compressive strengths, there were not any clear trends that demonstrated the addition of SCMs resulted in long-term compressive strengths greater than the control cylinders. Results from the *t*-tests indicated that there were very few SCM mixtures that had significantly higher compressive strengths than control cylinders and, of those mixtures, none of them demonstrated consistently higher compressive strengths throughout all the test days. It is uncertain why long-term compressive strength was not improved with the pozzolanic reaction of the SCMs compared to control specimens. Additionally, due to the 180-day control cylinders not being from the same batch of concrete, it is difficult to say with any certainty that the SCM mixtures had increased long term compressive strength at 180 days compared to control cylinders. Although, for the most part, cylinders containing SCMs had similar compressive strengths as control cylinders at 7, 28, and 90 days (at least 85%). Compressive strengths for SCM mixtures 1 day after casting were typically less than that of the control cylinders, with some mixtures less than 75% of the control cylinders strength. In general, ternary blends with glass performed better than binary mixtures with glass. SAI percentages for each of SCM mixtures are summarized in Table 4.1.

## 4.2 Flexural Strength

### 4.2.1 Cracking Moment

The cracking moment for the beams in positive bending occurs when the tensile stress in the bottom of the beam exceeds the concrete tensile capacity, ultimately causing

the bottom of the beam to crack. After initiation of the first crack, the steel reinforcement in the bottom of the beam is engaged. The steel reinforcement resisted the tensile forces in the beam, while the uncracked concrete resisted compressive forces.

The control beams cracked at an applied moment of 5.9 kip-ft; this was approximately 5% less than the ACI calculated value of 6.2 kip-ft (calculated in Appendix E). The 20FA1 beams displayed higher cracking moments than control beams, between 6.9 to 8.0 kip-ft, while the 20FA2 beams had consistent cracking moments compared to each other at around 7.3 kip-ft. The average cracking moments for beams made with W-glass, Q-glass, and UV-glass were around 8.2, 7.6, and 7.1 kip-ft, respectively. However, before the testing of one of the UV-glass beams an accidental load was briefly applied to the beam, which subjected the beam to a 1.0 in. displacement. The loading was immediately unapplied; however, cracking moment data was lost due to the beam being subjected to such a large displacement. This beam is not reflected in the 7.1 kip-ft average (i.e., only two values were averaged). Additionally, the cracking moments were relatively similar between 10W10FA2, 10W10FA1, and 10UV10FA2 beams at a magnitude of 7.1, 7.3, and 7.6 kip-ft, respectively. The 10Q10FA2 beams cracked at less applied moment than other ternary blends (6.4 kip-ft). Overall, the mixtures with SCMs cracked at a higher applied moment compared to the control beams, but all of the beams cracked around a 0.1 in. displacement.

### 4.2.2 Average Peak Applied Moment

The peak moment for beams in positive bending is achieved when the compressive stress in the top flange exceed the compressive capacity of the concrete. This is visually determined when the compression flange of the concrete beam begins to crush and the applied moment drastically decreases.

The control beams reached an average peak applied moment of 21.5 kip-ft, which was 2% higher than the calculated ACI peak actuator applied moment of 21.1 kip-ft calculated in Appendix E. The 20FA1 beams reached a similar, but slightly higher (1% higher) average peak moment as the control beams, and the 20FA2 beams had 7% less flexural strength than the control beams. Considering the average peak applied moment for

the beams with 20% glass replacement levels, both the 20Q and 20W beams had higher averaged peak moments than the control beams, which were less than 1% and 4% higher, respectively. The 20UV beams were the only 20% glass replacement specimens that had lower flexural strengths (4% less) than control beams. As stated previously, one 20UV beam was subjected to an accidental loading, which could have affected the peak applied moment of that beam (20.8 kip-ft). However, the peak applied moment for this beam was still used in the calculation of the average peak applied moment for the 20UV beams. The average peak applied moments were similar for 10W10FA1, 10W10FA2, and 10UV10FA2 beams with corresponding values of 21.6, 21.1, and 21.0 kip-ft. Unfortunately, one of the 10W10FA2 beams was in the process of being tested before the actuator lost power, ultimately crushing the beam before peak moment was recorded. The data for this beam was not used in the calculation of average peak moment. The 10Q10FA2 beams had the lowest average peak applied moment of the ternary blend specimens at 20.4 kip-ft. 10W10FA1 beams were the only ternary blend beams that had higher flexural strengths (less than 1%) than control beams. Otherwise, the 10W10FA2, 10UV10FA2, and 10Q10FA2 beams all had 2-5% less flexural strength than the control beams. All of the peak applied moments along with average peak moments are shown in Table 4.2. Figures with applied moment versus displacement for each beam are shown in Appendix B.

The nine concrete mixtures with 20% SCM replacement levels had similar flexural strengths compared to concrete without SCMs, which may have been from the pozzolanic reaction of the SCMs. Four out of the nine mixtures with SCMs had higher flexural strengths than control beams. The remaining five SCM mixtures had a flexural strength within 6% of the flexural strength of the control beams. However, the flexural strength results were inconsistent with the compressive strength results. For example, the 20UV specimens had a higher compressive strength but a lower flexural strength than the 20W and 20Q specimens. Additionally, in general, the ternary blend specimens performed better than the binary blend specimens in regards to compressive strength but worse in regards to flexural strength. It is unclear why the results would be different between the compressive strength results and the flexural strength results, but one possible reason could be the

different curing conditions between the beams and cylinders. However, overall, both the flexural strength results and compressive strength results showed that mixtures containing SCMs performed similar to control mixtures without SCMs. A t-test was used to determine if the flexural strength results were statistically similar.

#### 4.2.2.1 Statistical Analysis

An independent sample *t*-test was performed to determine if there was any significant difference between the flexural strength of control beams and the flexural strength of the other nine SCM beams. The two-tailed test was set up with a null hypothesis shown in Equation 4.3 and an alternative hypothesis in Equation 4.4. The flexural strength data was similar between each of the mixtures so a two-tailed *t*-test would determine whether they were statistically similar.

Null Hypothesis: $H_0: \mu_1 - \mu_2 = 0$ Eq. 4.3

Alternative Hypothesis: $H_a: \mu_1 - \mu_2 \neq 0$ Eq. 4.4

The null hypothesis stated that there was no difference between the flexural strength of control beams and each of the 20% SCM replacement beams, while the alternative hypothesis stated there was a difference. The t-test used a significance level (α) of 1%. The results from the t-test concluded that all nine SCM mixtures did not have significantly different average flexural strengths than the control beams. This implies that the nine mixtures with 20% SCM replacement levels performed just as well as the control beams in terms of flexural performance. However, the pozzolanic reaction was not significant enough to improve flexural strength beyond the flexural strength of control beams. Even though the predictions that ground glass would improve flexural strength at 90 days compared to control beams was not true, all of the SCM mixtures statistically had the same flexural strength as the control beams. This suggested that soda lime glass, both container and plate, and E-glass could be used as a partial replacement for cement (a 20% replacement level was used in this study), either in a binary or ternary blend with fly ash) to obtain similar flexural strengths as concrete not incorporating SCMs. P-values

comparing the flexural strength of control beams to each of the nine SCM mixtures can be seen in Table 4.5.

## 4.3 Beam Displacement

The control beams had the largest average displacement (1.4 in.) out of all the mixtures at the peak applied moment. The 20FA1, 20Q, 20W, 10UV10FA2, and 10W10FA1 beams all had an average displacement of more than one in., but they still had 8-21% less average displacement than the control beams. Furthermore, four mixtures (20FA2, 20UV, 10Q10FA2, and 10W10FA2) had a one in. or less average displacement at the peak applied moment. Of these four mixtures, the 10W10FA2 and 20FA2 beams had the lowest displacement (0.9 in.), which was 36% less average displacement than the control beams. Individual beam displacements and average displacements are summarized in Table 4.2. The lower displacements of the mixtures containing SCMs may have been caused by differences in the modulus of elasticity. Therefore, it was predicted that the modulus of elasticity would be larger for concrete specimens with SCMs than concrete specimens without SCMs.

### 4.3.1 Modulus of Elasticity

Beam displacement depends on the modulus of elasticity ($E$), span length of the beam, moment of inertia ($I$), and location and magnitude of applied loading. All of these variables remained constant between all the beams except for the modulus of elasticity. Therefore, the modulus of elasticity was determined in ASTM C469 (2014) using 90-day concrete cylinders for each of the ten mixtures. The modulus of elasticity results demonstrated that all nine mixtures containing SCMs had an average modulus of elasticity that was higher than the control mixture without SCMs. The control cylinder had a modulus of elasticity of 6,400 ksi, while the SCM mixtures had modulus of elasticities ranging from 8,000-11,000 ksi. The modulus of elasticity for the control mixture was calculated in Appendix E to be 5,000 ksi per ACI 318-14 (2014).

Results from Ghavidel and Madandoust (2013) demonstrated that the modulus of elasticity for control cylinders were 440 ksi higher than specimens with rice husk ash and

glass even at 90 days. The data obtained in this research suggests that SCM specimens have higher modulus of elasticities compared to the control specimens, by as much as 4,500 ksi. However, higher modulus of elasticity values for the SCM mixtures corroborated with the displacement results obtained while flexural testing the beams. In other words, because the mixtures with SCMs had higher modulus of elasticity values (increased stiffness), the displacement of these beams were less at failure. Intuitively, it would seem that concrete with SCMs should have an increased concrete stiffness because the pozzolanic reaction converts CH into additional C-S-H, which creates a denser and seemingly stiffer concrete. The modulus of elasticity results are summarized in Table 4.3 and Figure 4.7.

Table 4.1. Strength Activity Index (SAI) of the nine SCM mixtures at 1, 7, 28, 90, and 180 days calculated based on the average control cylinder strengths at the same age.

| | Strength Activity Index (SAI) (%) | | | | |
|---|---|---|---|---|---|
| **Specimens** | **1 day** | **7 days** | **28 days** | **90 days** | **180 days*** |
| 20FA1 | 94 | 101 | 90 | 91 | 110 |
| 20FA2 | 87 | 103 | 99 | 99 | 110 |
| 20Q | 80 | 85 | 85 | 85 | 104 |
| 20W | 68 | 87 | 98 | 87 | 97 |
| 20UV | 87 | 106 | 107 | 91 | 111 |
| 10Q10FA2 | 101 | 98 | 100 | 106 | 115 |
| 10W10FA2 | 97 | 92 | 95 | 86 | 101 |
| 10UV10FA2 | 76 | 98 | 101 | 92 | 109 |
| 10W10FA1 | 61 | 94 | 98 | 90 | 117 |

*Control cylinders were from a different batch of concrete than 1, 7, 28, and 90-day concrete.

Notes:

(1) ASTM C618 (2019) only requires a SAI of at least 75% of the control cylinder strength at 7 and 28 days.

(2) Green highlight indicates a SAI equal to or greater than 100% of the control cylinder strength at 7 and 28 days.

(3) Red highlight indicates a SAI of less than 75% of the control cylinder strength at 7 and 28 days.

Table 4.2. Peak applied moments and corresponding displacements for all 30 beams, with average values and ranges between highest and lowest recorded values from each mixture.

| Specimens | Moment (kip-ft) | | | Displacement (in.) | | |
|---|---|---|---|---|---|---|
| | Peak | Avg. | Range | Peak | Avg. | Range |
| 100PC 1R | 20.3 | 21.5 | 2.0 | 1.4 | 1.4 | 0.0 |
| 100PC 2O | 22.3 | | | 1.4 | | |
| 100PC 3O | 21.9 | | | 1.4 | | |
| 20FA1 1R | 22.2 | 21.8 | 0.6 | 1.3 | 1.2 | 0.2 |
| 20FA1 2O | 21.6 | | | 1.1 | | |
| 20FA1 3O | 21.6 | | | 1.3 | | |
| 20FA2 1R | 20.3 | 20.1 | 0.6 | 0.9 | 0.9 | 0.1 |
| 20FA2 2O | 19.7 | | | 0.9 | | |
| 20FA2 3O | 20.3 | | | 1.0 | | |
| 20Q 1R | 22.4 | 21.6 | 0.3 | 1.2 | 1.1 | 0.3 |
| 20Q 2O | 21.1 | | | 0.9 | | |
| 20Q 3O | 21.2 | | | 1.1 | | |
| 20W 1R | 22.1 | 22.4 | 0.7 | 1.2 | 1.2 | 0.1 |
| 20W 2O | 22.4 | | | 1.1 | | |
| 20W 3O | 22.8 | | | 1.2 | | |
| 20UV 1R | 20.8 | 20.6 | 0.7 | 1.1 | 1.0 | 0.3 |
| 20UV 2O* | 20.8 | | | 0.7 | | |
| 20UV 3O | 20.1 | | | 1.1 | | |
| 10Q10FA2 1R | 20.2 | 20.4 | 0.8 | 0.9 | 1.0 | 0.1 |
| 10Q10FA2 2O | 20.1 | | | 1.0 | | |
| 10Q10FA2 3O | 20.9 | | | 1.0 | | |
| 10W10FA2 1R | 20.9 | 21.1 | 0.3 | 0.9 | 0.9 | 0.0 |
| 10W10FA2 2O** | ~~20.0~~ | | | ~~0.7~~ | | |
| 10W10FA2 3O | 21.2 | | | 0.9 | | |
| 10UV10FA2 1R | 21.4 | 21.0 | 1.2 | 1.1 | 1.2 | 0.2 |
| 10UV10FA2 2O | 21.3 | | | 1.3 | | |
| 10UV10FA2 3O | 20.2 | | | 1.2 | | |
| 10W10FA1 1R | 21.3 | 21.6 | 0.7 | 1.2 | 1.3 | 0.3 |
| 10W10FA1 2O | 21.5 | | | 1.3 | | |
| 10W10FA1 3O | 22.0 | | | 1.5 | | |

*An accidental load applied to the beam before testing.

**The accidental failure of the beam resulted in loss of peak data. The data were not included in the average or range values.

Note: The ACI peak actuator applied moment calculated in Appendix E is 21.1 kip-ft.

Table 4.3. Modulus of elasticity at 90 days for each of the ten mixtures along with a range between the two experimental values.

| Specimens | Modulus of Elasticity (ksi) 90-Day | Range (ksi) 90-Day |
|---|---|---|
| 100PC (Control) | 6,400 | 400 |
| 20FA1 | 9,100 | 250 |
| 20FA2 | 8,000 | 16 |
| 20Q | 9,100 | 280 |
| 20W | 8,300 | 200 |
| 20UV | 8,300 | 620 |
| 10Q10FA2 | 9,000 | 50 |
| 10W10FA2 | 8,400 | 80 |
| 10UV10FA2 | 11,000 | 420 |
| 10W10FA1 | 10,000 | 580 |

Table 4.4. P-values for each mixture based on compresive strength of the control cylinders.

| Specimens | P-Value | | | | |
|---|---|---|---|---|---|
| | 1 day | 7 days | 28 days | 90 days | 180 days |
| 20FA1 | 1.000 | 0.031 | 1.000 | 1.000 | 0.000 |
| 20FA2 | 1.000 | 0.005 | 0.993 | 0.978 | 0.000 |
| 20Q | 1.000 | 1.000 | 1.000 | 1.000 | 0.000 |
| 20W | 1.000 | 1.000 | 1.000 | 1.000 | 0.997 |
| 20UV | 1.000 | 0.001 | 0.000 | 1.000 | 0.000 |
| 10Q10FA2 | 0.012 | 0.997 | 0.975 | 0.000 | 0.000 |
| 10W10FA2 | 0.999 | 1.000 | 0.999 | 1.000 | 0.009 |
| 10UV10FA2 | 1.000 | 0.991 | 0.014 | 1.000 | 0.000 |
| 10W10FA1 | 1.000 | 1.000 | 1.000 | 1.000 | 0.000 |

Notes:

(1) Green highlight indicates that the SCM mixtures had significantly higher compressive strengths compared with control cylinders.

(2) No highlight indicates that there was no difference between the compressive strength of control cylinders and each of the 20% SCM replacement cylinders, or the control cylinders had significantly higher compressive strengths than SCM mixtures.

Table 4.5. P-values for each mixture based on the flexural strength of the control beams.

| Specimens | P-Value |
|---|---|
| 20FA1 | 0.68 |
| 20FA2 | 0.15 |
| 20Q | 0.93 |
| 20W | 0.27 |
| 20UV | 0.28 |
| 10Q10FA2 | 0.23 |
| 10W10FA2 | 0.32 |
| 10UV10FA2 | 0.49 |
| 10W10FA1 | 0.89 |

Note:

(1) there were no differences between the flexural strength of control beams and each of the 20% SCM replacement beams.

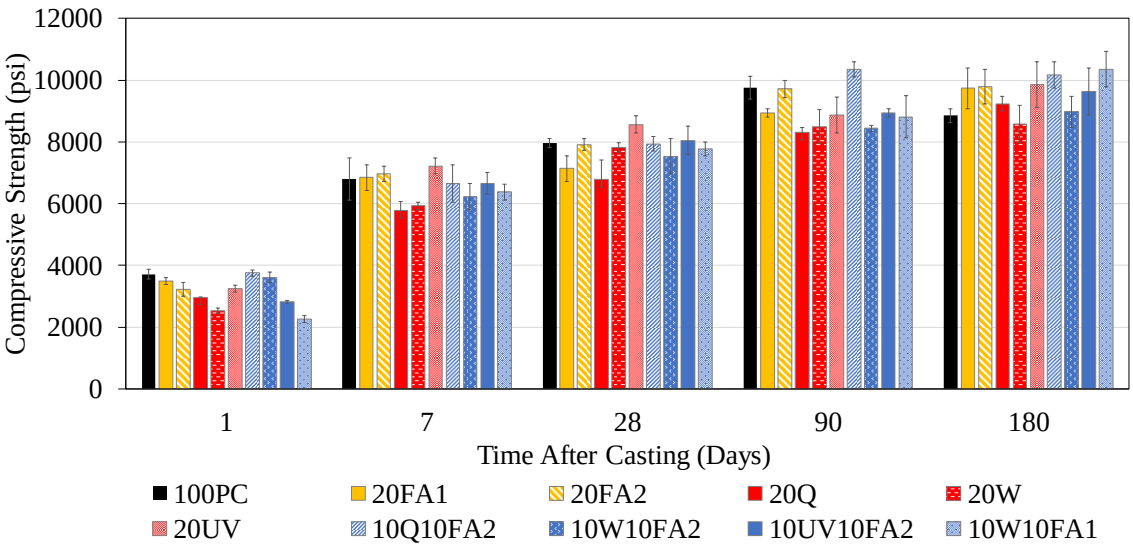


Figure 4.1. Average concrete compressive strengths ± one standard deviation from the average (shown with error bars).

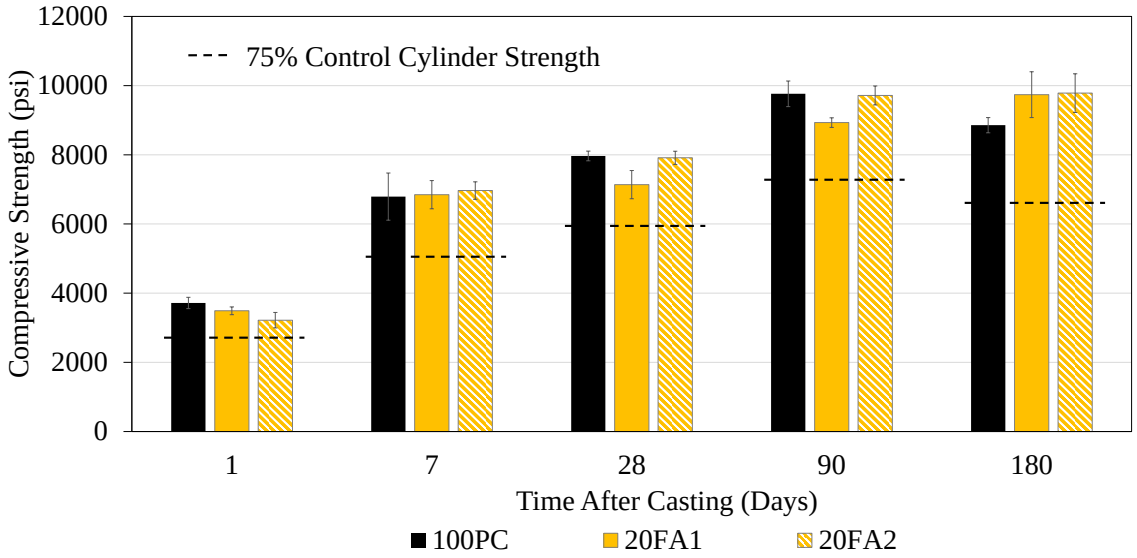


Figure 4.2. Fly ash specimens versus control: average concrete compressive strengths ± one standard deviation from the average (shown with error bars).

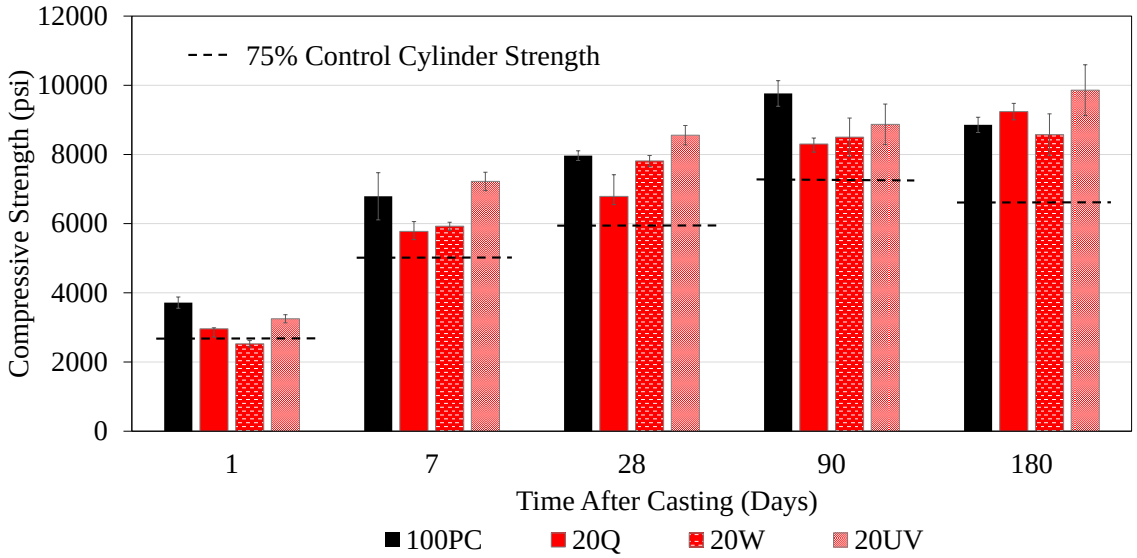


Figure 4.3. Glass specimens versus control: average concrete compressive strengths ± one standard deviation from the average (shown with error bars).

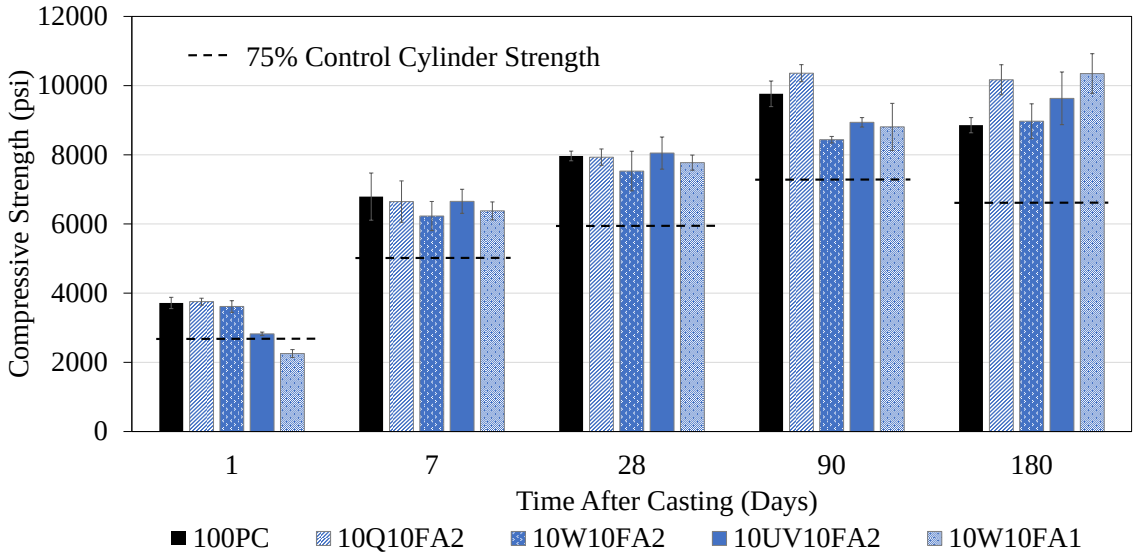


Figure 4.4. Ternary blend specimens versus control: average concrete compressive strengths ± one standard deviation from the average (shown with error bars).

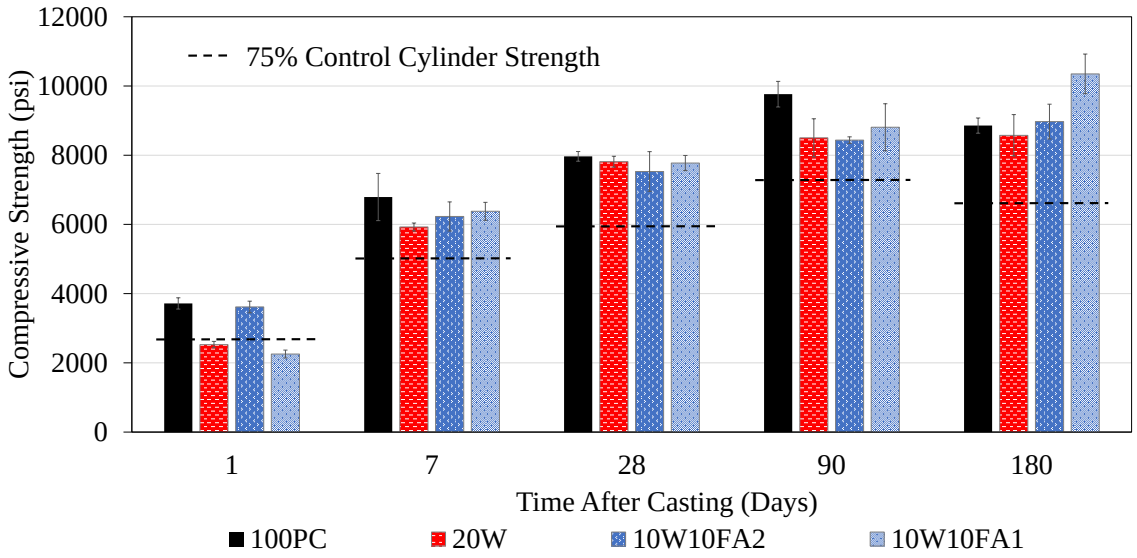


Figure 4.5. W-glass specimens versus control: average concrete compressive strengths ± one standard deviation from the average (shown with error bars).

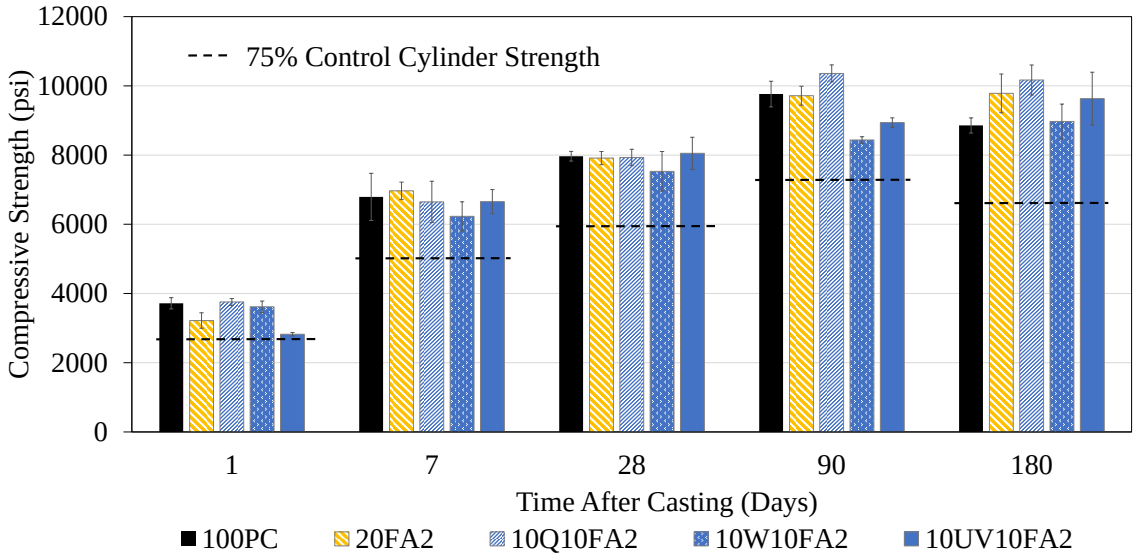


Figure 4.6. Fly Ash 2 specimens versus control: average concrete compressive strengths ± one standard deviation from the average (shown with error bars).

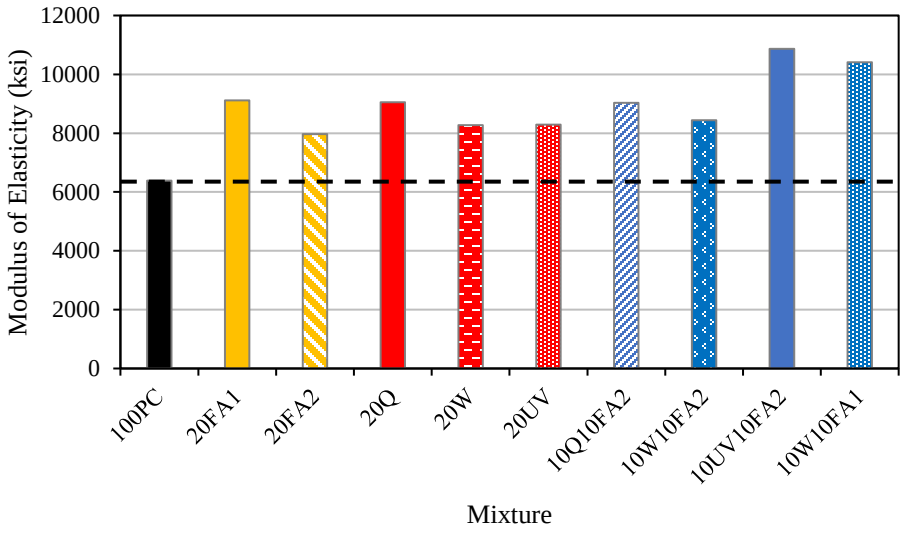


Figure 4.7. Modulus of elasticity at 90 days for the ten mixtures.

# Chapter 5: Summary and Conclusions

Eight of the nine mixtures containing SCMs had lower 1-day compressive strengths compared to the control mixture without SCMs, which was most likely due to the pozzolanic reaction. However, all nine mixtures not only satisfied the 75% SAI requirements of ASTM C618 (2019) at 7 and 28 days but had at least 85% of the control mixture compressive strength at 7, 28, 90 and 180 days. Therefore, all nine mixtures satisfied the physical properties, chemical properties, and strength requirements of ASTM C618 (2019). Soda-lime or E-glass could be incorporated in binary or ternary blend (with fly ash) concrete mixtures to achieve sufficient compressive strengths for construction purposes when ground to particle sizes less than 45 μm and used at a 20% replacement level.

There were only four instances (20FA2 at 7-day, 20UV at 7-day, 20UV at 28-day, and 10Q10FA2 at 90-day) when the SCM mixtures had significantly higher compressive strengths than control cylinders, not including 180-day *t*-test results. These results were different than the hypothesis that the pozzolanic reaction would increase compressive strength compared to control cylinders at 90-days. Eight of the nine mixtures had significantly higher compressive strengths than the control cylinders at 180 days. However, the 180-day control cylinders were from a separate batch of concrete, which likely had lower compressive strengths than what the original control concrete would have had. The ternary blends typically had higher compressive strengths at all ages compared to binary blends. It is likely that the nine SCM mixtures underwent a pozzolanic reaction to some degree, but the pozzolanic reaction was not strong enough to significantly increase the compressive strength compared to control cylinders.

Results from *t*-tests demonstrated that the flexural strengths of the nine mixtures containing SCMs were not significantly different than the flexural strength of the control beams. Additionally, any of the glasses (W, UV, or Q) could be used in concrete beams at a 20% replacement level with negligible difference in flexural strength; there was also negligible difference in flexural strength between the concrete beams with glass and the fly ash mixtures. The ternary blends with 10% glass and 10% fly ash did not increase the

flexural strength of the beams when compared to the mixtures with 20% glass. Instead, all of the beams made with a ternary blend had statistically similar flexural strength compared to their binary blend counterparts. For example, 20UV beams had the same flexural strength as 10UV10FA2 beams. Additionally, the flexural strength of the ternary blends with two different fly ashes (10W10FA1 and 10W10FA2) had statistically equal flexural strengths. Based on the flexural results, it would be acceptable to use ground soda-lime glass or E-glass in structural concrete. Since glass can be recycled an infinite amount of times without loss in quality, it would be preferable to improve glass recovery and recycling rates to reduce the consumption of raw materials for new glass. In the meantime, waste glass could be used as a cement substitute (at a 20% replacement level) in structural concrete mixtures, and these mixtures will achieve similar flexural strengths as concrete without SCMs. Needless to say, it is important to continue to test concrete mixtures made with ground glass as a replacement for cement because there are many types of glass that may behave differently.

All of the beams made with SCMs had lower displacement than the control beams (1.4 in.) at the peak applied load and some mixtures had as much as 36% less displacement. Furthermore, all of the beams made with SCMs had a higher modulus of elasticity compared to the control specimens. Some of the measured modulus of elasticity were 60-70% higher than control specimens. Additional research should be conducted to confirm if it is common for beams with SCMs (especially different glass types) to have less displacement compared to beams without SCMs. The possibility that displacement could be less for beams with SCMs could come with advantages and disadvantages. An advantage of lower displacements could be in displacement-critical areas of structures, where displacement allowances are strict. Mixtures with SCMs could provide stiffer concrete while maintaining similar flexural strengths compared to concrete without SCMs. A disadvantage of concrete with less flexural displacement could be fewer warning signs before failure. For example, greater displacement in structural members are likely to gain more attention than members that displace less, ultimately providing more warning time to the occupants before failure.

Overall, it was possible to produce concrete with acceptable compressive strength and statistically similar flexural strength compared to 100% portland cement concrete by partially replacing a 20% of the cement with one of the most common types of glass (soda-lime or E-glass) in either a binary or ternary blend. Beams made with E-glass did not perform as well as anticipated (significantly higher than control specimens), but they performed just as well as the control specimens considering compressive and flexural strength. From a strength prospective, it was shown to be viable to use ground glass as a pozzolan in structural concrete where curing time isn't a concern. Other advantages of waste glass used as a partial replacement of cement include possible lower concrete costs, lower carbon dioxide emissions, more space in landfills, and potentially opening waste glass markets for waste facilities.

Future studies related to concrete made with ground glass should investigate larger sample sizes of beams, different types of glasses, different cement replacement levels, testing beams at different ages (e.g., 28 days), and ternary blends with different SCMs (e.g., Class C fly ash or GBFS). Also, more research on the relationship between displacement and modulus of elasticity of SCM mixtures is required to determine if SCM mixtures consistently have a higher modulus of elasticity value compared to conventional concrete, which would ultimately resulting in less displacement of the concrete beams made with SCMs.

# References


ACI Committe 318. (2014). Building Code Requirments for Structural Concrete (ACI 318-14). Farmington Hills, MI.

Aggarwal, V., & Shekhawat, B. S. (2014). Investigation of strength and durability parameters of glass powder based concrete. *International Journal of Engineering Research & Technology (IJERT), 3*(7).

American Concrete Institute (ACI). (2019). *Definition of a Pozzolan.* Retrieved from https://www.concrete.org/topicsinconcrete/topicdetail/pozzolan?search=pozzolan

Aphale, A. S., & Sahare, S. A. (2016). Effect of particle size of recycled glass on concrete properties - A review. *International Journal of Advances in Mechanical and Civil Engineering, 3*(5).

ASTM A706 - 16. (2016). Standard Specification for Deformed and Plain Low-Alloy Steel Bars for Concrete Reinforcement. *American Society for Testing and Materials (ASTM)*. West Conshohocken , PA.

ASTM C29 -17a. (2017). Standard Test Method for Bulk Density ("Unit Weight") and Voids in Aggregate. *American Society for Testing and Materials (ASTM)*. West Conshohocken, PA.

ASTM C39 - 18. (2018). Standard Test Method for Compressive Strength of Cylindrical Concrete Specimens. *American Society for Testing and Materials (ASTM)*. West Conshohocken, PA.

ASTM C78 - 18. (2018). Standard Test Method for Flexural Strength of Concrete (Using Simple Beam with Third-Point Loading). *American Society for Testing and Materials (ASTM)*. West Conshohocken, PA.

ASTM C127 -15. (2015). Standard Test Method for Relative Density (Specific Gravity) and Absorption of Coarse Aggregate. American Society for Testing and Materials (ASTM). West Conshohocken , PA.

ASTM C128 - 15. (2015). Standard Test Method for Relative Density (Specific Gravity) and Absorption of Fine Aggregate. *American Society for Testing and Materials (ASTM)*. West Conshohocken , PA.

ASTM C136 - 14. (2014). Standard Test Method for Sieve Analysis of Fine and Coarse Aggregates. *American Society for Testing and Materials (ASTM)*. West Conshohocken, PA.

ASTM C138 -17. (2017). Standard Test Method for Density (Unit Weight), Yield, and Air Content (Gravimetric) of Concrete. *American Society for Testing and Materials (ASTM)*. West Conshohocken, PA.

ASTM C143 - 15a. (2015). Standard Test Method for Slump of Hydraulic-Cement Concrete. *American Society for Testing and Materials (ASTM)*. West Conshohocken , PA.

ASTM C150 - 19a. (2019). Standard Specification for Portland Cement. *American Society for Testing and Materials (ASTM)*. West Conshohocken, PA.

ASTM C192 - 16a. (2016). Making and Curing Concrete Test Specimens in the Labratory. *American Society for Testing and Materials (ASTM)*. West Conshohocken, PA.

ASTM C231 - 17a. (2017). Standard Test Method for Air Content of Freshly Mixed Concrete by the Pressure Method. *American Society for Testing and Materials (ASTM)*. West Conshohocken , PA.

ASTM C469 - 14. (2014). Standard Test Method for Static Modulus of Elasticity and Poisson's Ratio of Concrete in Compression. *American Society for Testing and Materials (ASTM)*. West Conshohocken, PA.

ASTM C566 - 13. (2013). Standard Test Method for Total Evaporable Moisture Content of Aggregate by Drying. *American Society for Testing and Materials (ASTM)*. West Conshohocken, PA.

ASTM C618 - 19. (2019). Standard Specification for Coal Fly Ash and Raw or Calcined Natural Pozzolan for Use in Concrete. *American Society for Testing and Materials (ASTM)*. West Conshohocken , PA.

ASTM C1064 - 17. (2017). Standard Test Method for Temperature of Freshly Mixed Hydraulic-Cement Concrete. *American Society for Testing and Materials (ASTM)*. West Conshohocken, PA.

ASTM C1157 - 17. (2017). Standard Performance Specification for Hydraulic Cement. *American Society for Testing and Materials (ASTM)*. West Conshohocken, PA.

ASTM E8 - 16a. (2016). Standard Test Methods for Tension Testing of Metallic Materials. *American Society for Testing and Materials (ASTM)* . West Conshohocken , PA.

Baxter, S., & Meyer, C. (1998). *Use of recycled glass and fly ash for precast concrete.* (4292-IABR-IA-96). New York: Columbia University.

Chen, C. H., Huang, R., Wu, J. K., & Yang, C. C. (2006). Waste E-glass particles used in cementitious mixtures. *Cement and Concrete Research, 36*(2006), 449-456.

Chindaprasirt, P., & Rukzon, S. (2014). Use of ternary blend of Portland cement and two pozzolans to improve durability of high-strength concrete. *KSCE Journal of Engineering*, 1745-1752. doi:10.1007/s12205-014-0461-y

Christiansen, M. U., & Dymond, B. Z. (2019). The effect of composition on the performance of ground glass pozzolan. *ACI Materials Journal*.

Corning Museum of Glass. (2002). *Corning museum of glass*. Retrieved 4 27, 2020, from https://www.cmog.org/article/types-glass

Enviornmental Protection Agency. (2019, May 7). *Facts and figures about materials, waste and recycling*. Retrieved 4 27, 2020, from United States Environmental Protection Agency (EPA): https://www.epa.gov/facts-and-figures-about-materials-waste-and-recycling/glass-material-specific-data

Erdem, T. K., & Kirca, O. (2008). Use of binary and ternary blends in high strength concrete. *Construction and Building Materials, 22*(7). Retrieved from https://link-gale-com.libpdb.d.umn.edu:2443/apps/doc/A179533512/AONE?u=mnauduluth&sid=AONE&xid=307cd21d

Gartner, E. M., John, V. M., & Scrivener, K. L. (2018). Eco-efficient cements: Potential economically viable solutions for a low-CO2 cement-based materials industry. *Cement and Concrete Research, 114*(2018), 2-26.

Ghavidel, R., & Madandoust, R. (2013). Mechanical properties of concrete containing waste glass powder and rice husk ash. *Biosystems Engnineering, 116*(2013), 113-119.

Han, R., Wei, Y.-M., & Zhang, C.-Y. (2018). Accounting process-related CO2 emissions from global cement production under shared socioeconomic pathways. *Cleaner Production, 184*(2018), 451-465.

Ionescu, D., Kilpatrick, A., & Petrolito, J. (2018). *Use of recycled glass in concrete production.* The International Structural Engineering and Construction Society (ISEC). doi:10.14455/ISEC.res.2018.58

Jennings, H., & Thomas, J. (2018, August 14). Retrieved from The science of concrete: http://iti.northwestern.edu/cement/index.html

Juenger, M. C., & Siddique, R. (2015). Recent advances in understanding the role of supplementary cementitious materials in concrete. *Cement and Concrete Research, 78*(2015), 71-80.

Kazi, N., Rahman, M. H., & Sadiqul Islam, G. M. (2016). Waste glass powder as partial replacement of cement for sustainable concrete practice. *Science Direct*.

Kumar, D., & Raju, S. (2014). Effect of using glass powder in concrete. *IJIRSRET, 3*(5).

Lalande, J.-M., & Tremblay, A. (2005). *United States of America Patent No. US6908507B2*.

Lee, D., Sutan , N. M., Tamanna, N., & Yakub, I. B. (2013). Utilization of waste glass in concrete. *ResearchGate*. doi:10.3850/978-981-07-6059-5_090

Lefort, T., Moras, S., Rodriguez, D., & Shao, Y. (2000). Studies on concrete containing ground waste glass. *Cement and Concrete Research, 30*(2000), 91-100.

Malhotra, V. M., & Mehta, P. K. (1996). Pozzolanic and cementitious materials. *American Concrete Institute materials journal, 93*(6), 1-6.

Meyer, C., & Xi, Y. (1999). Use of recycled glass and fly ash for precast concrete. *Journal of Materials in Civil Engineering, 11*(2).

Najm, H., Nassif, H. H., & Suksawang, N. (2005). Effect of pozzolanic materials and curing methods on the elastic modulus of HPC. *Cement & Concrete Composites, 27*(2005), 661-670.

Nassar, R. D., & Soroushian, P. (2011). Field investigation of concrete incorporating milled waste glass. *Solid Waste Technology Managment, 37*(4), 307-319.

Pavia, S., & Walker, R. (2011). Physical properties and reactivity of pozzolans, and their influence on the properties of lime–pozzolan pastes. *Materials and Structures, 44*(6), 1139-1150. doi:10.1617/s11527-010-9689-2

Portland Cement Association (PCA). (2016). In S. H. Kosmatka, & M. L. Wilson , *Design and Control of Concrete Mixtures* (16th ed.). Skokie, Illinois: Portland Cement Association.

Samtur, H. R. (1974). *Glass recycling and reuse.* (Report No. 17). University of Wisconsin, Madison. Institute for Environmental Studies.

Shayan, A., & Xu, A. (2004). Value-added utilisation of waste glass in concrete. *Cement and Concrete Research, 34*(2004), 81-84.

Slag Cement Association (SCA). (2019). *Ternary Concrete Mixtures With Slag Cement*. Retrieved from www.slagcement.org/aboutslagcement/is-20.aspx

# Appendix A Material Properties

Table A.1. Cement manufacture material certification report.

**GCC of America**
Cherry Creek Plaza 1, 600 S. Cherry Street, 10th Floor, Glendale, CO 80246
Sales (303) 739-5900 Customer Service (800) CALL GCC

**MATERIAL CERTIFICATION REPORT**

**Plant:** Rapid City
**Address:** 501 N. St Onge Street
Rapid City, South Dakota
**Contact:** Gail B. Amicucci
**Phone:** (605) 721-7100

**Cement Type:** I/II, I/II(MH), Low Alkali, GU
**Date Issued:** 01-Mar-18
**Production Period:** 1-Feb-18
**To:** 28-Feb-18

**STANDARD REQUIREMENTS ASTM C150/AASHTO M85/ASTM C1157**

| CHEMICAL | | |
|---|---|---|
| **Item** | **ASTM C150 Spec. Limit** | **Test Result** |
| $SiO_2$ (%) | [A] | 20.2 |
| $Al_2O_3$ (%) | 6.0 max | 4.6 |
| $Fe_2O_3$ (%) | 6.0 max | 3.3 |
| CaO (%) | [A] | 64.0 |
| MgO (%) | 6.0 max | 1.2 |
| $SO_3$ (%) | 3.5 max[B] | 3.0 |
| Loss on Ignition (%) | 3.5 max | 1.7 |
| $Na_2O$ (%) | [A] | 0.12 |
| $K_2O$ (%) | [A] | 0.70 |
| Insoluble Residue (%) | 1.5 max | 0.36 |
| $CO_2$ (%) | [A] | 0.8 |
| Limestone (%) | 5.0 max | 2.5 |
| $CaCO_3$ in Limestone (%) | 70 min | 93 |
| Potential Phase Composition [C] | | |
| $C_3S$ (%) | [A] | 59 |
| $C_2S$ (%) | [A] | 13 |
| $C_3A$ (%) | 8 max | 6.6 |
| $C_4AF$ (%) | [A] | 10 |
| $C_3S + 4.75C_3A$ (%) | 100 max | 91 |

| PHYSICAL | | | |
|---|---|---|---|
| **Item** | **ASTM C150 Spec. Limit** | **ASTM C1157 Spec. Limit** | **Test Result** |
| Air Content (volume %) | 12 max | 12 max | 9 |
| Blaine Fineness ($cm^2/g$) | 2600-4300 | [A] | 3937 |
| Residue 45 µm (No. 325) Sieve (%) | [A] | [D] | 2.7 |
| Autoclave Expansion (%) | 0.80 max | 0.80 max | -0.02 |
| Compressive Strength | | | |
| 1 day, MPa (psi) | [A] | [A] | 13.8 (2010) |
| 3 days, MPa (psi) | 12.0 (1741) min | 13 (1890) min | 26.4 (3820) |
| 7 days, MPa (psi) | 19.0 (2760) Min | 20.0 (2900) min | 37.0 (5360) |
| 28 days, MPa (psi)[E] | [A] | 28.0 (4160) min | 46.6 (6760) |
| Time of Setting, Initial Vicat (minutes) | 45-375 | 45-420 | 125 |
| Heat of Hydration, 7 days, kJ/kg (cal/g) | [F] | [A] | 350 |
| Mortar Bar Expansion C-1038 (%) | [B] | 0.020 max | 0.002 |

| INORGANIC PROCESSING ADDITION (If Applicable) | | | |
|---|---|---|---|
| Type | None | Base Phase Cement Composition | |
| $SiO_2$ (%) | NA | $C_3S$ (%) | 60 |
| $Al_2O_3$ (%) | NA | $C_2S$ (%) | 13 |
| $Fe_2O_3$ (%) | NA | $C_3A$ (%) | 7 |
| CaO (%) | NA | $C_4AF$ (%) | 10 |
| $SO_3$ (%) | NA | | |

**OPTIONAL REQUIREMENTS ASTM C150/AASHTO M85/ASTM C1157**

| CHEMICAL | | |
|---|---|---|
| **Item** | **ASTM C150 Spec. Limit** | **Test Result** |
| Equivalent Alkalies (%) | 0.60 max | 0.58 |

| PHYSICAL | | | |
|---|---|---|---|
| **Item** | **ASTM C150 Spec. Limit** | **ASTM C1157 Spec. Limit** | **Test Result** |
| False Set (%) | 50 min | 50 min | 77 |

[A] Not applicable
[B] It is permissible to exceed the specification limit provided that ASTM C1038 Mortar Bar Expansion does not exceed 0.020 % at 14 days.
[C] Adjusted per Annex A1.6
[D] No limit specified, data reported for information purpose only
[E] Test result of prior month
[F] Test result represents most recent value. Heat of hydration test has been carried out by American Engineering Testing, Saint Paul, MN.

GCC of America Cement is warranted to conform at the time of shipment with current ASTM C150/AASHTO M85/ASTM C1157. No other warranty is made or implied. Having no control over the use of its cements, GCC of America does not guarantee finished work. GCC is not responsible for any additives not stated in the Certificate of Compliance. GCC of America certifies that the data described above under "Processing Addition" represents the materials in the cement manufactured during the production period indicated.

Table A.2. Concrete material quantities used in each of the ten mixtures; all values in lb. Moisture content of aggregates were accounted for in water quantities.

| | **100PC** | **20FA1** | **20FA2** | **20Q** | **20W** | **20UV** | **10Q10FA2** | **10W10FA2** | **10UV10FA2** | **10W10FA1** |
|---|---|---|---|---|---|---|---|---|---|---|
| **Water** | 102.4 | 97.6 | 96.9 | 87.6 | 98.8 | 98.9 | 96.0 | 92.2 | 110.1 | 90.1 |
| **Portland Cement** | 248.4 | 198.8 | 198.8 | 198.8 | 198.8 | 198.8 | 198.8 | 198.8 | 198.8 | 198.8 |
| **CA** | 593.4 | 595.2 | 593.8 | 594.0 | 593.9 | 593.8 | 592.3 | 597.6 | 589.3 | 596.4 |
| **FA** | 492.9 | 486.8 | 488.9 | 498.0 | 486.8 | 486.9 | 491.3 | 489.8 | 480.2 | 493.0 |
| **W-glass** | - | - | - | - | 49.7 | - | - | 24.8 | - | 24.8 |
| **Q-glass** | - | - | - | 49.7 | - | - | 24.8 | - | - | - |
| **UV-glass** | - | - | - | - | - | 49.7 | - | - | 24.8 | - |
| **Fly Ash 1** | - | 49.7 | - | - | - | - | - | - | - | 24.8 |
| **Fly Ash 2** | - | - | 49.7 | - | - | - | 24.8 | 24.8 | 24.8 | - |

Table A.3. Average width and height dimensions taken from three locations within the middle third of the beams for all 30 beams.

| Concrete Beam Labels | Beam Number | Average Width, *b* (in.) | Average Height, *h* (in.) |
|---|---|---|---|
| 100PC | 1 | 6.0 | 9.8 |
| | 2 | 6.1 | 10.5 |
| | 3 | 6.1 | 10.3 |
| 20FA1 | 1 | 6.0 | 10.3 |
| | 2 | 6.0 | 10.2 |
| | 3 | 6.1 | 10.0 |
| 20FA2 | 1 | 5.8 | 10.3 |
| | 2 | 6.0 | 10.3 |
| | 3 | 6.0 | 10.3 |
| 20W | 1 | 6.1 | 10.5 |
| | 2 | 5.7 | 10.5 |
| | 3 | 6.2 | 10.5 |
| 20Q | 1 | 6.1 | 10.6 |
| | 2 | 6.0 | 10.4 |
| | 3 | 6.3 | 10.3 |
| 20UV | 1 | 5.9 | 10.1 |
| | 2 | 6.2 | 10.4 |
| | 3 | 5.7 | 10.4 |
| 10W10FA2 | 1 | 6.0 | 10.6 |
| | 2 | 5.6 | 10.5 |
| | 3 | 6.3 | 10.5 |
| 10Q10FA2 | 1 | 6.0 | 10.5 |
| | 2 | 5.8 | 10.4 |
| | 3 | 6.2 | 10.5 |
| 10UV10FA2 | 1 | 5.8 | 10.2 |
| | 2 | 5.75 | 10.3 |
| | 3 | 6.0 | 10.4 |
| 10W10FA1 | 1 | 6.0 | 10.3 |
| | 2 | 6.2 | 10.3 |
| | 3 | 5.9 | 10.3 |

Table A.4. Average concrete densities of the 3 in. by 6 in. cylinders at 1, 7, 28, 90, and 180 days for each of the ten mixtures.

| **Concrete Mixtures** | **Average Density of Concrete Cylinders (pcf)** | | | | |
|---|---|---|---|---|---|
| | **1 Day** | **7 Days** | **28 Days** | **90 Days** | **180 Days** |
| 100PC (Control) | 154.4 | 154.0 | 153.6 | 154.0 | 154.0 |
| 20FA1 | 155.2 | 154.4 | 155.2 | 154.8 | 154.4 |
| 20FA2 | 154.0 | 153.2 | 154.0 | 154.0 | 154.1 |
| 20Q | 152.8 | 152.4 | 152.4 | 152.4 | 152.8 |
| 20W | 152.4 | 151.6 | 152.0 | 151.6 | 152.0 |
| 20UV | 152.4 | 151.6 | 153.2 | 151.6 | 153.2 |
| 10Q10FA2 | 154.0 | 153.6 | 152.8 | 153.6 | 153.2 |
| 10W10FA2 | 154.0 | 154.0 | 154.4 | 153.6 | 153.6 |
| 10UV10FA2 | 153.6 | 152.0 | 152.9 | 152.0 | 152.8 |
| 10W10FA1 | 153.6 | 152.0 | 152.8 | 152.8 | 153.2 |

# Appendix B Applied Moment Versus Displacement Figures

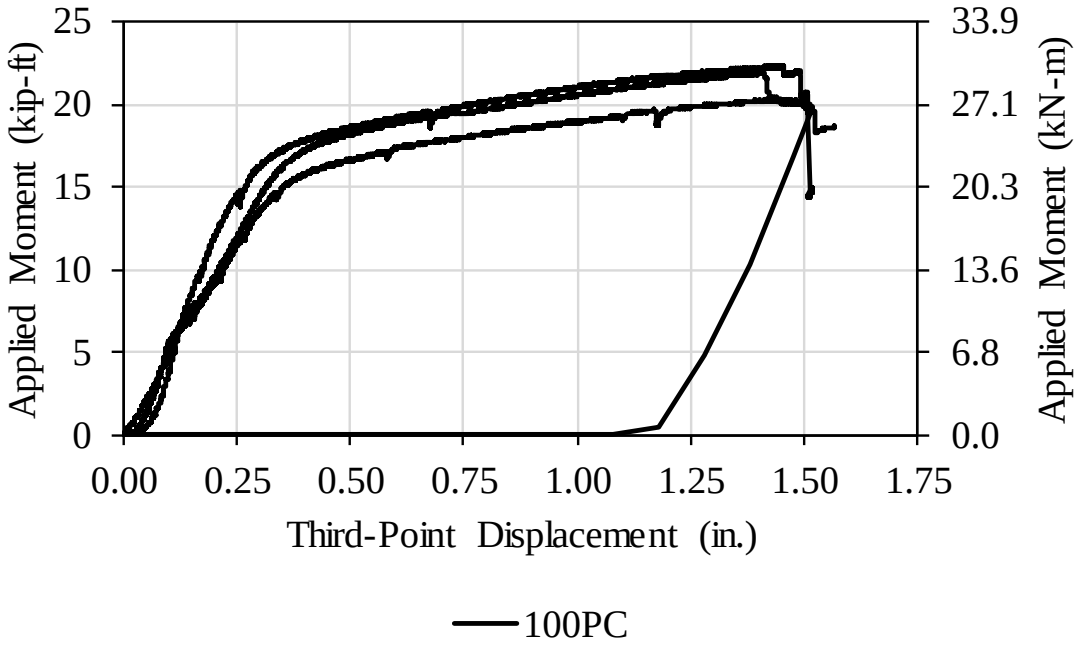


Figure B.1. Control beams: applied moment on the beam third-points versus displacement of the beam at the third-points.

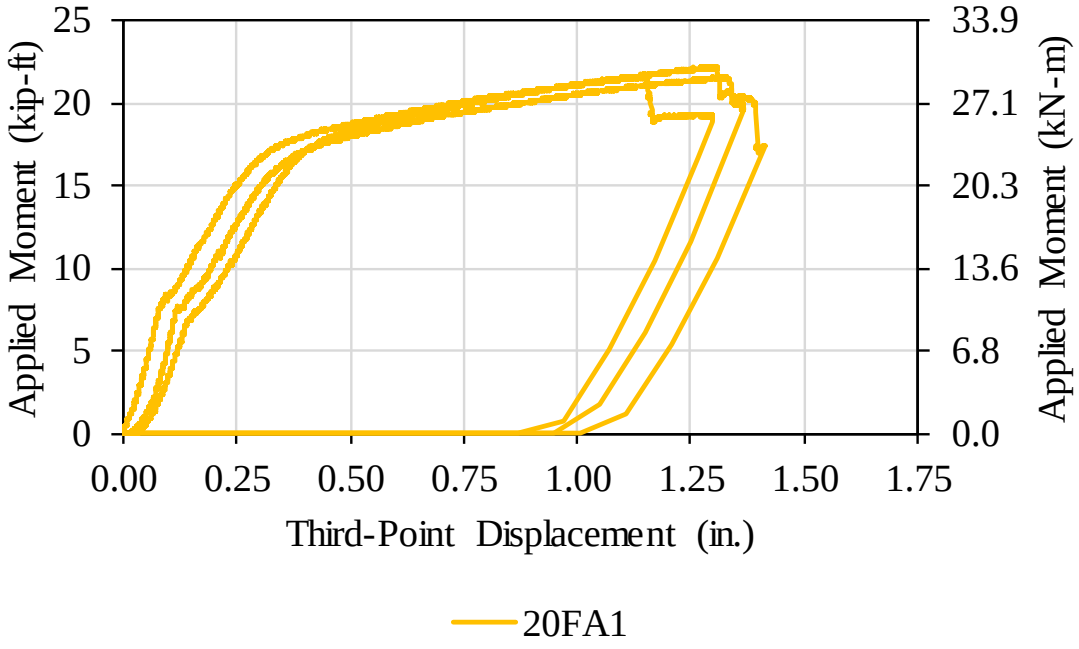

Figure B.2. 20FA1 beams: applied moment on the beam third-points versus displacement of the beam at the third-points.

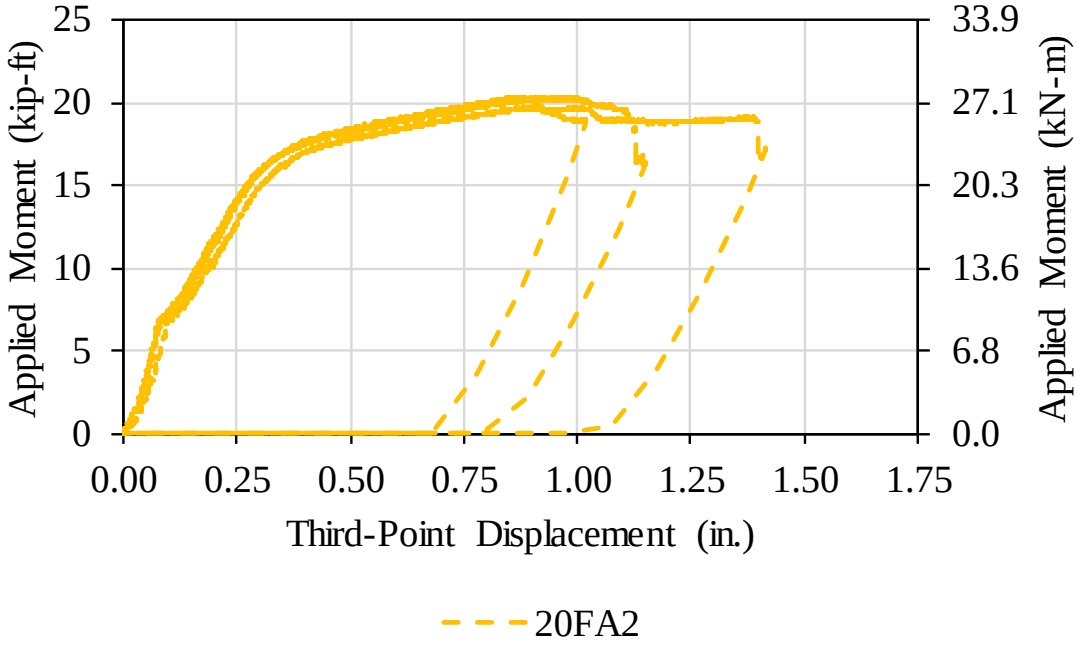


Figure B.3. 20FA2 beams: applied moment on the beam third-points versus displacement of the beam at the third-points.

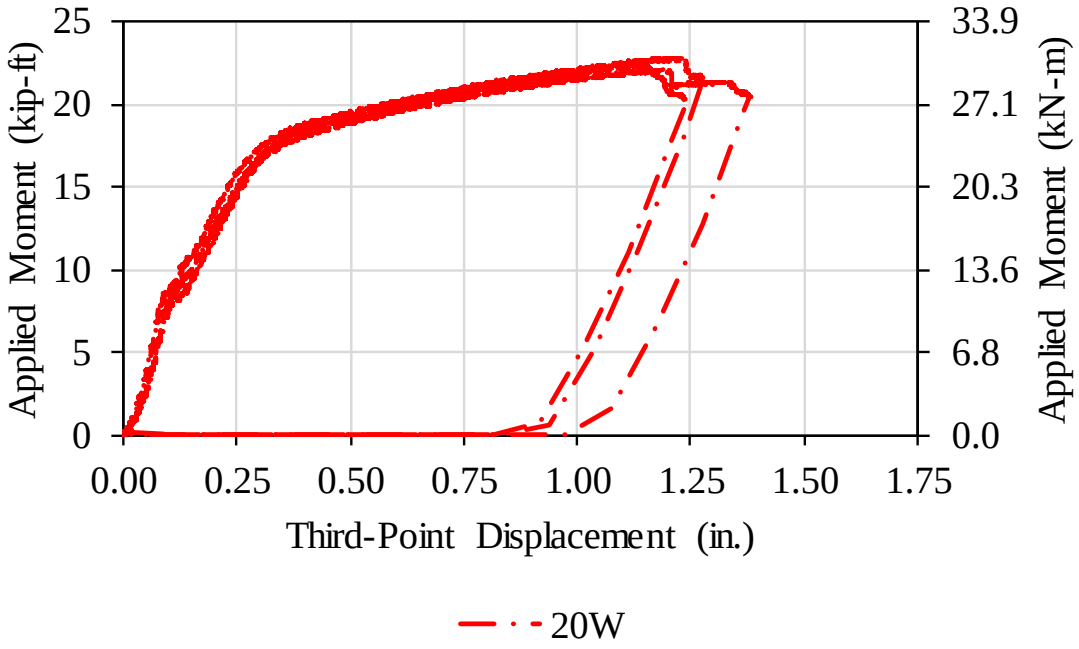


Figure B.4. 20W beams: applied moment on the beam third-points versus displacement of the beam at the third-points.

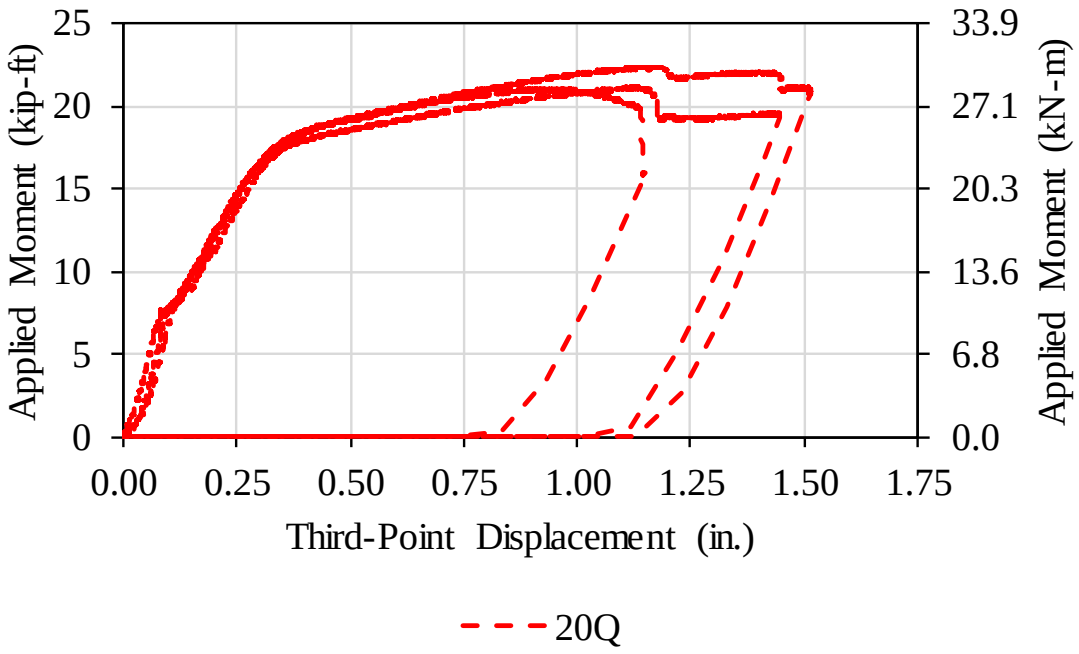


Figure B.5. 20Q beams: applied moment on the beam third-points versus displacement of the beam at the third-points.

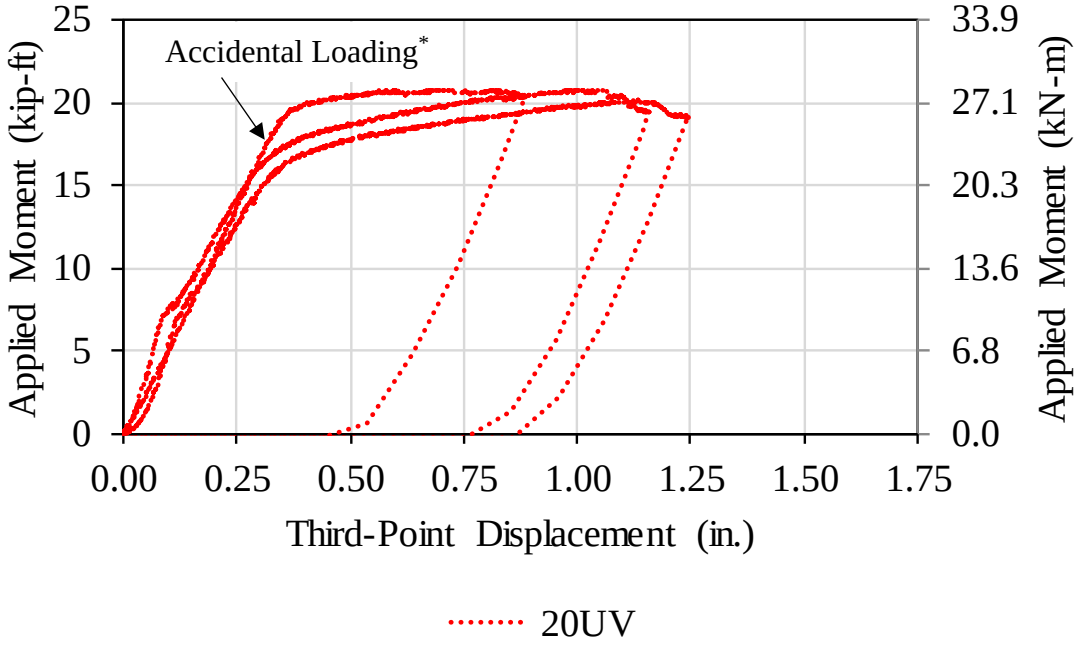


Figure B.6. 20UV beams: applied moment on the beam third-points versus displacement of the beam at the third-points. *An accidental load applied to the beam before testing.

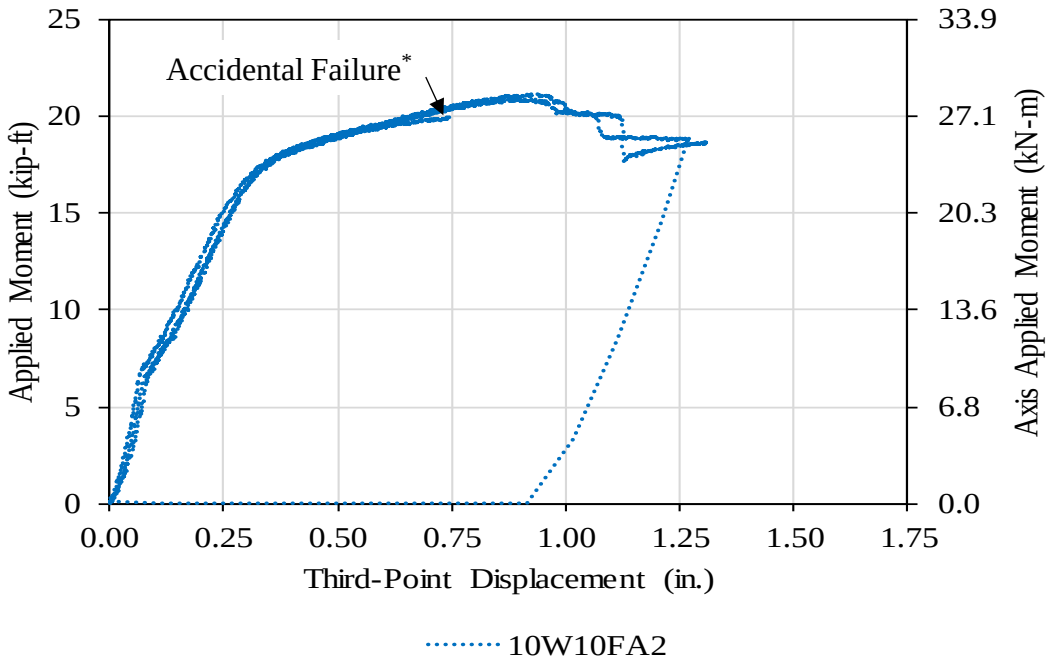


Figure B.7. 10W10FA2 beams: applied moment on the beam third-points versus displacement of the beam at the third-points. *The accidental failure of the beam resulted in loss of peak data.

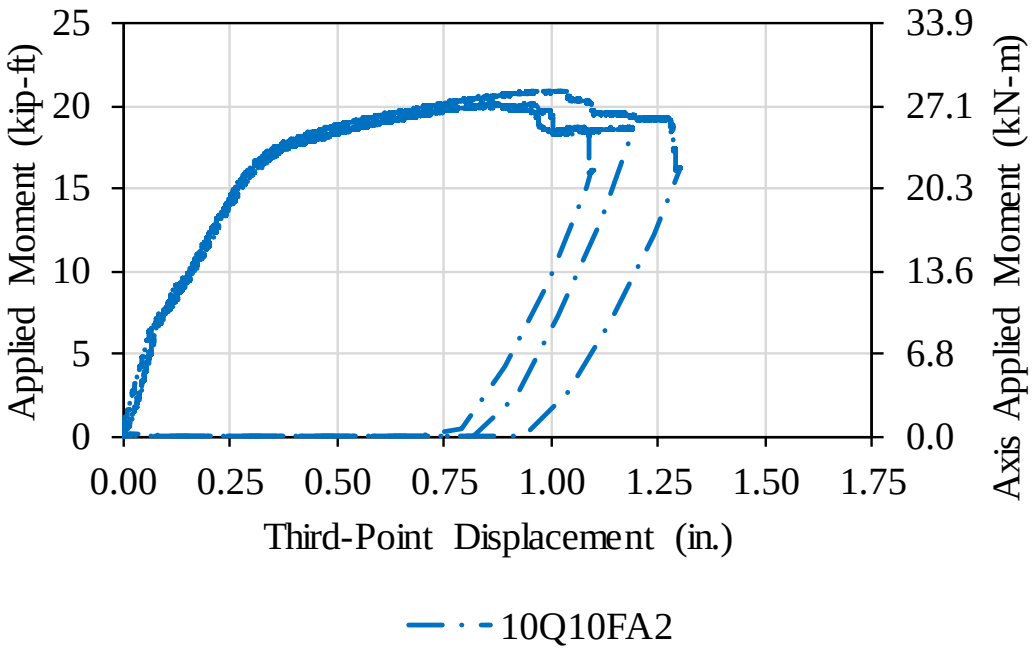


Figure B.8. 10Q10FA2 beams: applied moment on the beam third-points versus displacement of the beam at the third-points.

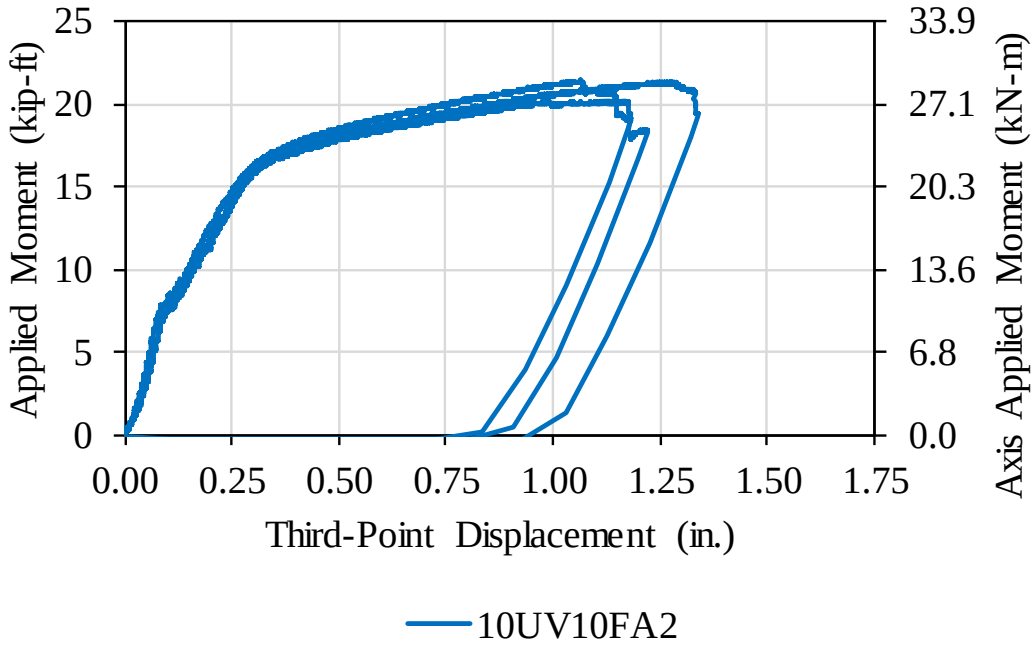


Figure B.9. 10UV10FA2 beams: applied moment on the beam third-points versus displacement of the beam at the third-points.

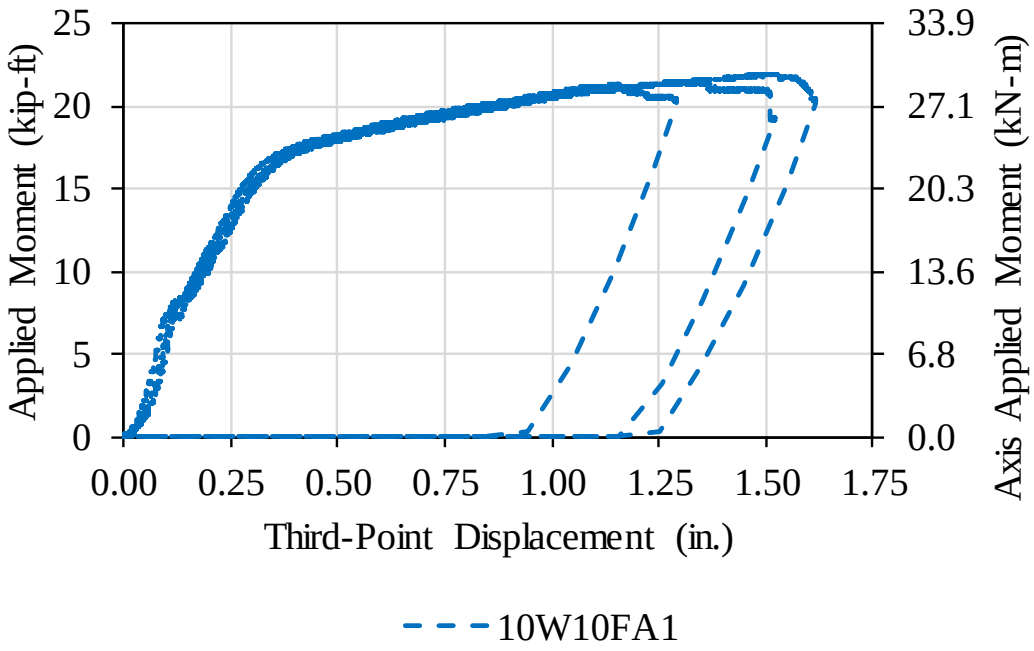


Figure B.10. 10W10FA1 beams: applied moment on the beam third-points versus displacement of the beam at the third-points.

# Appendix C Concrete Beams Before and After Testing

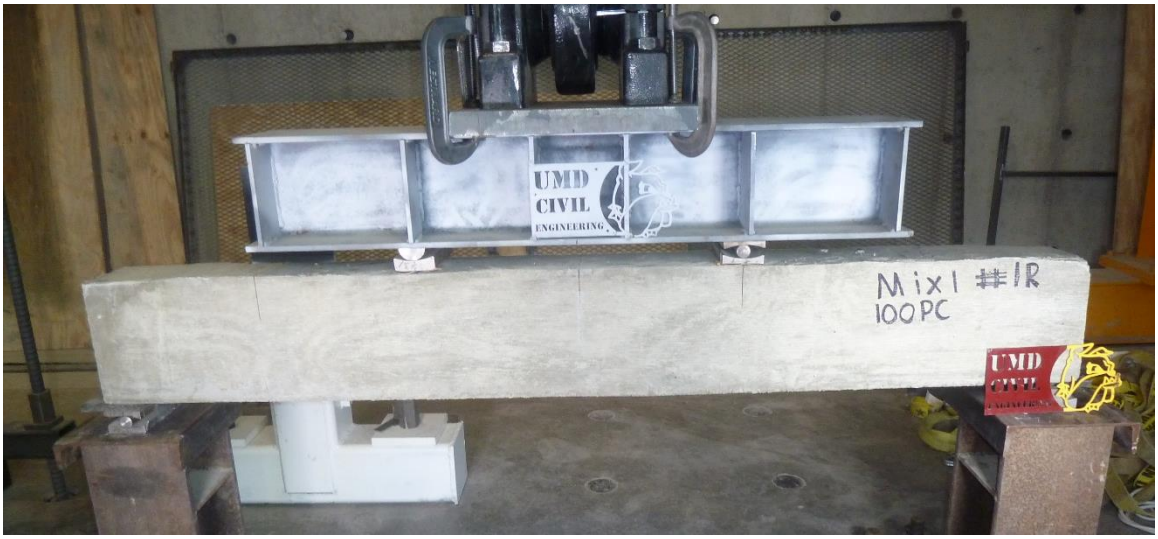


Figure C.1. Mixture 1 (100PC) beam #1R: concrete beam before testing.

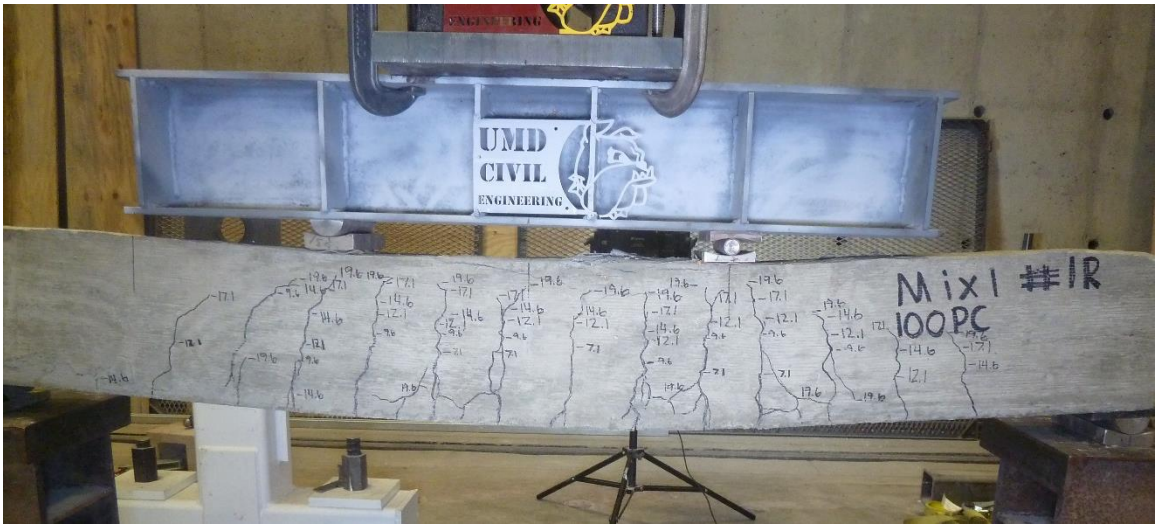


Figure C.2. Mixture 1 (100PC) beam #1R: concrete beam after testing.

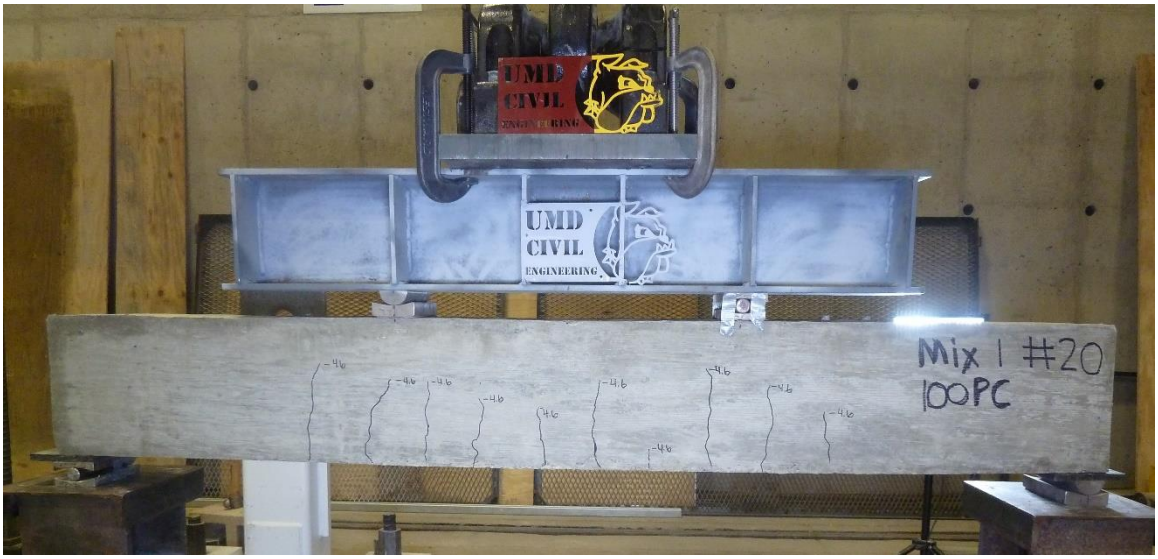


Figure C.3. Mixture 1 (100PC) beam #2O: concrete beam before testing.

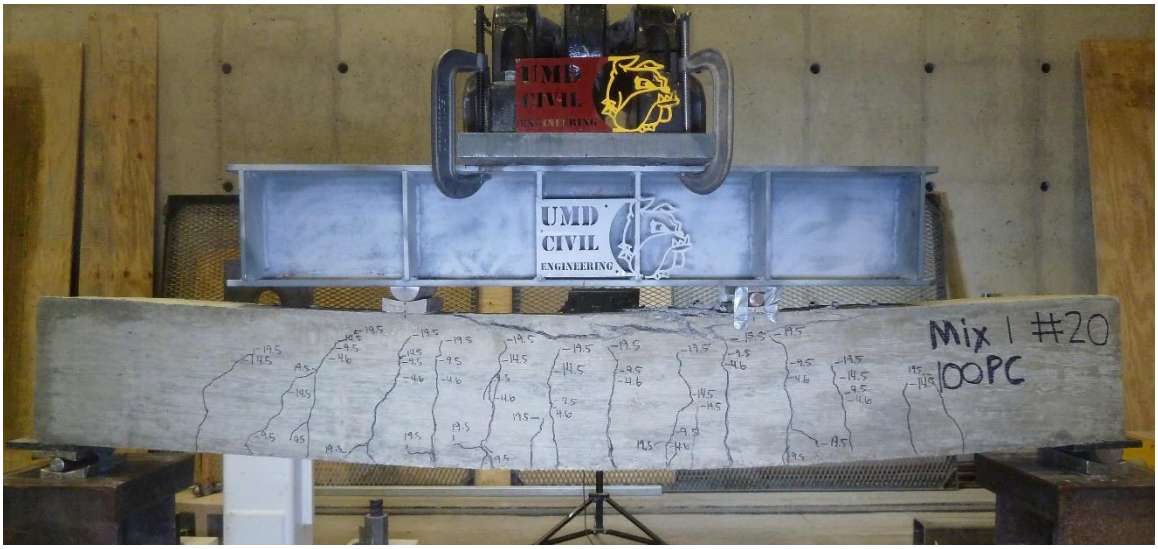


Figure C.4. Mixture 1 (100PC) beam #2O: concrete beam after testing.


Figure C.5. Mixture 1 (100PC) beam #3O: concrete beam before testing.


Figure C.6. Mixture 1 (100PC) beam #3O: concrete beam after testing.

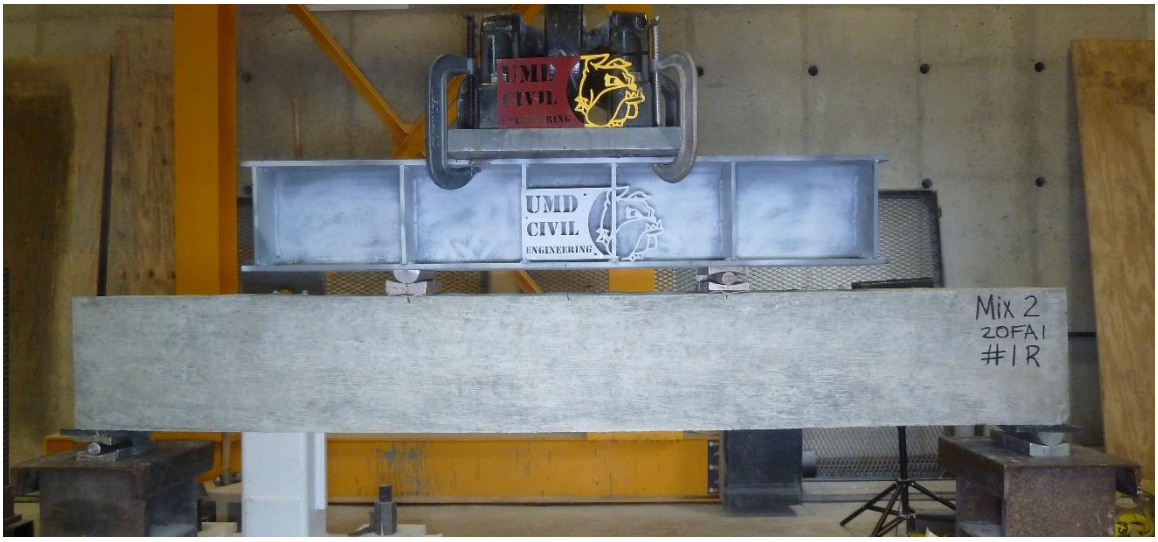


Figure C.7. Mixture 2 (20FA1) beam #1R: concrete beam before testing.

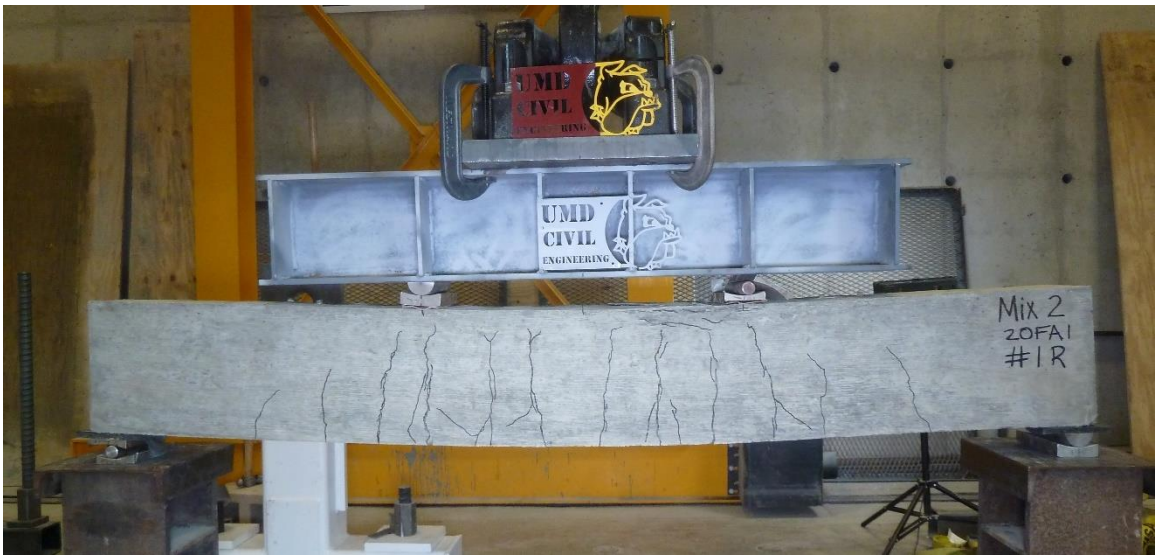


Figure C.8. Mixture 2 (20FA1) beam #1R: concrete beam after testing.

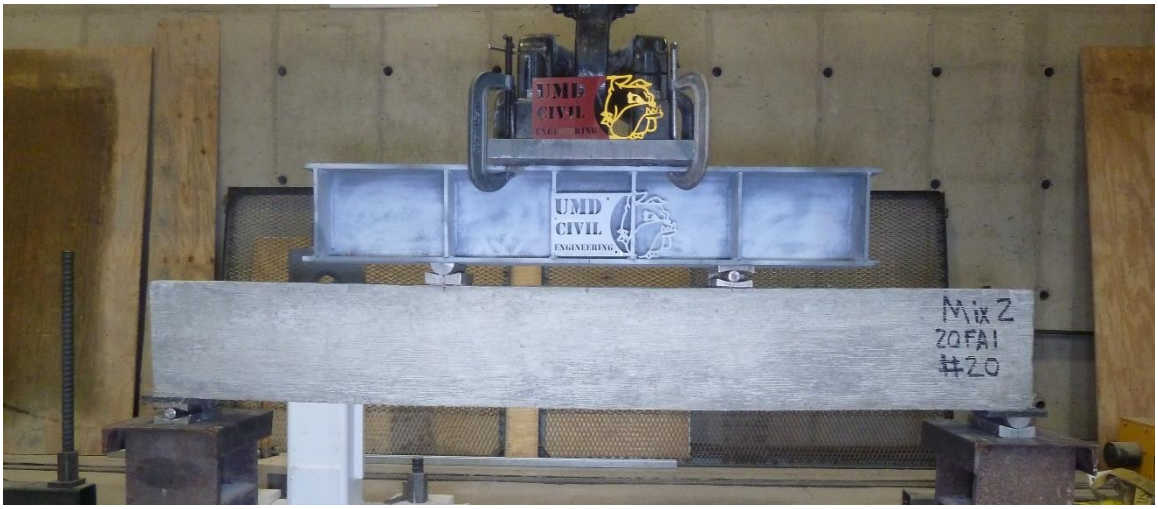


Figure C.9. Mixture 2 (20FA1) beam #2O: concrete beam before testing.


Figure C.10. Mixture 2 (20FA1) beam #2O: concrete beam after testing.

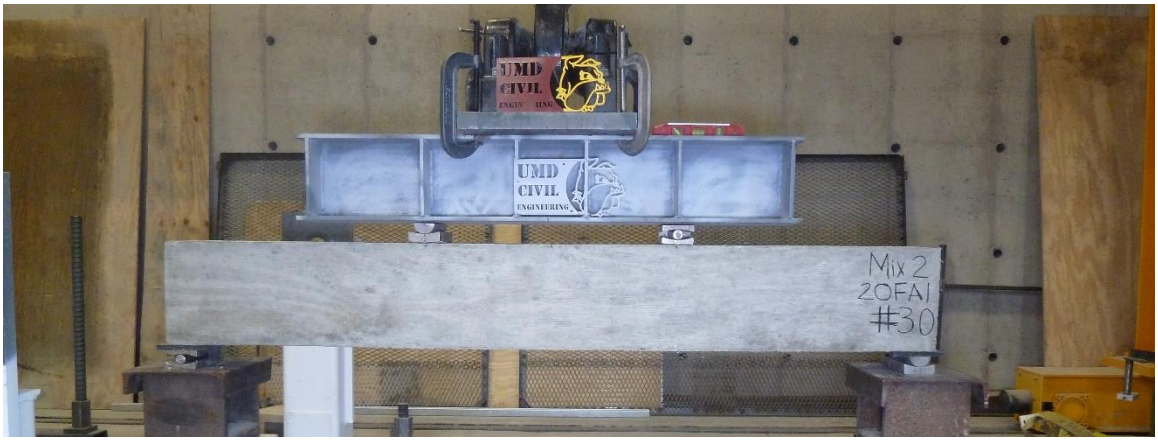


Figure C.11. Mixture 2 (20FA1) beam #3O: concrete beam before testing.


Figure C.12. Mixture 2 (20FA1) beam #3O: concrete beam after testing.

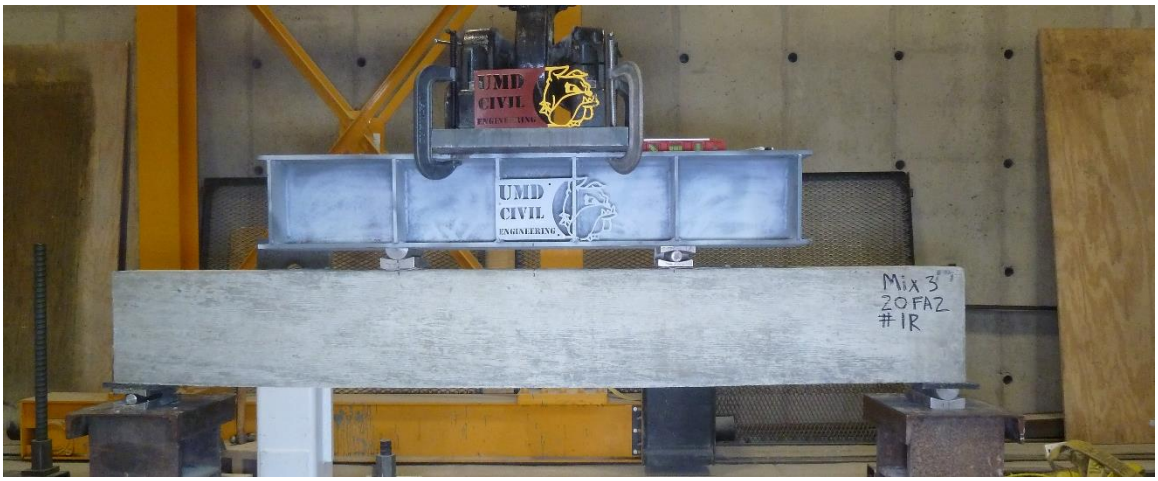


Figure C.13. Mixture 3 (20FA2) beam #1R: concrete beam before testing.


Figure C.14. Mixture 3 (20FA2) beam #1R: concrete beam after testing.

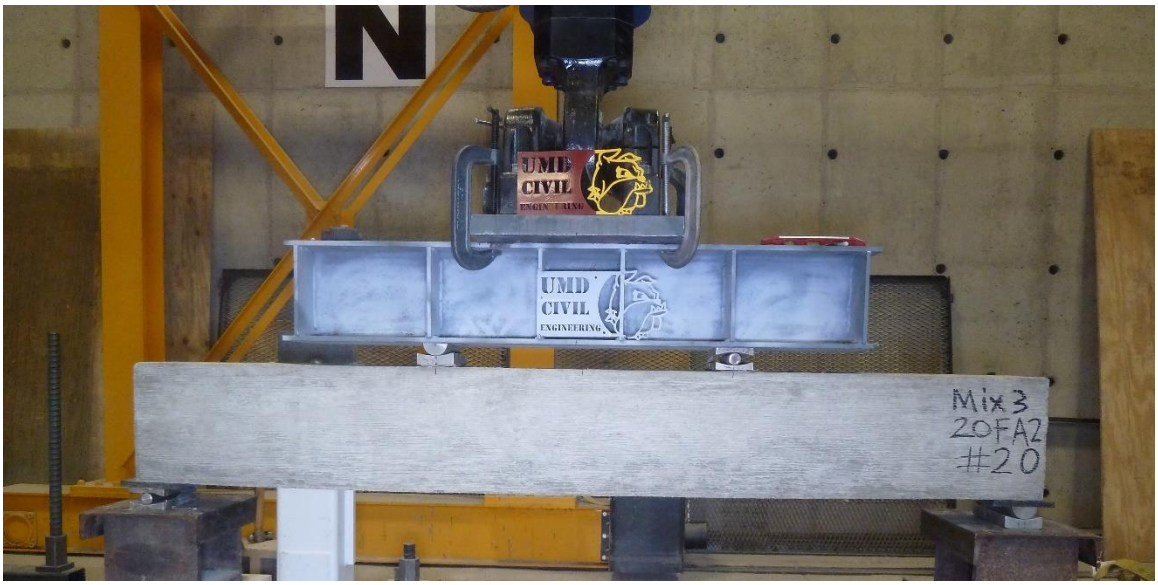


Figure C.15. Mixture 3 (20FA2) beam #2O: concrete beam before testing.


Figure C.16. Mixture 3 (20FA2) beam #2O: concrete beam after testing.

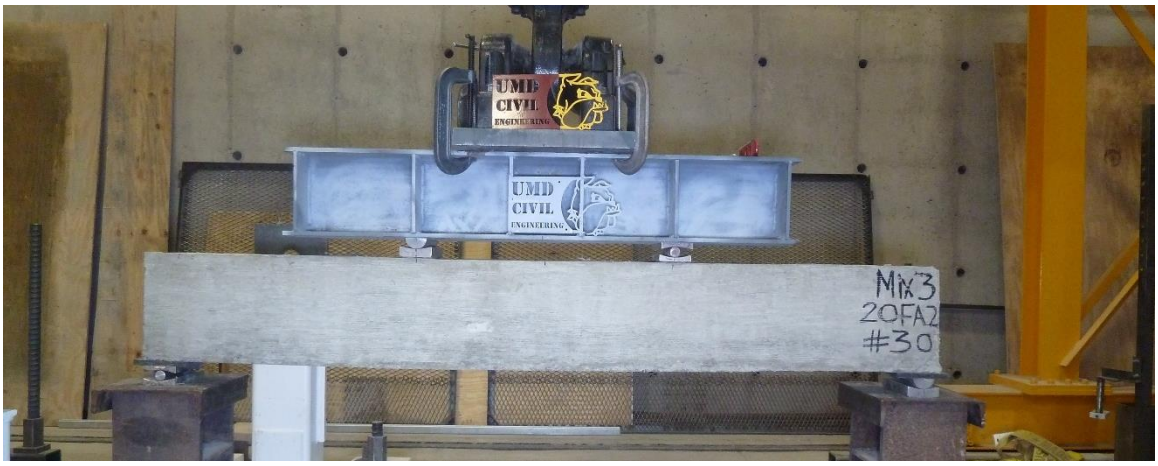


Figure C.17. Mixture 3 (20FA2) beam #3O: concrete beam before testing.

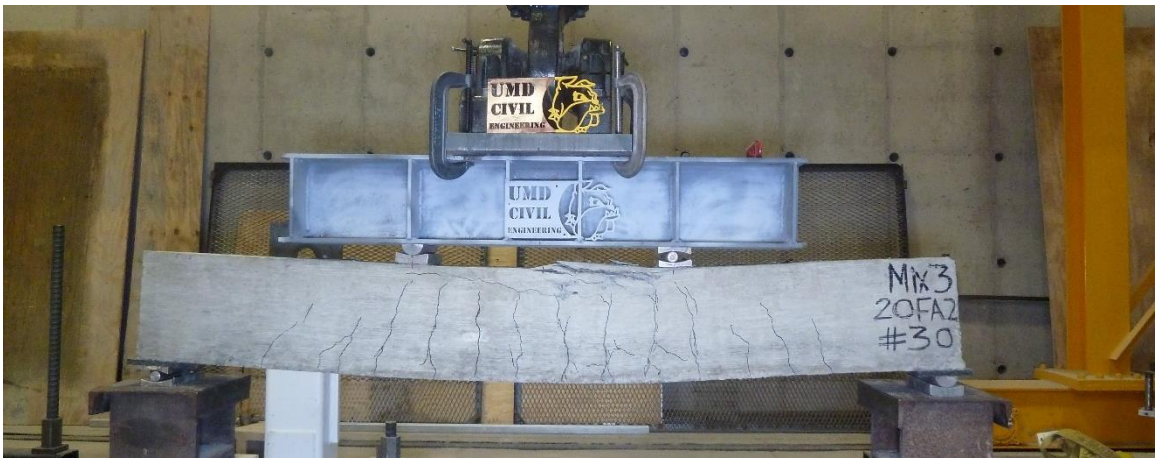


Figure C.18. Mixture 3 (20FA2) beam #3O: concrete beam after testing.


Figure C.19. Mixture 4 (20Q) beam #1R: concrete beam before testing.


Figure C.20. Mixture 4 (20Q) beam #1R: concrete beam after testing.

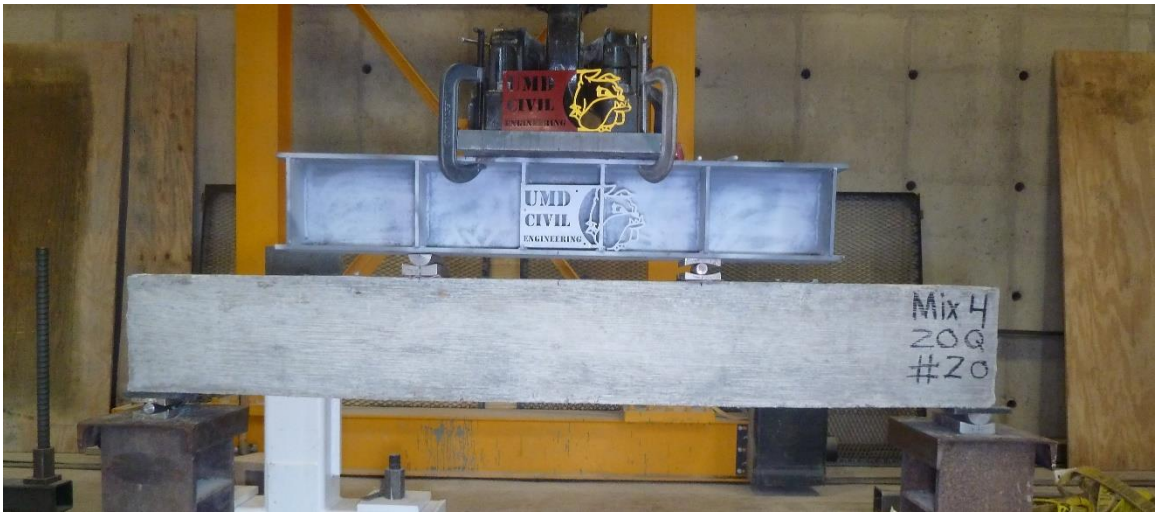


Figure C.21. Mixture 4 (20Q) beam #2O: concrete beam before testing.

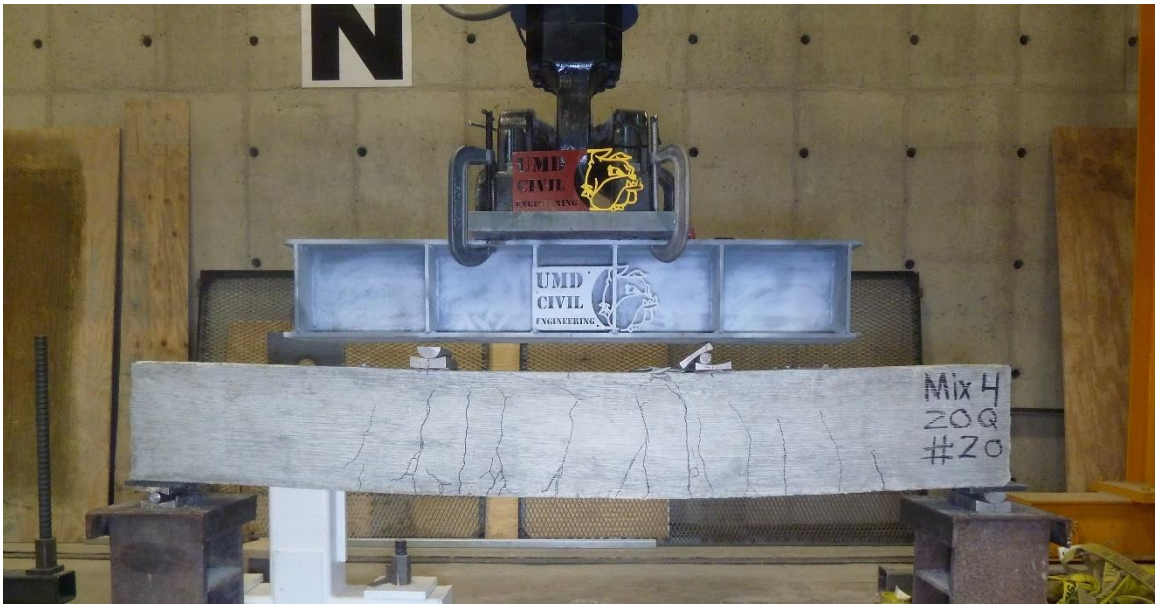


Figure C.22. Mixture 4 (20Q) beam #2O: concrete beam after testing.

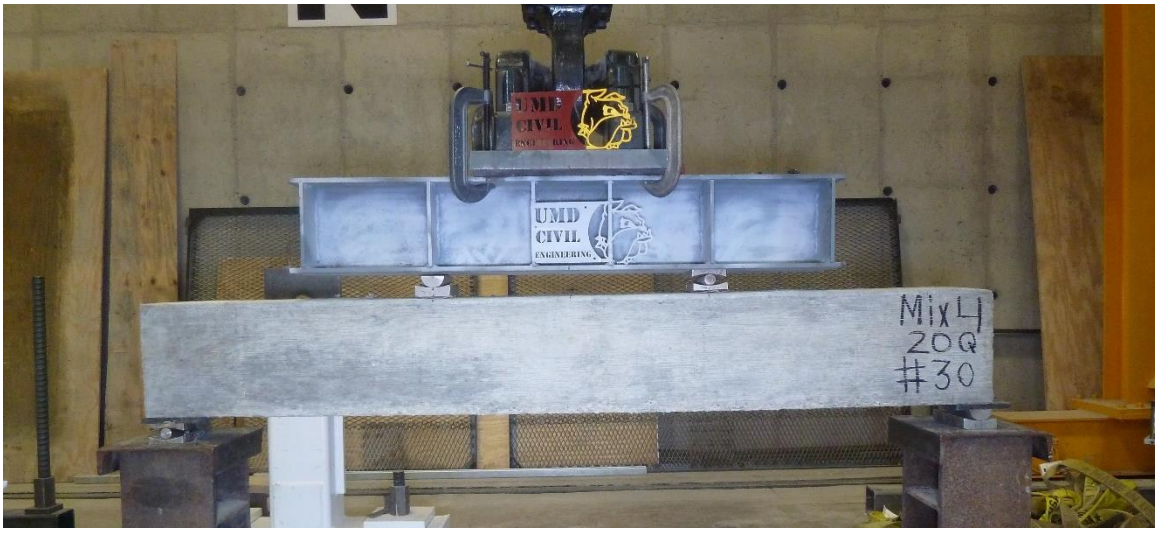


Figure C.23. Mixture 4 (20Q) beam #3O: concrete beam before testing.


Figure C.24. Mixture 4 (20Q) beam #3O: concrete beam after testing.

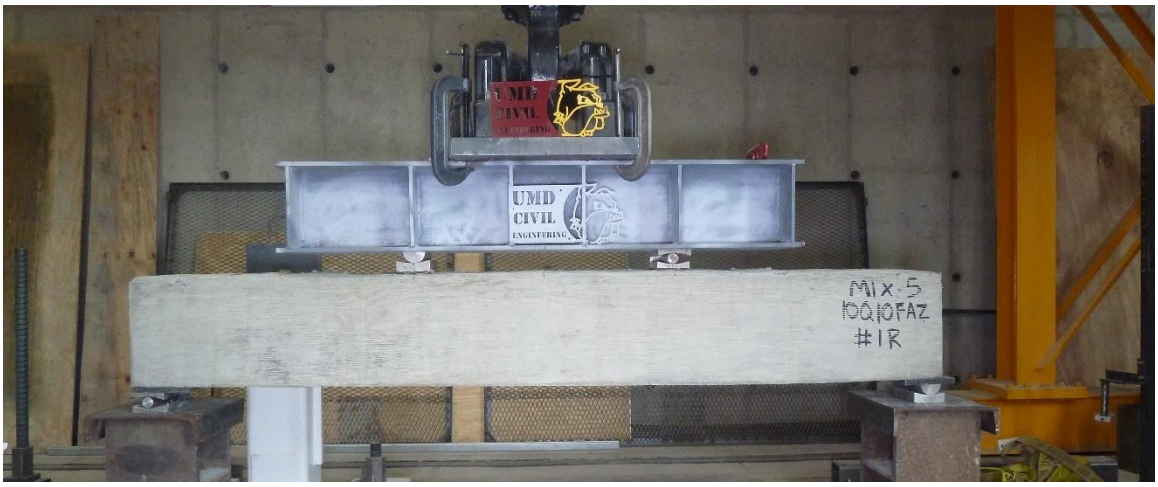


Figure C.25. Mixture 5 (10Q10FA2) beam #1R: concrete beam before testing.


Figure C.26. Mixture 5 (10Q10FA2) beam #1R: concrete beam after testing.

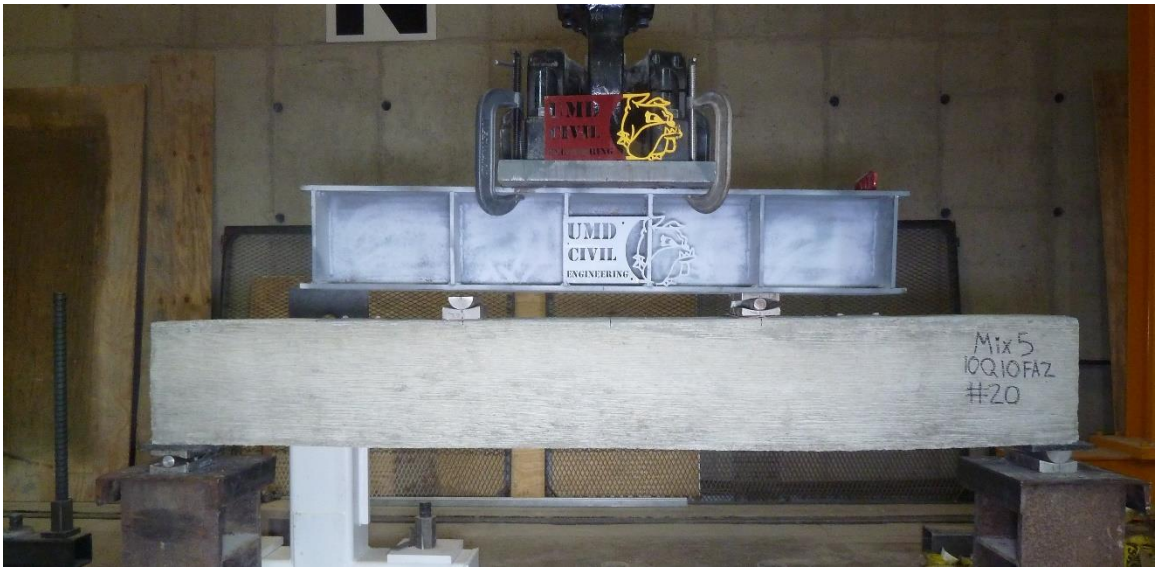


Figure C.27. Mixture 5 (10Q10FA2) beam #2O: concrete beam before testing.


Figure C.28. Mixture 5 (10Q10FA2) beam #2O: concrete beam after testing.

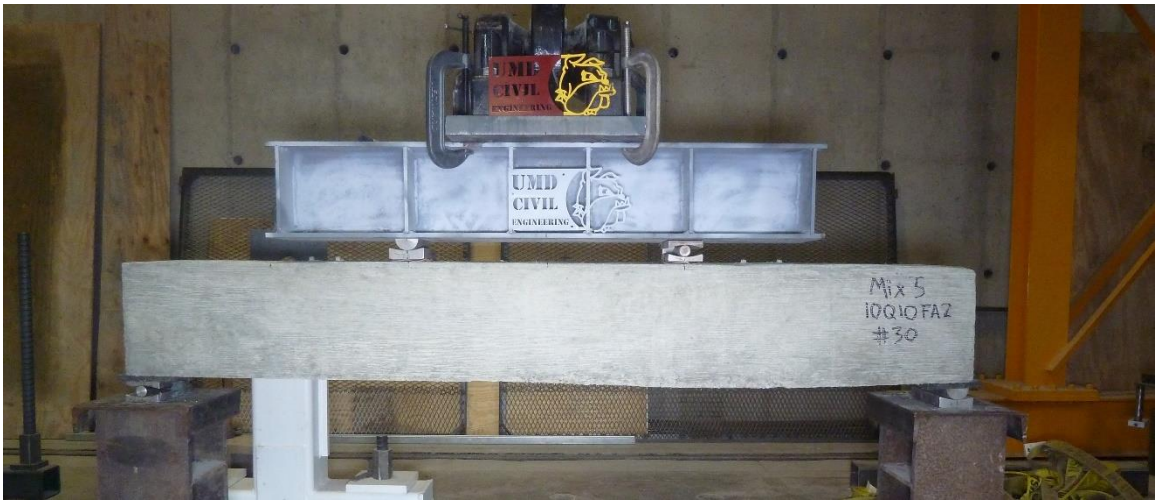


Figure C.29. Mixture 5 (10Q10FA2) beam #3O: concrete beam before testing.

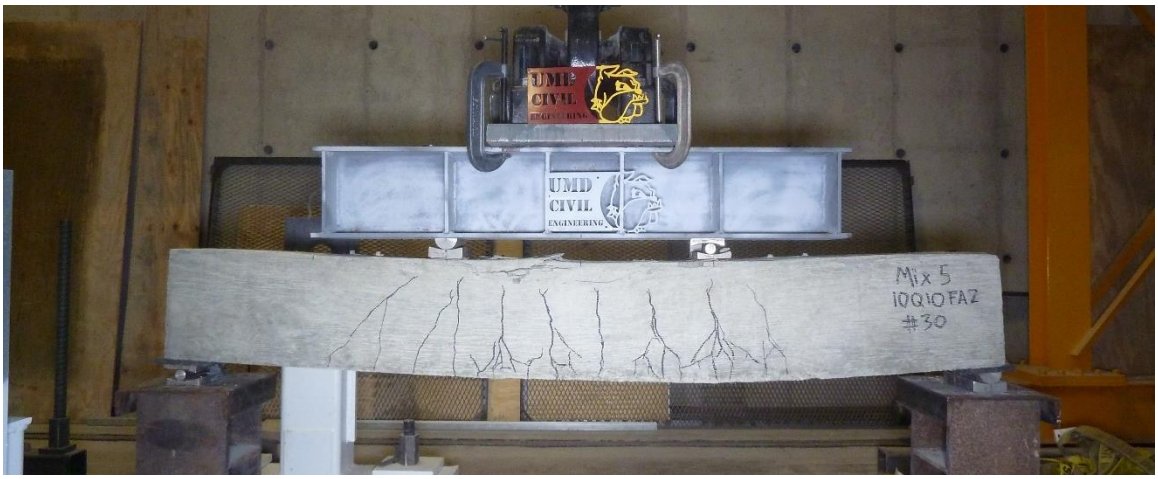


Figure C.30. Mixture 5 (10Q10FA2) beam #3O: concrete beam after testing.


Figure C.31. Mixture 6 (10W10FA2) beam #1R: concrete beam before testing.


Figure C.32. Mixture 6 (10W10FA2) beam #1R: concrete beam after testing.

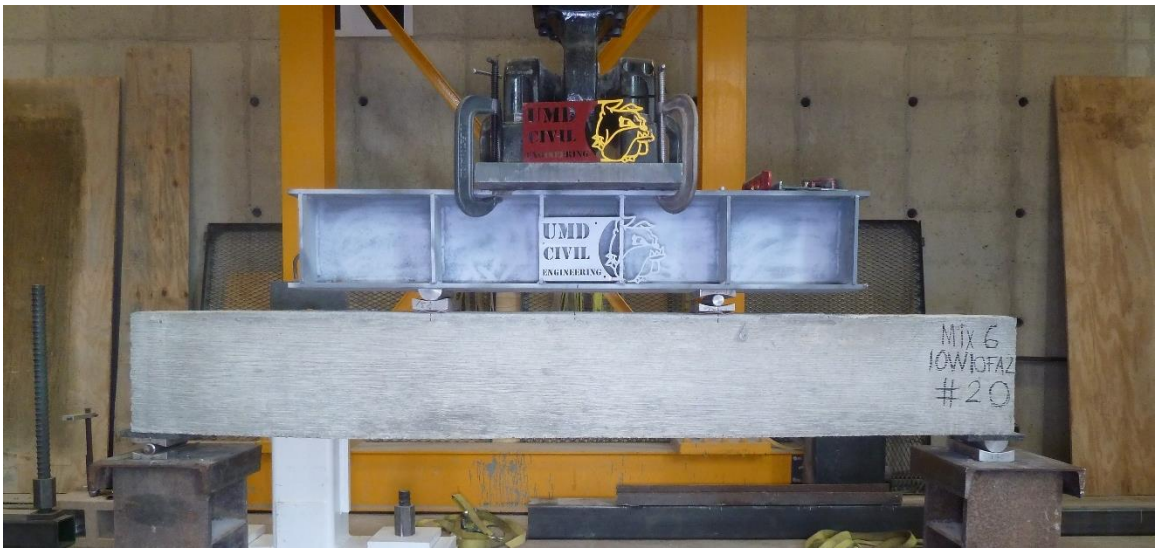


Figure C.33. Mixture 6 (10W10FA2) beam #2O: concrete beam before testing.


Figure C.34. Mixture 6 (10W10FA2) beam #2O: concrete beam after testing.


Figure C.35. Mixture 6 (10W10FA2) beam #3O: concrete beam before testing.


Figure C.36. Mixture 6 (10W10FA2) beam #3O: concrete beam after testing.


Figure C.37. Mixture 7 (20W) beam #1R: concrete beam before testing.


Figure C.38. Mixture 7 (20W) beam #1R: concrete beam after testing.


Figure C.39. Mixture 7 (20W) beam #2O: concrete beam before testing.


Figure C.40. Mixture 7 (20W) beam #2O: concrete beam after testing.


Figure C.41. Mixture 7 (20W) beam #3O: concrete beam before testing.


Figure C.42. Mixture 7 (20W) beam #3O: concrete beam after testing.


Figure C.43. Mixture 8 (10W10FA1) beam #1R: concrete beam before testing.


Figure C.44. Mixture 8 (10W10FA1) beam #1R: concrete beam after testing.


Figure C.45. Mixture 8 (10W10FA1) beam #2O: concrete beam before testing.


Figure C.46. Mixture 8 (10W10FA1) beam #2O: concrete beam after testing.


Figure C.47. Mixture 8 (10W10FA1) beam #3O: concrete beam before testing.


Figure C.48. Mixture 8 (10W10FA1) beam #3O: concrete beam after testing.


Figure C.49. Mixture 8 (20UV) beam #1R: concrete beam before testing.


Figure C.50. Mixture 8 (20UV) beam #1R: concrete beam after testing.


Figure C.51. Mixture 8 (20UV) beam #2O: concrete beam before testing.


Figure C.52. Mixture 8 (20UV) beam #2O: concrete beam after testing.


Figure C.53. Mixture 8 (20UV) beam #3O: concrete beam before testing.


Figure C.54. Mixture 8 (20UV) beam #3O: concrete beam after testing.


Figure C.55. Mixture 10 (10UV10FA2) beam #1R: concrete beam before testing.


Figure C.56. Mixture 10 (10UV10FA2) beam #1R: concrete beam after testing.

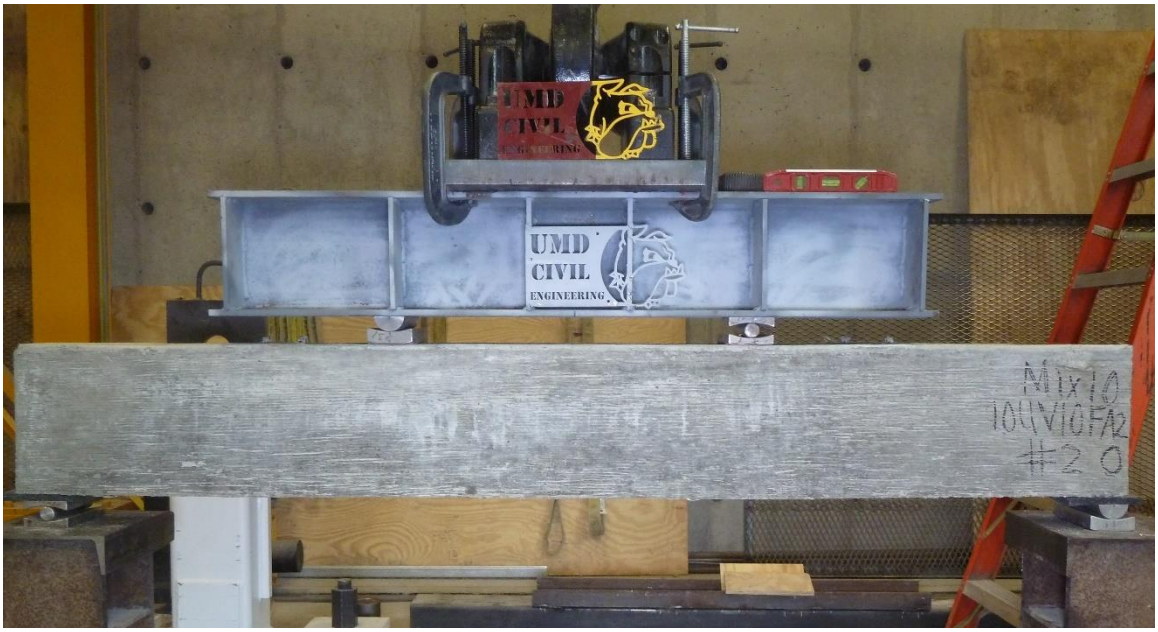


Figure C.57. Mixture 10 (10UV10FA2) beam #2O: concrete beam before testing.


Figure C.58. Mixture 10 (10UV10FA2) beam #2O: concrete beam after testing.


Figure C.59. Mixture 10 (10UV10FA2) beam #3O: concrete beam before testing.

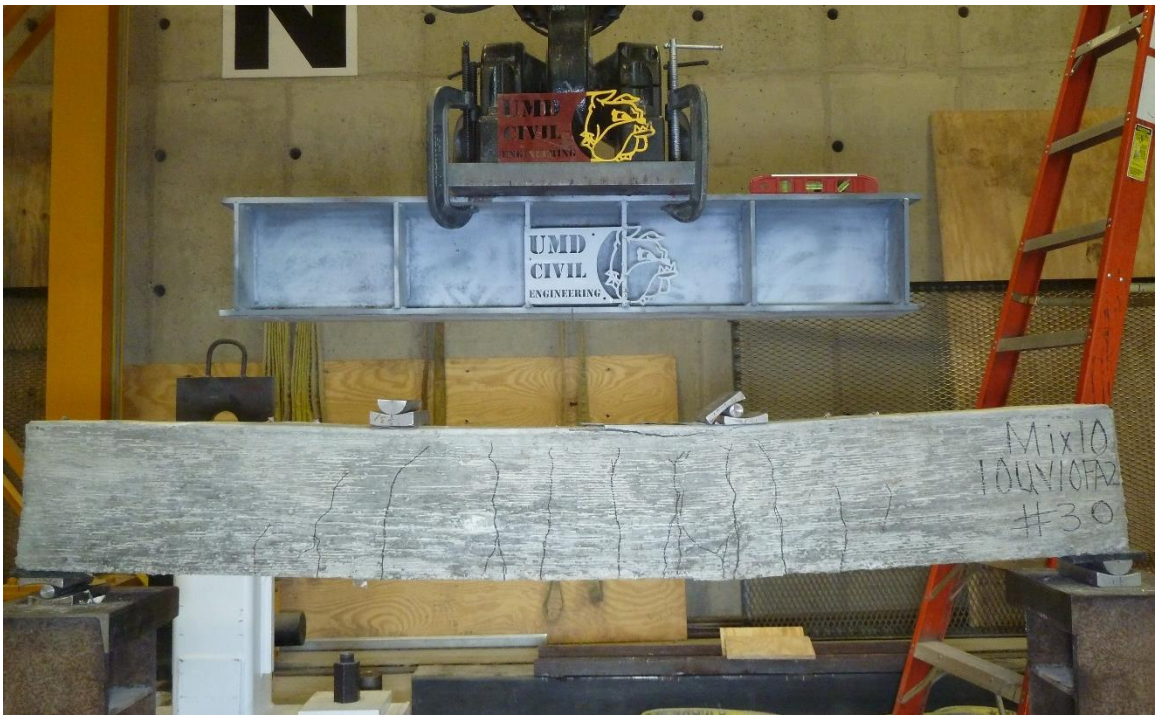


Figure C.60. Mixture 10 (10UV10FA2) beam #3O: concrete beam after testing.

# Appendix D Concrete Beam Crack Patterns

Figure D.1. Mixture 1 (100PC) beam #1R: concrete beam top view.

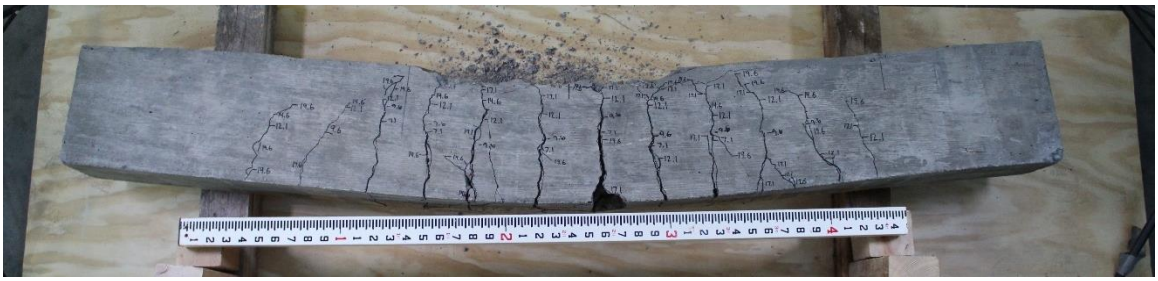

Figure D.2. Mixture 1 (100PC) beam #1R: concrete beam side view.

Figure D.3. Mixture 1 (100PC) beam #1R: concrete beam bottom view.

Figure D.4. Mixture 1 (100PC) beam #2O: concrete beam top view.

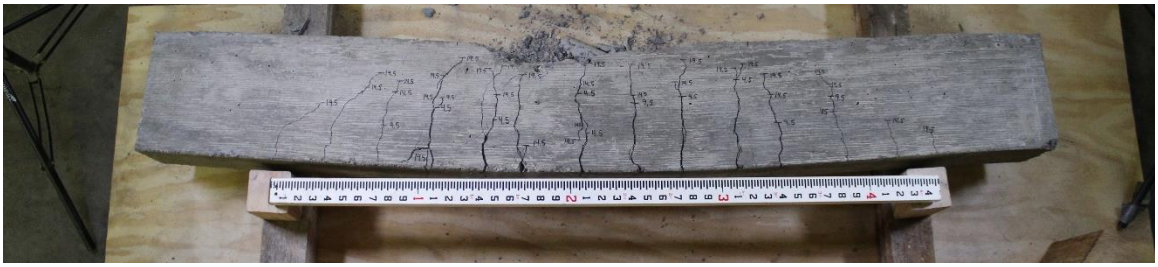

Figure D.5. Mixture 1 (100PC) beam #2O: concrete beam side view.

Figure D.6. Mixture 1 (100PC) beam #2O: concrete beam bottom view.

Figure D.7. Mixture 1 (100PC) beam #3O: concrete beam top view.

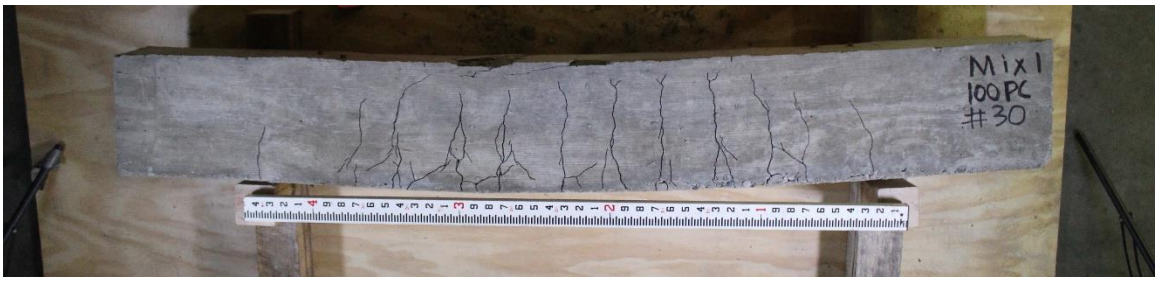


Figure D.8. Mixture 1 (100PC) beam #3O: concrete beam side view.

Figure D.9. Mixture 1 (100PC) beam #3O: concrete beam bottom view.

Figure D.10. Mixture 2 (20FA1) beam #1R: concrete beam top view.

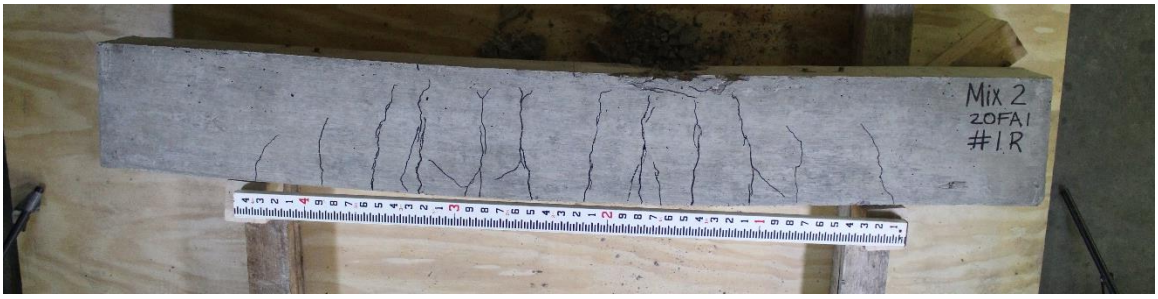


Figure D.11. Mixture 2 (20FA1) beam #1R: concrete beam side view.

Figure D.12. Mixture 2 (20FA1) beam #1R: concrete beam bottom view.

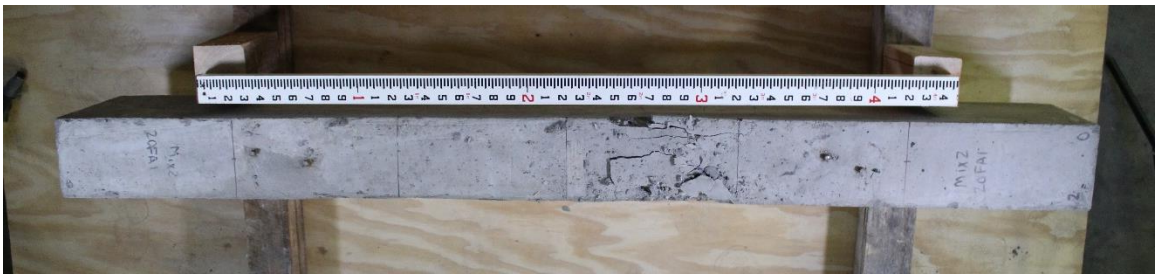

Figure D.13. Mixture 2 (20FA1) beam #2O: concrete beam top view.

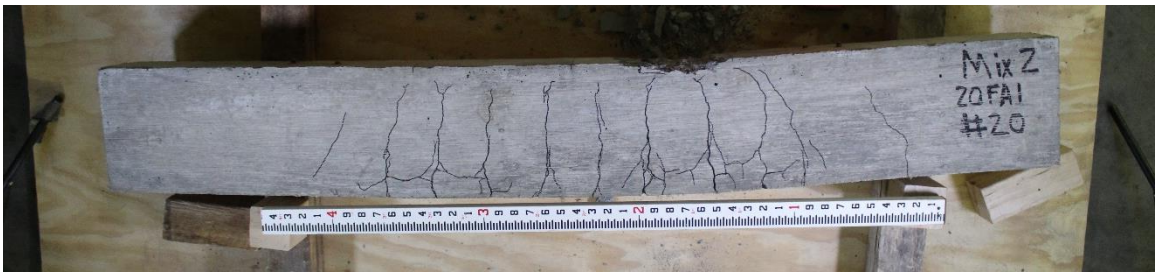


Figure D.14. Mixture 2 (20FA1) beam #2O: concrete beam side view.

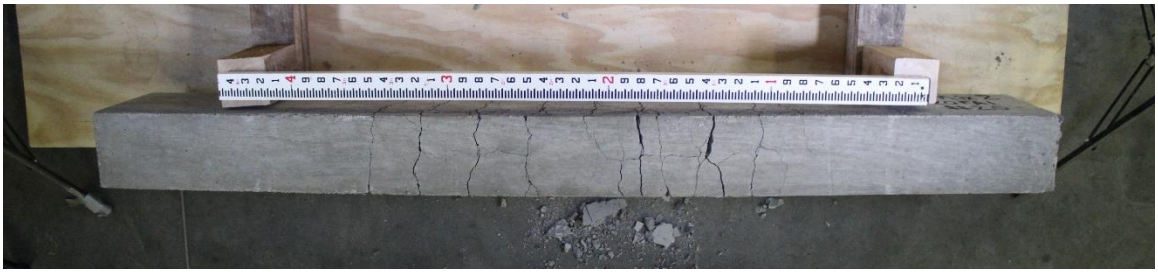

Figure D.15. Mixture 2 (20FA1) beam #2O: concrete beam bottom view.

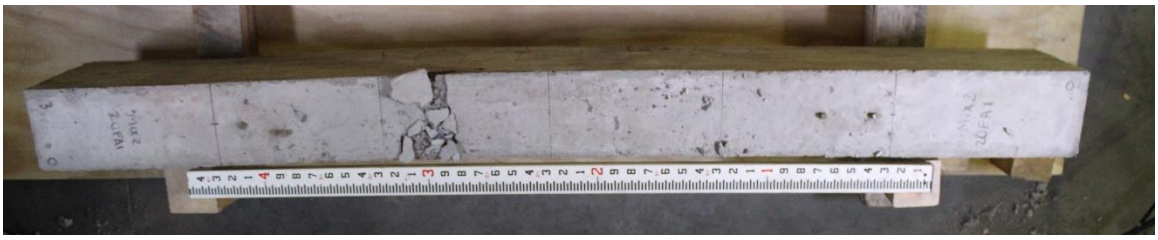

Figure D.16. Mixture 2 (20FA1) beam #3O: concrete beam top view.

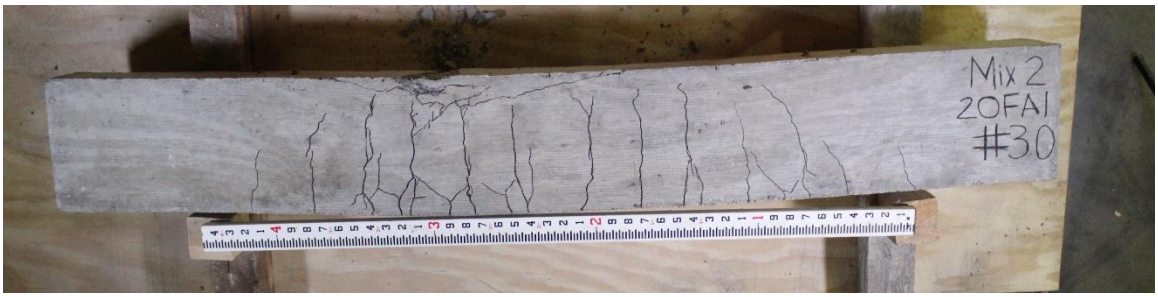


Figure D.17. Mixture 2 (20FA1) beam #3O: concrete beam side view.

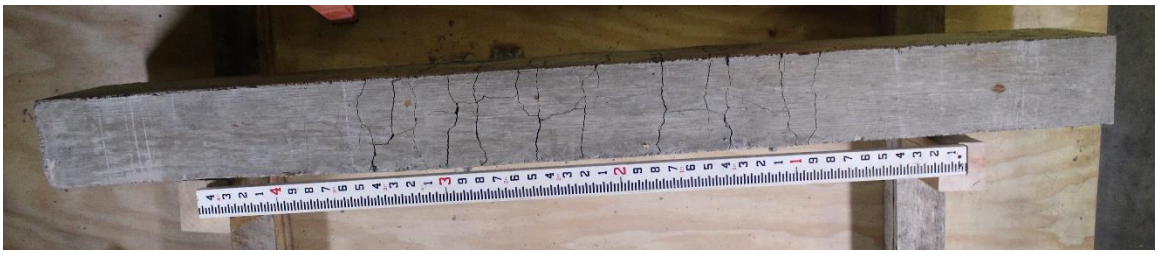

Figure D.18. Mixture 2 (20FA1) beam #3O: concrete beam bottom view.

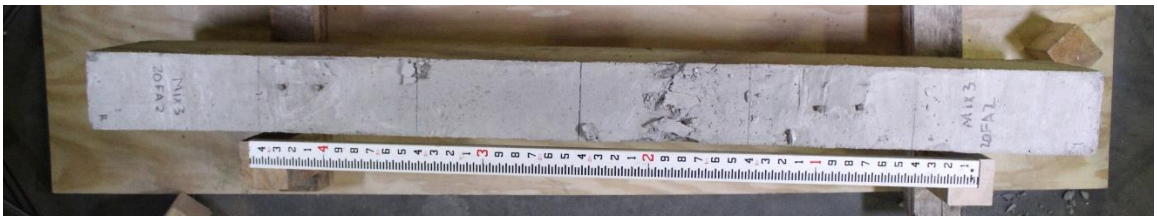

Figure D.19. Mixture 3 (20FA2) beam #1R: concrete beam top view.

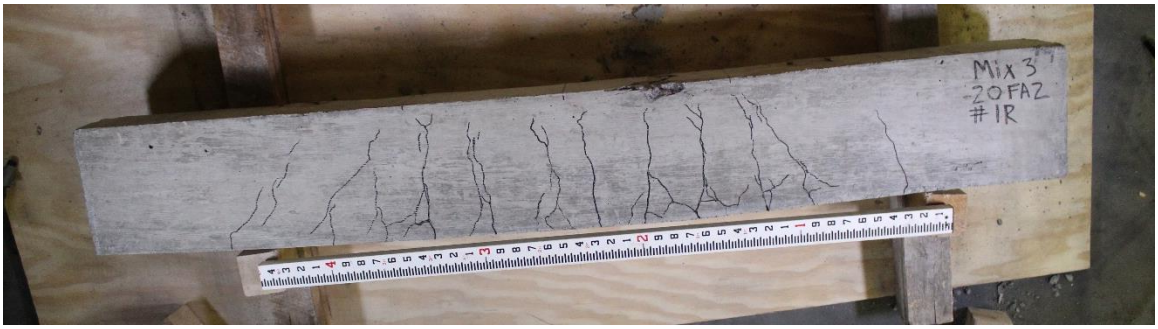


Figure D.20. Mixture 3 (20FA2) beam #1R: concrete beam side view.

Figure D.21. Mixture 3 (20FA2) beam #1R: concrete beam bottom view.

Figure D.22. Mixture 3 (20FA2) beam #2O: concrete beam top view.


Figure D.23. Mixture 3 (20FA2) beam #2O: concrete beam side view.

Figure D.24. Mixture 3 (20FA2) beam #2O: concrete beam bottom view.

Figure D.25. Mixture 3 (20FA2) beam #3O: concrete beam top view.

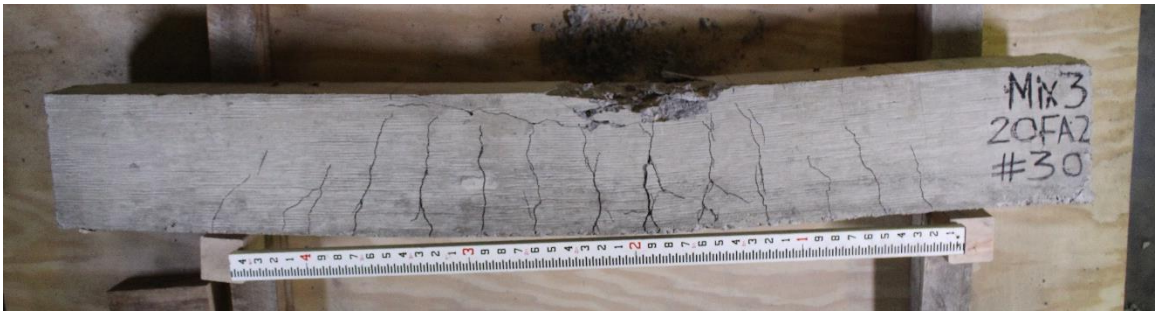


Figure D.26. Mixture 3 (20FA2) beam #3O: concrete beam side view.

Figure D.27. Mixture 3 (20FA2) beam #3O: concrete beam bottom view.

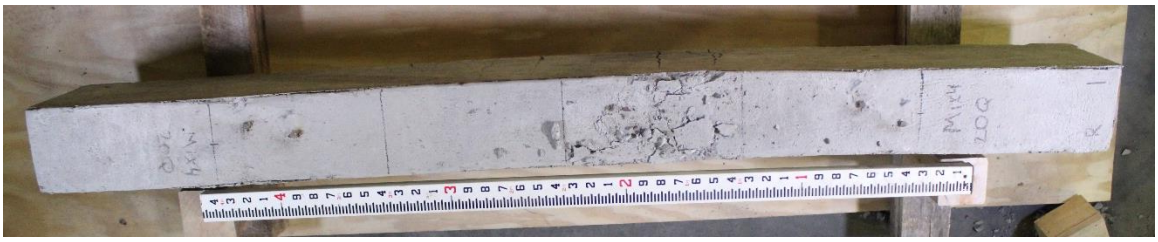

Figure D.28. Mixture 4 (20Q) beam #1R: concrete beam top view.

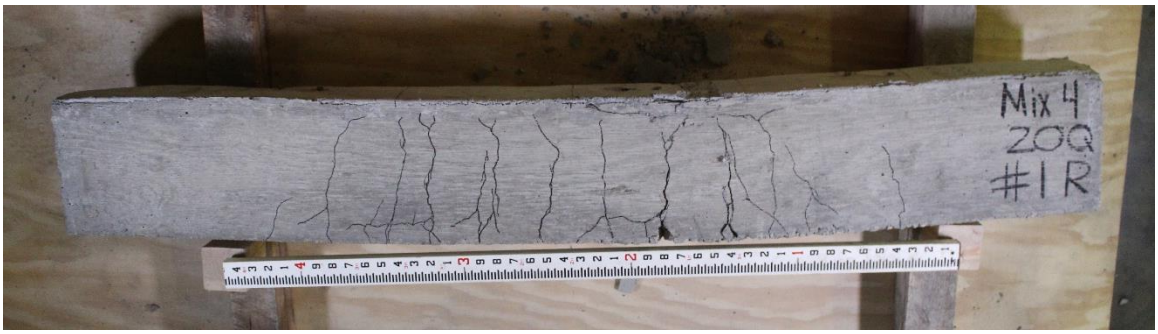


Figure D.29. Mixture 4 (20Q) beam #1R: concrete beam side view.

Figure D.30. Mixture 4 (20Q) beam #1R: concrete beam bottom view.

Figure D.31. Mixture 4 (20Q) beam #2O: concrete beam top view.

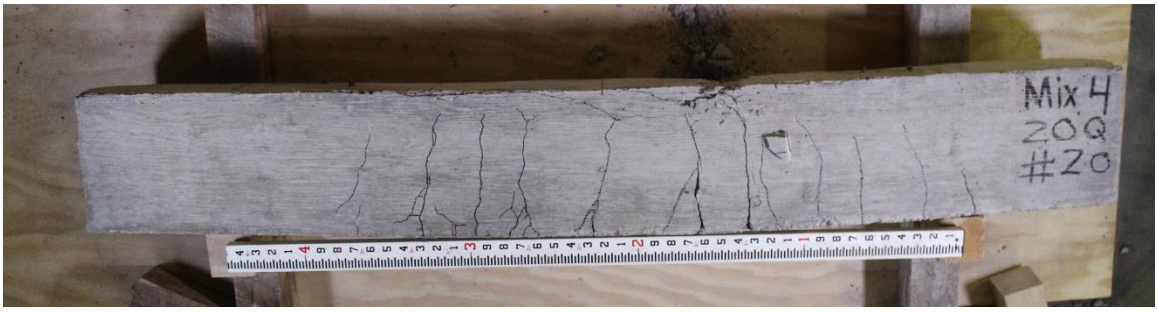


Figure D.32. Mixture 4 (20Q) beam #2O: concrete beam side view.

Figure D.33. Mixture 4 (20Q) beam #2O: concrete beam bottom view.

Figure D.34. Mixture 4 (20Q) beam #3O: concrete beam top view.

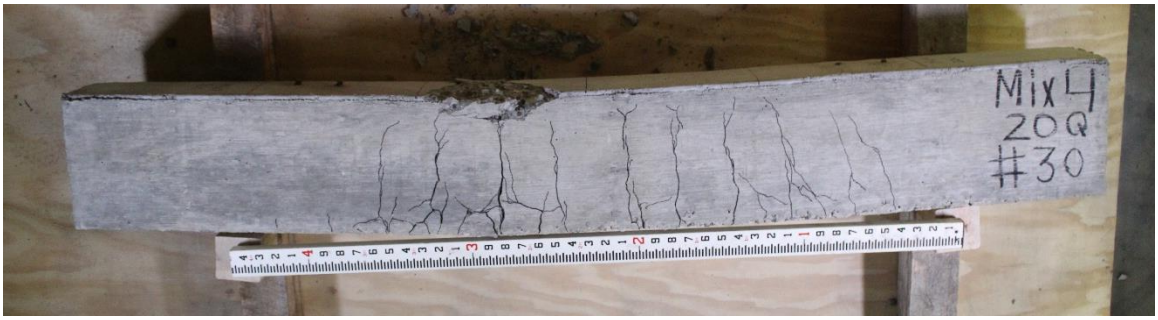


Figure D.35. Mixture 4 (20Q) beam #3O: concrete beam side view.

Figure D.36. Mixture 4 (20Q) beam #3O: concrete beam bottom view.

Figure D.37. Mixture 5 (10Q10FA2) beam #1R: concrete beam top view.

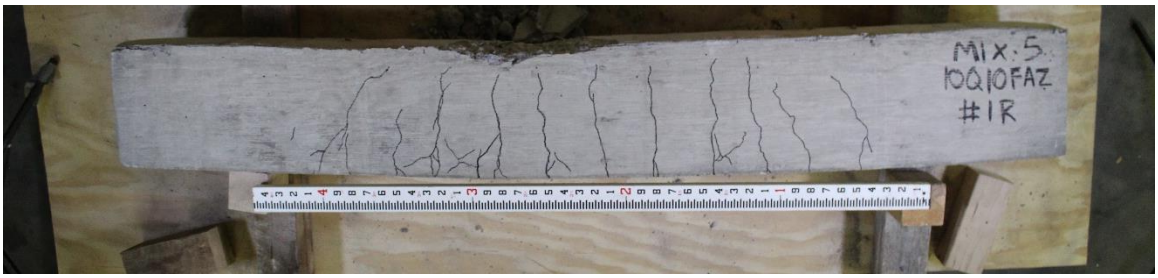


Figure D.38. Mixture 5 (10Q10FA2) beam #1R: concrete beam side view.

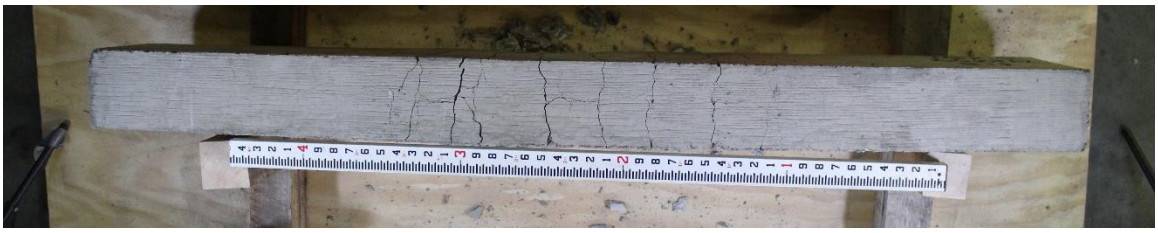

Figure D.39. Mixture 5 (10Q10FA2) beam #1R: concrete beam bottom view.

Figure D.40. Mixture 5 (10Q10FA2) beam #2O: concrete beam top view.

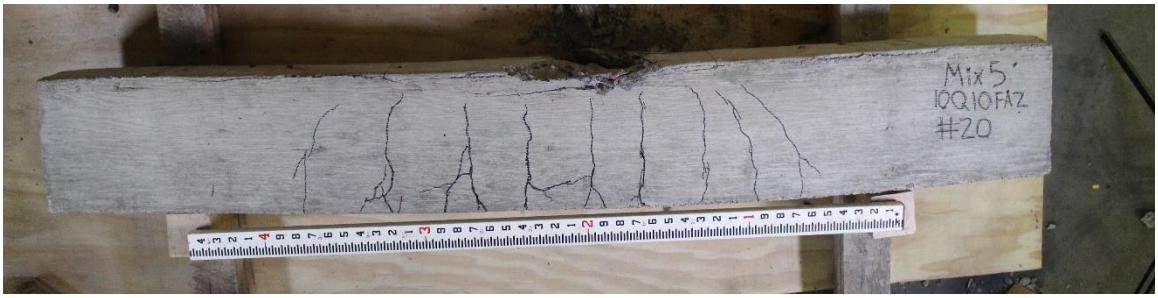


Figure D.41. Mixture 5 (10Q10FA2) beam #2O: concrete beam side view.

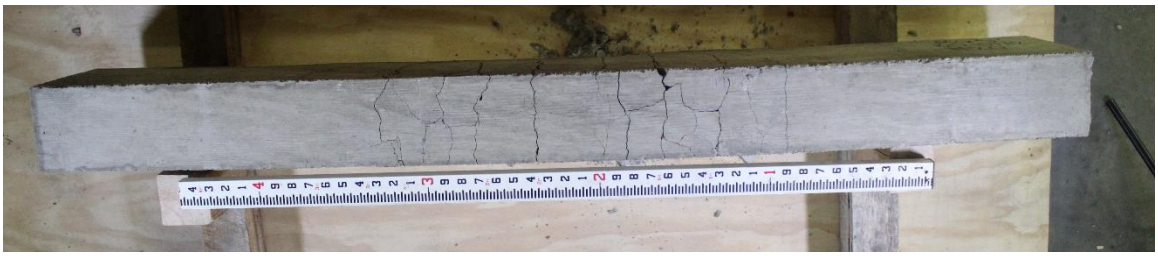

Figure D.42. Mixture 5 (10Q10FA2) beam #2O: concrete beam bottom view.

Figure D.43. Mixture 5 (10Q10FA2) beam #3O: concrete beam top view.

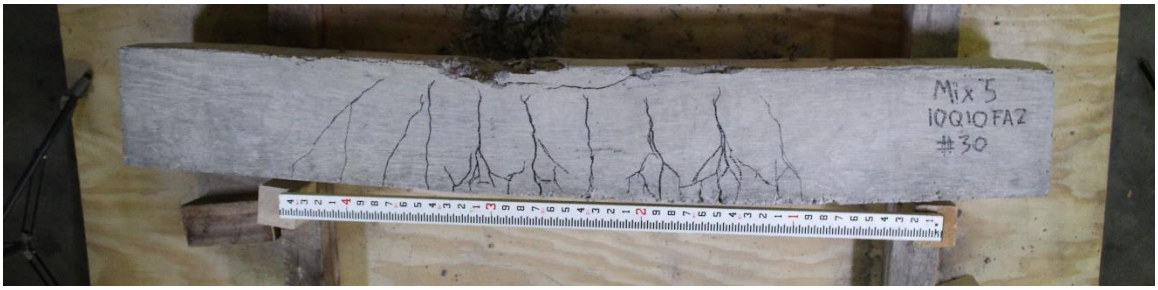


Figure D.44. Mixture 5 (10Q10FA2) beam #3O: concrete beam side view.

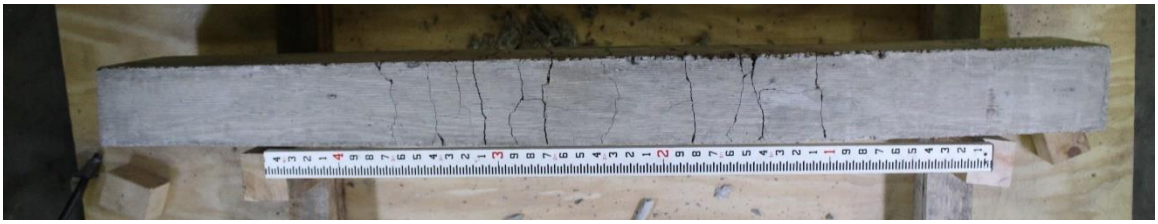

Figure D.45. Mixture 5 (10Q10FA2) beam #3O: concrete beam bottom view.

Figure D.46. Mixture 6 (10W10FA2) beam #1R: concrete beam top view.

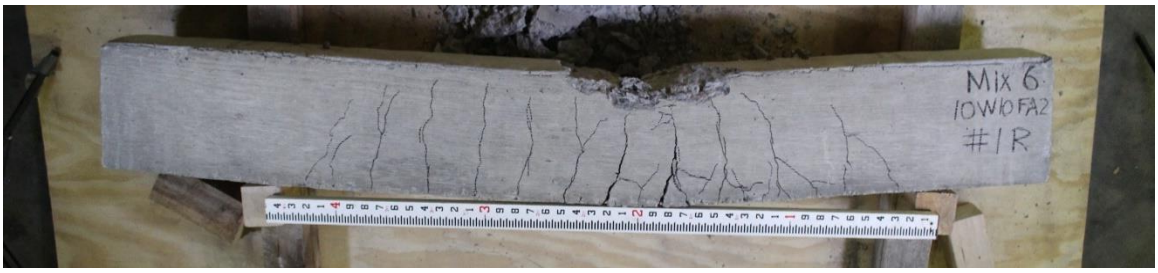


Figure D.47. Mixture 6 (10W10FA2) beam #1R: concrete beam side view.

Figure D.48. Mixture 6 (10W10FA2) beam #1R: concrete beam bottom view.

Figure D.49. Mixture 6 (10W10FA2) beam #2O: concrete beam top view.


Figure D.50. Mixture 6 (10W10FA2) beam #2O: concrete beam side view.

Figure D.51. Mixture 6 (10W10FA2) beam #2O: concrete beam bottom view.

Figure D.52. Mixture 6 (10W10FA2) beam #3O: concrete beam top view.

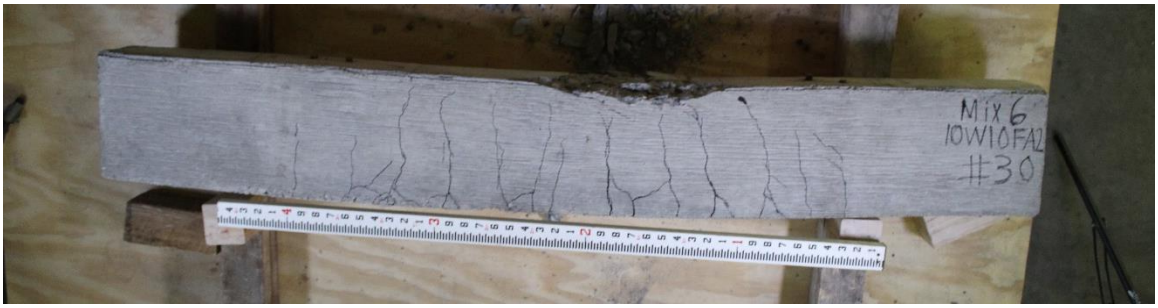


Figure D.53. Mixture 6 (10W10FA2) beam #3O: concrete beam side view.

Figure D.54. Mixture 6 (10W10FA2) beam #3O: concrete beam bottom view.

Figure D.55. Mixture 7 (20W) beam #1R: concrete beam top view.

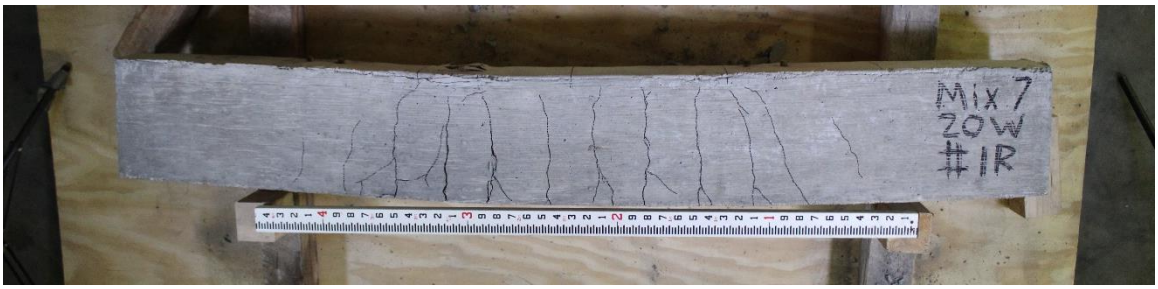


Figure D.56. Mixture 7 (20W) beam #1R: concrete beam side view.

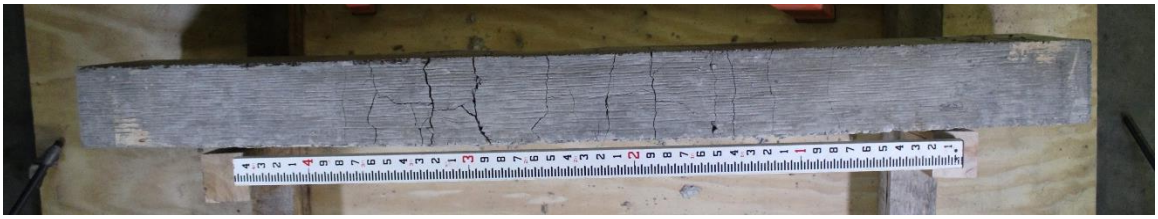

Figure D.57. Mixture 7 (20W) beam #1R: concrete beam bottom view.

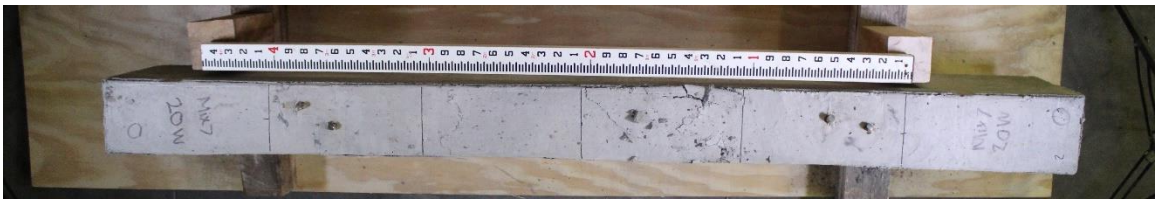

Figure D.58. Mixture 7 (20W) beam #2O: concrete beam top view.

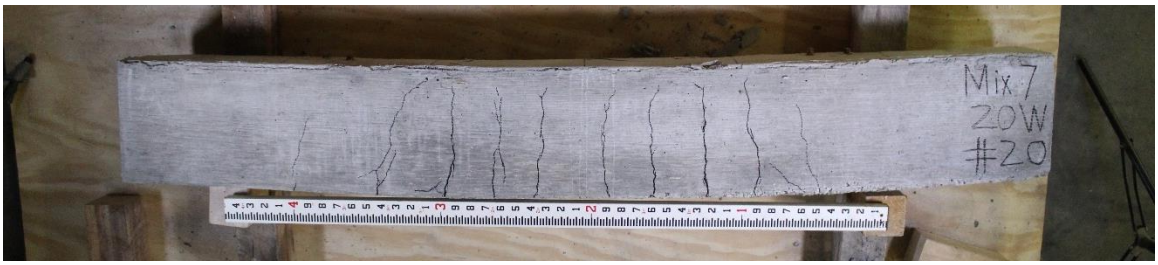


Figure D.59. Mixture 7 (20W) beam #2O: concrete beam side view.

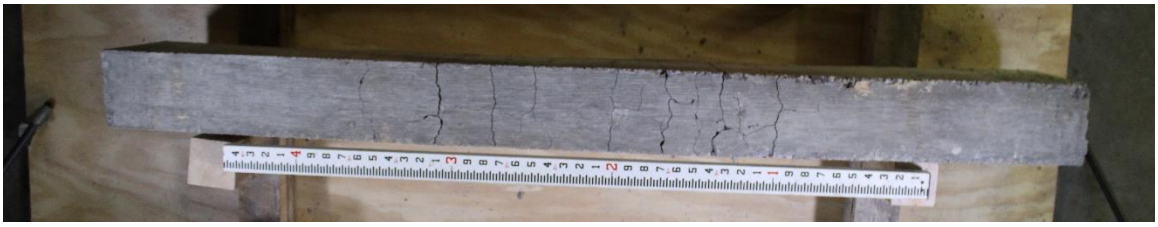

Figure D.60. Mixture 7 (20W) beam #2O: concrete beam bottom view.


Figure D.61. Mixture 7 (20W) beam #3O: concrete beam top view.

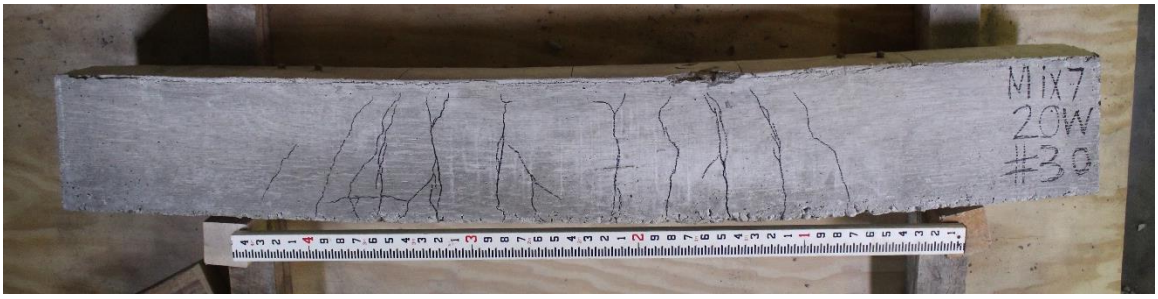


Figure D.62. Mixture 7 (20W) beam #3O: concrete beam side view.

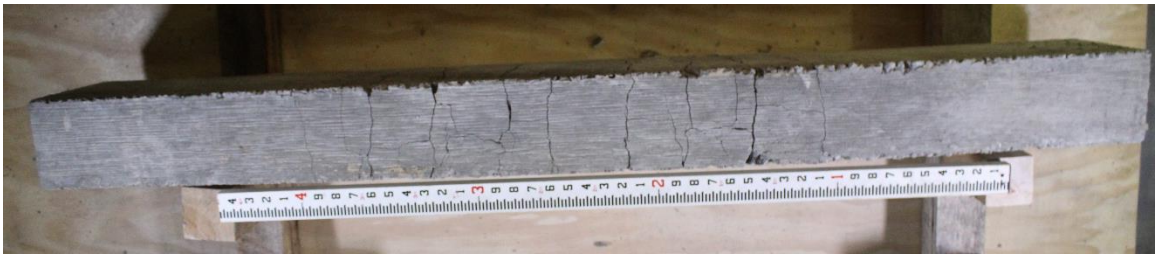

Figure D.63. Mixture 7 (20W) beam #3O: concrete beam bottom view.

Figure D.64. Mixture 8 (10W10FA1) beam #1R: concrete beam top view.

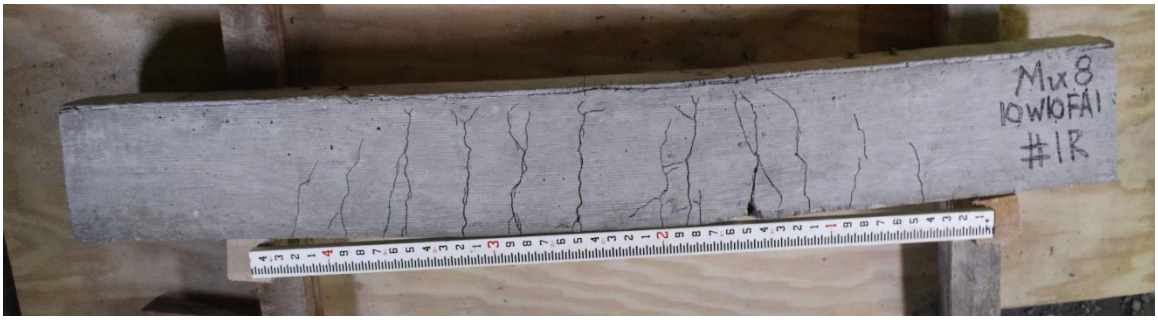


Figure D.65. Mixture 8 (10W10FA1) beam #1R: concrete beam side view.

Figure D.66. Mixture 8 (10W10FA1) beam #1R: concrete beam bottom view.

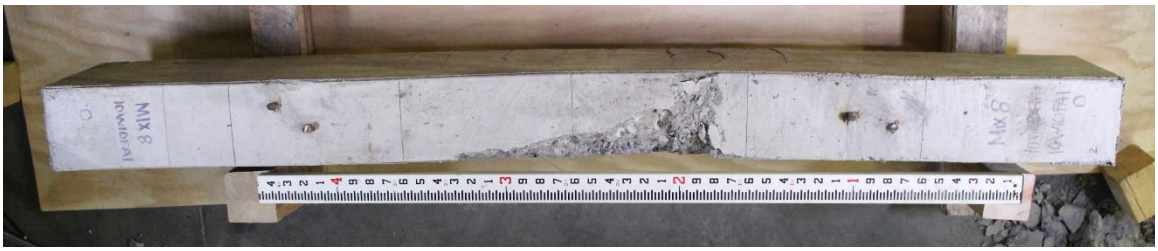

Figure D.67. Mixture 8 (10W10FA1) beam #2O: concrete beam top view.


Figure D.68. Mixture 8 (10W10FA1) beam #2O: concrete beam side view.

Figure D.69. Mixture 8 (10W10FA1) beam #2O: concrete beam bottom view.

Figure D.70. Mixture 8 (10W10FA1) beam #3O: concrete beam top view.

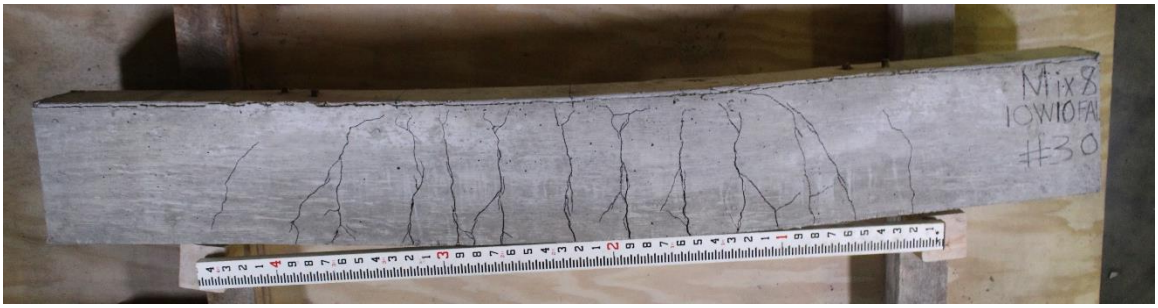


Figure D.71. Mixture 8 (10W10FA1) beam #3O: concrete beam side view.

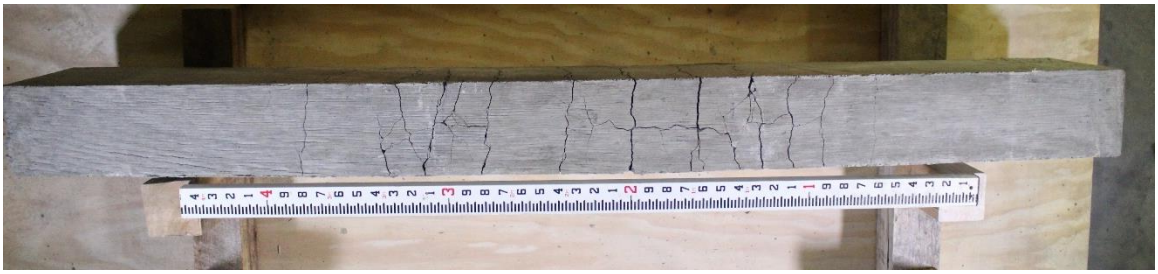

Figure D.72. Mixture 8 (10W10FA1) beam #3O: concrete beam bottom view.

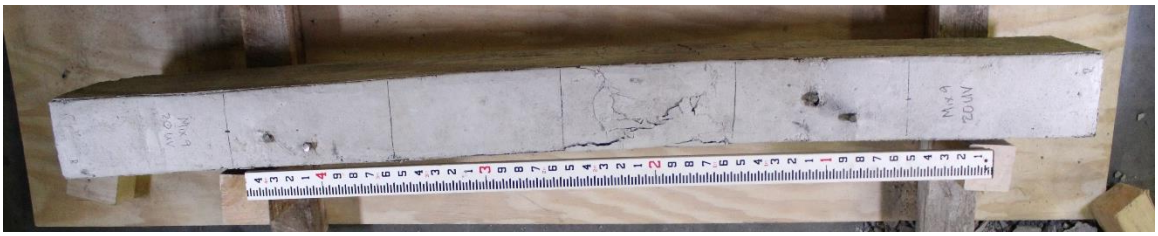

Figure D.73. Mixture 9 (20UV) beam #1R: concrete beam top view.

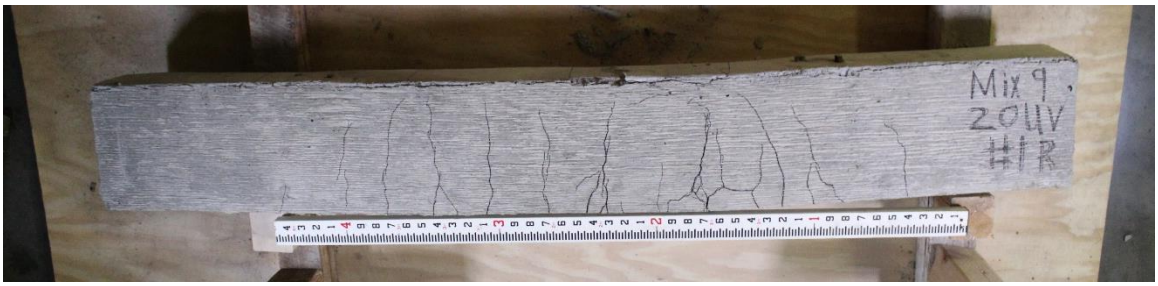


Figure D.74. Mixture 9 (20UV) beam #1R: concrete beam side view.

Figure D.75. Mixture 9 (20UV) beam #1R: concrete beam bottom view.

Figure D.76. Mixture 9 (20UV) beam #2O: concrete beam top view.

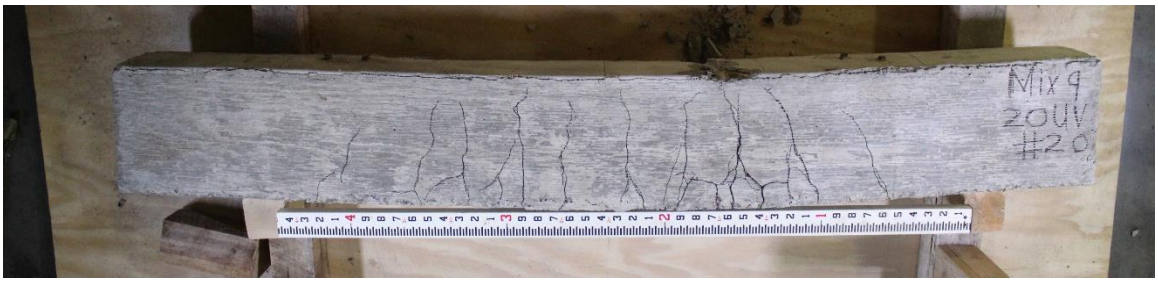


Figure D.77. Mixture 9 (20UV) beam #2O: concrete beam side view.

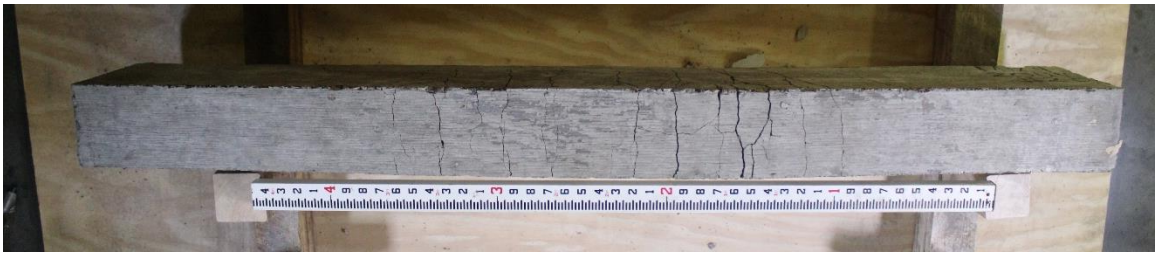

Figure D.78. Mixture 9 (20UV) beam #2O: concrete beam bottom view.

Figure D.79. Mixture 9 (20UV) beam #3O: concrete beam top view.

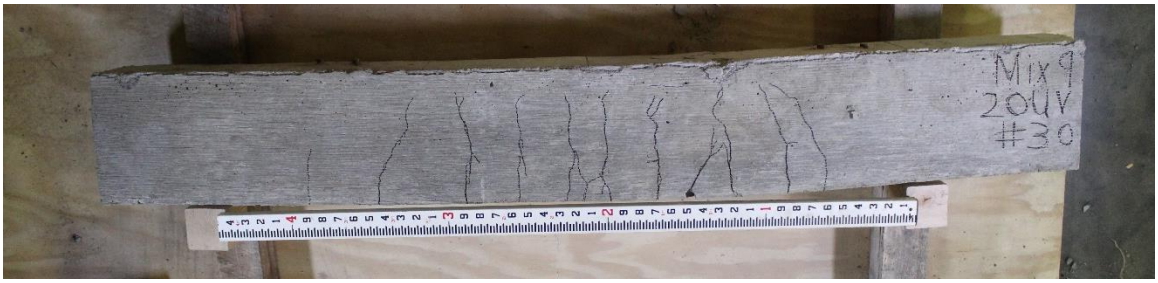


Figure D.80. Mixture 9 (20UV) beam #3O: concrete beam side view.

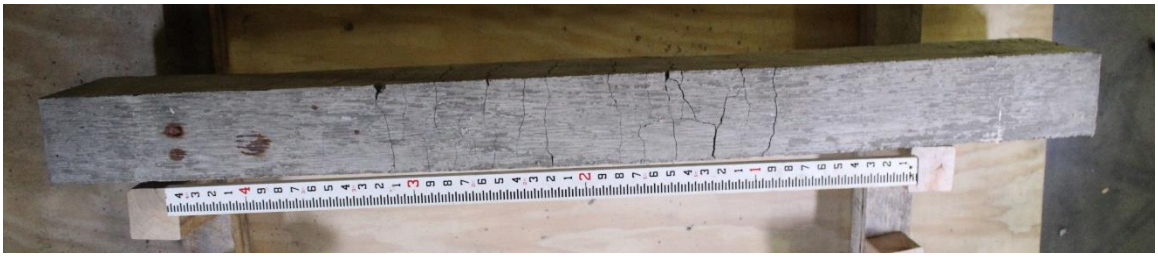

Figure D.81. Mixture 9 (20UV) beam #3O: concrete beam bottom view.

Figure D.82. Mixture 10 (10UV10FA2) beam #1R: concrete beam top view.

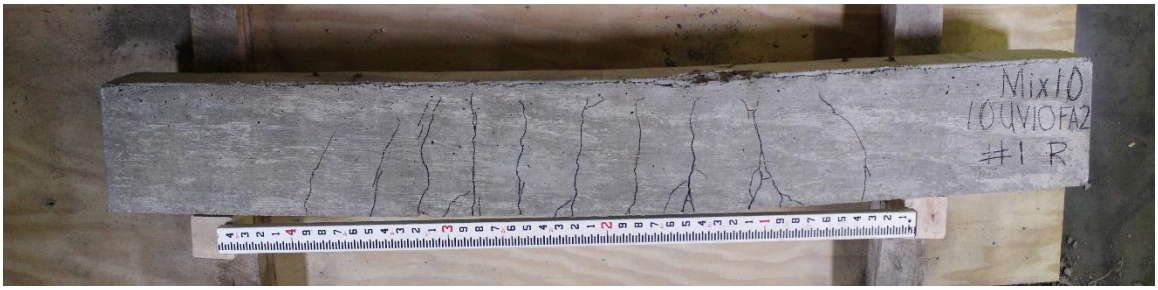


Figure D.83. Mixture 10 (10UV10FA2) beam #1R: concrete beam side view.

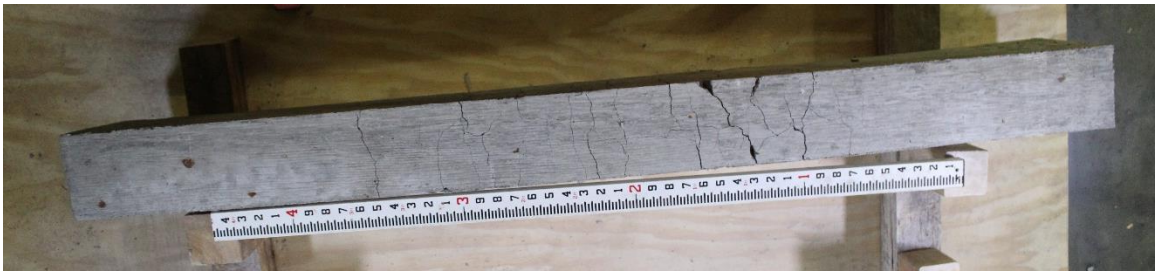

Figure D.84. Mixture 10 (10UV10FA2) beam #1R: concrete beam bottom view.

Figure D.85. Mixture 10 (10UV10FA2) beam #2O: concrete beam top view.

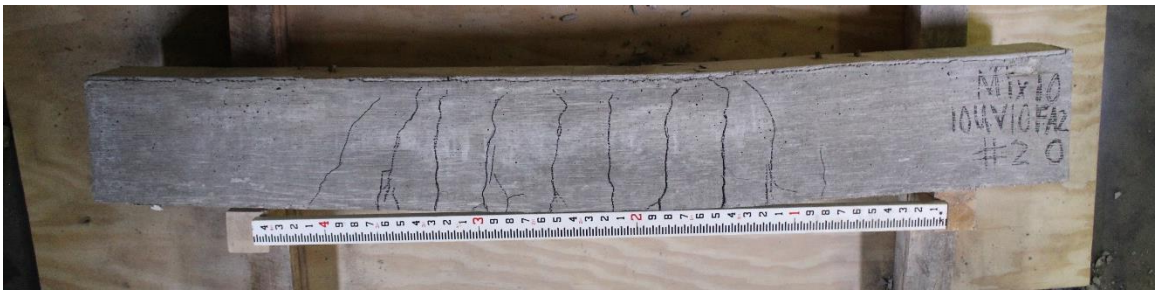


Figure D.86. Mixture 10 (10UV10FA2) beam #2O: concrete beam side view.

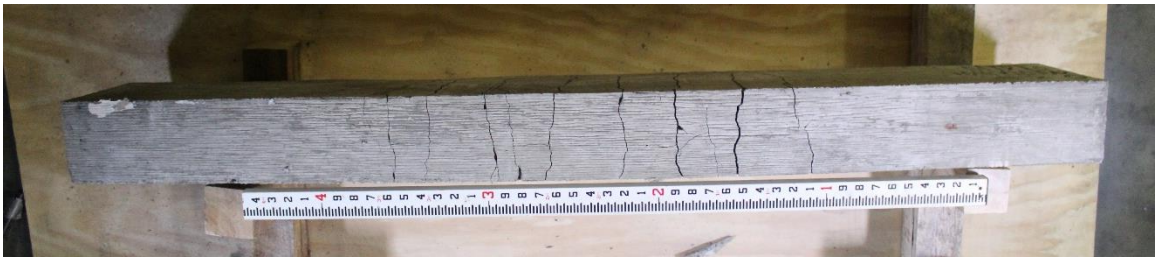

Figure D.87. Mixture 10 (10UV10FA2) beam #2O: concrete beam bottom view.

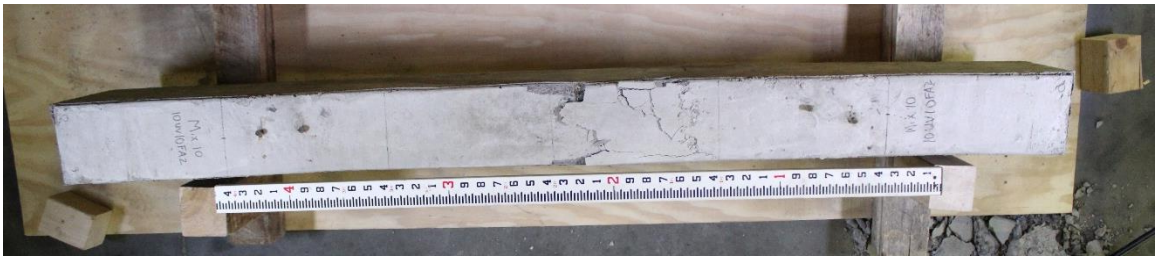

Figure D.88. Mixture 10 (10UV10FA2) beam #3O: concrete beam top view.

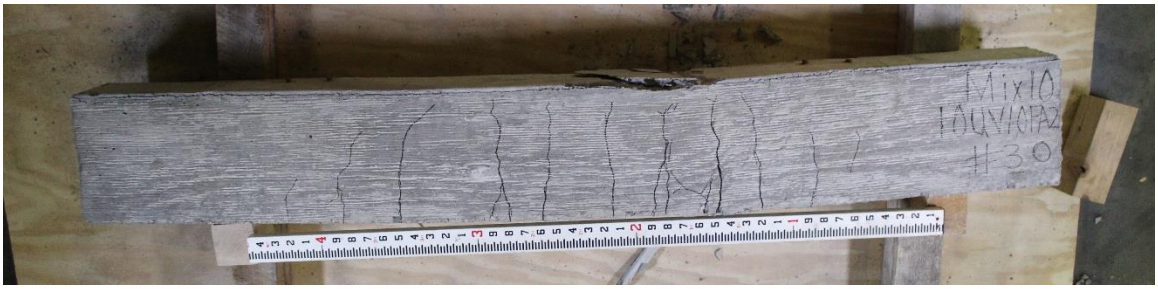


Figure D.89. Mixture 10 (10UV10FA2) beam #3O: concrete beam side view.

Figure D.90. Mixture 10 (10UV10FA2) beam #3O: concrete beam bottom view.

# Appendix E Calculations

Equations per ACI 318 (2014)

**Average Nominal Flexural Strength of Control Beams**

Width of compression face of member $b = 6.07\ in$

Overall height of member $h = 10.20\ in$

Distance from extreme compression fiber to centroid of longitudinal tension reinforcement $d = 8.95\ in$

Measured yield strength for nonprestressed reinforcement $f_y = 90{,}000\ psi$

Span length of beam $l = 6\ ft$

Measured Unit weight of concrete $w_c = 152.0\ pcf$

Measured compressive strength of concrete at 90 days $f_c' = 9{,}763\ psi$

Area of nonprestressed longitudinal tension reinforcement $A_s = 0.33\ in^2$

Factor relating depth of equivalent rectangular compressive stress block to depth of neutral axis $\beta_1 = 0.65$

Self-weight of concrete member

$$w_{self\_weight} = w_c \cdot b \cdot h \cdot \left(\frac{1}{144\ in^2}\right) = 152.0\ pcf \cdot 6.07\ in \cdot 10.20\ in \cdot \left(\frac{ft^2}{144\ in^2}\right)$$

$$= 65.4\ plf$$

Depth of equivalent rectangular stress block

$$a = \frac{f_y \cdot A_s}{0.85 \cdot f_c' \cdot b} = \frac{90{,}000\ psi\ \cdot 0.33\ in^2}{0.85 \cdot 9{,}763\ psi \cdot 6.07\ in} = 0.590\ in$$

Distance from extreme compression fiber to neutral axis

$$c = \frac{a}{\beta_1} = \frac{0.590\ in}{0.65} = 0.908\ in$$

Net tensile strain in extreme layer of longitudinal tension reinforcement at nominal strength

$$\varepsilon_t = \frac{0.003 \cdot (d - c)}{c} = \frac{0.003 \cdot (8.95\ in - 0.908\ in)}{0.908\ in} = 0.027$$

Moment caused by self-weight of beam

$$M_{sw} = \frac{w \cdot l^2}{8} = \frac{65.4\ plf \cdot (6\ ft)^2}{8} = 294\ lb \cdot ft = 0.294\ kip \cdot ft$$

Tension in steel reinforcement

$$T = F_y \cdot A_s = 90{,}000\ psi \cdot 0.33\ in = 29{,}700\ lb = 29.7\ kip$$

Nominal flexural strength at section

$$M_n = T \cdot \left(d - \frac{a}{2}\right) = 29.7\ kip \cdot \left(8.95\ in - \frac{0.590\ in}{2}\right) = 257\ kip \cdot in = 21.4\ kip \cdot ft$$

Theoretical actuator applied moment at nominal flexural strength at section

$$M_n = 21.4\ kip \cdot ft - 0.294\ kip \cdot ft = 21.1\ kip \cdot ft$$

**Cracking Moment Calculations**

Modulus of rupture of concrete

$$f_r = 7.5 \cdot \sqrt{f_c'} = 7.5 \cdot \sqrt{9{,}763\ psi} = 741.1\ psi$$

Moment of inertia of gross concrete section about centroidal axis

$$I_g = \left(\frac{1}{12}\right) \cdot b \cdot h^3 = \left(\frac{1}{12}\right) \cdot 6.07\ in \cdot (10.20\ in)^3 = 536.8\ in^4$$

Moment caused by self-weight of beam

$$M_{sw} = \frac{w \cdot l^2}{8} = \frac{65.4\ plf \cdot (6\ ft)^2}{8} = 294\ lb \cdot ft = 0.294\ kip \cdot ft$$

Cracking moment

$$M_{cr} = \frac{f_r \cdot I_g}{y} = \frac{741.1\ psi \cdot 536.8\ in^4 \cdot (\frac{kip}{1{,}000\ lb})}{5.10\ in} = 78.0\ kip \cdot in = 6.50\ kip \cdot ft$$

Theoretical actuator applied cracking moment

$$M_{cr} = 6.50\ kip \cdot ft - 0.294\ kip \cdot ft = 6.2\ kip \cdot ft$$

**Modulus of Elasticity Calculation**

Unit weight of concrete for control cylinder $w_c = 153\ pcf$

Measured compressive strength of concrete at 90 days $f_c' = 6{,}385\ psi$

Modulus of elasticity

$$E_c = w_c^{1.5} \cdot 33 \cdot \sqrt{f_c'} = (153\ pcf)^{1.5} \cdot 33 \cdot \sqrt{6{,}385\ psi} = 4{,}990\ ksi$$